CITY UNIVERSITY LONDON

MODELLING OF SCREW COMPRESSOR PLANT OPERATION UNDER INTERMITTENT CONDITIONS

by Ekaterina Chukanova

Thesis submitted for the
Degree of Doctor Philosophy
in Mechanical Engineering

City University London
December 2015

Contents

List of Figures

List of Tables

Nomenclature

A – cross section area of control valve, [m^2]

A_g – clearance gap cross-sectional area, [m^2]

c_{oil} – specific heat, [J/kgK]

D_g – effective diameter of clearance gap, [m]

d – screw compressor rotor diameter, [m]

d_h – pipe hydraulic diameter, [m]

f_d – Darcy friction factor,

h – specific enthalpy, [J/kg]

L – length of the rotor, [m]

l_g – leakage clearance length, [m]

M – torque, [Nm]

m – mass, [kg]

$\dot{m}_{in}$–mass flow entering the tank, [kg/s]

$\dot{m}_{out}$ –mass flow leaving the tank, [kg/s]

p_0 – atmospheric pressure, [Pa]

p_1 – pressure in the compressor tank, [Pa]

p_2 – pressure in the tank at the next time step, [Pa]

$\dot{Q}$– heat transfer between fluid and compressor surroundings, [J]

R - gas constant, [J/molK]

Re – Reynolds number,

T_2 - Temperature in the tank, [K]

T_{in} – temperature of the gas entering the tank, [K]

T_{out} – temperature of the gas leaving the tank, equal to T_2, [K]

t_{fl} – flow time, [s]

Δt – time step, [s]

U - internal energy, [J]

u - specific internal energy, [J/kg]

V – volume of the plant containing tank and pipes, [m^3]

V – local volume of the compressor working chamber, [m^3]

v – fluid velocity, [m/s]

w – suction/discharge port velocity, [m/s]

w_l – leaking gas velocity, [m/s]

γ – isentropic gas constant

δ_g – leakage clearance width, [μm]

φ – angular coordinate,

φ – transported property in generic transport equation

θ – main rotor angle,

μ – flow coefficient,

ν – kinematic viscosity, [m^2/s]

ρ_l – leaking gas density, [kg/m^3]

ρ_2 – density of the gas in the tank, [kg/m^3]

ω – angular velocity, [rad/s].

Acknowledgments

I feel very honoured to be a student of Professor Stosic – a brilliant engineer, a great teacher and a man with a big heart. Without his support, guidance and encouragement my PhD thesis would have never been completed. His patience, knowledge and enthusiasm have no limit.

I would also like to thank Professor Kovacevic, without whom this thesis had never been started, who initially trusted to my ideas and continued guiding me through the whole process of it.

Also, my very best gratitude to my colleagues for the continuous help and discussions over the years: Dr Sham Rane, Dr Matthew Read, Dr Ashvin Dhunput, Ms Madhulika Kethidi, Mr Mohammad Arjeneh. Special thanks to Mr Mike Smith for his help with the test rig.

I want to thank company Howden where I got inspiration and ideas for my research and people who supported me there: Mr Eric Schwab, Mr Peter Goddard, Mr Paul Hendry and Mr Kirill Zaitsev.

Also, I would like to thanks my friends, my relatives and my husband Mikhail for their unconditional support and patience.

Abstract

Compressor plant frequently operates under unsteady conditions. This is due to pressure fluctuations, variable flow demand, or unsteady inlet conditions, as well as shaft speed variation. Also, following demand, compressor plants often work intermittently with frequent starts and stops. This may cause premature wear, decrease of compressor performance and even failure, which might cost millions of pounds to industry in downtime. However, there is still a lack of published data which describes intermittent plant behaviour, or predicts the effects of unsteady operation upon compressor plant performance. Thus, there appears to be a need to develop a mathematical model to calculate compressor plant performance during intermittent operating conditions and to verify this model with experimental data.

Accordingly, this thesis describes an experimental and analytical study of screw compressor plant operating under unsteady conditions. For this purpose a one-dimensional model of the processes within a compressor was used, based on the differential equations of conservation of mass and energy, extended to include other plant components, such as storage tanks, control valves and connecting pipes. The model can simulate processes in both oil-free and oil-injected compressor plants during transient operation, including the effects of sudden changes in pressure, speed and valve area. Performance predictions obtained from the model gave good agreement with test results.

This model can, therefore, be used to predict a variety of events, which may occur in everyday compressor plant operation.

1. Introduction

Screw compressors are extensively used in industry and their application is so wide that it is difficult to overestimate the role that they play in the contemporary engineering world. As described by Stosic et al (2003), during the past 30 years traditional reciprocating compressors have been replaced, by those of the twin screw type, in many applications. Since most of them operate mainly under unsteady conditions, there has been an increasing need to investigate their behaviour under transient conditions. Despite this, there is still a lack of published information on both predictive methods and test results that describe how they operate under such conditions.

Figure 1: Twin screw compressor

As shown in Figure 1, screw compressors are rotary positive displacement machines of simple design, with their moving parts comprising only two rotors revolving in four to six bearings. Their working principle is described in Appendix 1. Due to their pure rotary motion, they are capable of efficient operation at high speeds over a wide range of operating pressures and flow rates. They are thus both compact and reliable. Consequently, the majority of industrial positive displacement compressors now

produced are of this type. Their remarkable success is due to improvements in their rotor profiles, detailed computer modelling of the flow processes within them, and the development of profile milling and grinding machine tools that produce rotor profiles, with linear tolerances of less than 10 μm, at an economic cost. Machines can thus be manufactured with rotor interlobe clearances of 30-50 μm, thereby greatly reducing internal leakages and, consequently making them more efficient than other types.

Gas compression constitutes a core part of many industrial processes, such as refrigeration, air conditioning, ice and snow production, food processing, the oil and gas industries, power generation, chemical factories, and mining. Also, compressed air is widely used to operate control systems.

Figure 2: Oil-injected process screw compressor plant, the compressor is on the right, the oil-separator on the left, the suction pipe on the top and service ladders in the middle *(Courtesy of Howden. Compressors)*

A typical industrial compressor plant is presented in Figure 2. This includes a screw compressor, together with an electric drive motor, an oil-separator/oil tank, oil or gas coolers, pumps, pipes, filters and automatic controls. The power input for such systems varies from 100kW to 3MW depending on required flow. Large industrial compressor plants can cost millions of pounds and their failure usually causes the plant

to shut down. This can result in production losses that cost more than the equipment itself. So, simulation of their performance under extreme operating conditions is vital at the design stage in order to choose all the components correctly, to reduce equipment cost and to avoid plant failure. Thus, the plant design process should include performance estimates under varying, as well as steady state conditions. Various general commercial software packages have therefore been developed for this purpose. Those, which treat power and process plant dynamics, are well known by their commercial names, such as Aspen Hysys by Aspen Technology, Dynsim by Schneider Technology and Scada by Inductive Automation. These and other similar programs are available to determine and follow dynamic plant behaviour. Their specialists constantly stress the importance of dynamic studies. Nicholas Brownrigg, AspenTech, says that "dynamic simulation of gas processing and petroleum refining processes is vital for the prevention of catastrophic equipment occurrences; the protection of compressors from mechanical failure is essential to maximise operating time and ensure safer operations".

However, their role is limited to the estimation of overall plant dynamics and this does not to include the dynamic behaviour of the compressor plant in sufficient detail for reliable detailed design of the compressor and its associated components.

Apart from their insufficient detail in the treatment of compressors, these generalised software packages, usually, do not contain detailed information about the models, used to describe the plant elements and, in general, do not give the equations used in them and their methods of solution, while they operate through predefined menus, which do not contain enough information to define the compressor itself. Thus it is only possible to use these programs to check predefined situations without understanding the model on which the processes is based. Moreover, none of these solvers use detailed compressor models, but are usually based on empirical data.

Thus there is a clear need for a detailed analysis of the compressor process, included in a complete plant dynamic study.

1.1. Phenomena Associated with Transient Behaviour of Screw Compressors

The most significant transients and their effect on a compressor system, during unsteady plant operation, are summarised in Table 1 below.

Table 1: Types of screw compressor plant and their associated transient phenomena

Transient Type	Area of Occurrence	Effect
Frequent startup and shutdown	Small air and refrigeration compressor plants	Increased power consumption, premature wear and failure
Effect of parameter changes: pressure fluctuations, shaft speed variation, variable flow demand and variable inlet conditions	Offshore platforms, Chemical and Process gas plants, Refrigeration plants, Air-conditioning	Use of overdesign factors from previous experience leads to equipment cost increase. Curves and diagrams used for extreme cases lead to risk of early failure. Compressor work in off-design mode leads to compressor performance decrease.

1.2. Thesis Outline

This thesis has been prepared in 10 Chapters. Chapter 1 gives a detailed explanation of the motivation for this research, stresses the value of dynamic simulation studies and also describes phenomena associated with the transient behaviour of compressor plant. Chapter 2 contains a literature review and describes the problems of compressor dynamic modelling and the effects of transient behaviour on compressor performance. Chapter 3 states the research aims, objectives and the contribution made. Chapter 4 describes the experimental work done. This includes a description of the test rigs used. Chapter 5 describes the mathematical model developed for the analysis of screw

compressor plant. Chapters 6 and 7 describe the results of 2 major experiments, and how these compare with the model predictions. Chapter 8 describes a number of simulated cases of screw compressor plant intermittent behaviour. Chapter 9 gives conclusions, derived from the work carried out and Chapter 10 suggests some proposals for further investigation.

2. Literature review

2.1. Transient behaviour and its effects

2.1.1. Startup and Shutdown of Process Plant

Ogbonda (1987) investigated the dynamic simulation of chemical plant and stated that "information about the stability of the startup and shutdown processes can help process engineers to evolve better startup and shutdown procedures". The Honeywell Dynamic Engineering Studies Group (2012) confirmed that dynamic models of new plant designs, their review and testing, can make shorter commissioning, thus making significant money and time savings for large process plants.

Jun and Yezheng (1988, 1990) carried out experimental studies on the effects of working fluid migration in a refrigeration system operating with a reciprocating compressor, during the startup and shutdown processes. They developed a program to estimate energy losses and how to calculate their effect, with the aim of reducing energy consumption.

Fleming et al (1996) published a paper on the simulation of shutdown processes in screw compressor driven refrigeration plant. Their idea was to investigate the replacement of a suction non-return valve by a reverse rotation brake because a non-return valve causes an additional pressure drop in the line and is prone to malfunction, caused by the accumulation of debris in the refrigerant. A reverse rotation brake holds the compressor rotors stationary, to avoid backflow into the evaporator and prevents the compressor being driven like a motor in reverse by the high-pressure gas. However, for safe system shutdown, the shutdown torque should not exceed the normal running torque. Thus, a reverse rotation brake is a good option in the case of off-loaded compressor shutdown but in the case of an emergency shutdown, it might cause plant failure. A mathematical model was presented in this paper, but without experimental validation.

Li and Alleyne (2009) investigated transient processes in the startup and shutdown of vapour compression cycle systems, operating with semi-hermetic reciprocating compressors. They established a model of a moving boundary heat exchanger and validated it experimentally. Ndiaye and Bernier, 2010 developed a dynamic model for

a reciprocating compressor during on-off cycle operation and validated it as a part of an experiment to justify water-to-air heat pump models. A recent paper, by Link and Deschamps (2011), deals with numerical methods and the experimental validation of their results, during transient startup and shutdown processes in reciprocating compressors.

2.1.2. Effects of Parameter Changes

Mokhatab (2007) confirmed the purpose and relevance of plant dynamic modelling. That paper describes the dynamic simulation of offshore production plant where the parameters, such as flow, may change frequently. A dynamic model to predict the effects of severe slugging or unstable flow of the offshore process plant was developed. That model was verified by experiment and it is shown that the model can be used as "a useful engineering tool for the reliable simulation of separation facilities during normal transients and more serious upsetting conditions". Another benefit of this model, which has been confirmed by other authors, is that "by using this model one can check whether the production system handles unstable flows or if the proposed production control system is stressed". It is mentioned that slugging leads to unstable plant operation and even to its shutdown and restart. Also, it is said that it is very important to have an accurate dynamic model, which allows for the accurate design of the separator size, to avoid over-dimensioning, because every kilogram of material counts on offshore platforms.

The same paper mentions two other unstable types of plant behaviour: "At the conceptual design stage, dynamic simulation studies are particularly valuable in evaluating process design options and carrying out controllability studies. During the detailed design phase, dynamic simulation can be used as a tool to check and develop startup and shutdown procedures and examine case scenarios".

2.1.3. Control Systems Design

The Honeywell Dynamic Engineering Studies group (2012) worked on various aspects of dynamic simulations, including compressor control and process design and controllability. They stressed that "the cost of damage to compressor systems can quickly run into tens of millions of dollars, not only due to the cost of equipment but also due to the loss of profit during plant downtime". Also, it is stated that it is essential

for large process plants to be shut down just once in 2-3, sometimes even in 5 years. That is why it is critically important to provide dynamic models which include detailed compressor models, as well as valves, tanks and pipes to know answers to questions of the type "what would happen if.." Some of these answers can be provided by dynamic simulation studies and will play a vital role in decision making in improvement of the design, or in testing of new designs before they are built, as it was concluded by Ogbonda (1987).

Bezzo et al (2004), who studied both steady state and dynamic simulation of the purification stage for a vinyl chloride synthesis industrial plant, stated that dynamic modelling is a powerful tool to assess control system performance and for hazard analysis in case of abnormal events. Dynamic simulators can be used to design a control system and to verify its effectiveness. Also that paper demonstrated that both steady state and dynamic simulations can be used by plant engineers for better understanding of process behaviour. Similar conclusions were drawn by other authors mentioned above.

2.2. Dynamic modelling

Some issues of screw compressor dynamic modelling have been considered, as simulation potential was increased, due to the availability of much more powerful computers. The papers of Sauls, Weathers and Powell (2006) presented a transient thermal analysis of screw compressors. A control volume model based on the principles of conservation of mass and internal energy was applied in the first instance and then the derived values of pressure and temperature were used as boundary conditions for a 3-D Finite Element Method. Detailed descriptions of such methods are presented in books by Stosic et al, 2005 for the chamber model and Kovacevic et al, 2007 for the 3-D Computational Fluid Dynamics. An integrated model was presented at the IMechE Conference by Kovacevic et al (2007). This model combines the benefits of both methods and enables faster calculation than from full 3-D CFD modelling with more accurate results than from 1 quasi-dimensional modelling. Krichel and Sawodny (2011) presented a model for the dynamic simulation of an oil-injected screw compressor. They split the plant into four subsystems, namely: throttle-valve, motor, screw compressor block, and oil/air separator, and presented them as separate mathematical models. It was emphasized in that paper that the warm-up and

shutdown phases require a lot of energy and that this is often ignored when studying steady state compressor plant operation. This again confirms that screw compressor transient operation is worth investigating and that both existing and advanced mathematical models should be adapted, extended and improved in order to predict compressor performance during unsteady operation.

3. Aims of the Research and its Contribution to Science and Engineering

3.1. Aims of the research

The aim of the studies described in this thesis was to investigate, develop and verify a mathematical model suitable for the analysis of screw compressor plant operating under transient conditions. To achieve this, the following objectives were set:

- Development of a mathematical model and additional procedures to predict compressor plant system performance, when operating under unsteady conditions;
- To determine how variable operation parameters influence compressor system performance;
- The development of software that enables various kinds of unsteadiness, which may appear during the plant operation, to be simulated;
- Validation of the results obtained from simulation by comparison with measurements obtained from real screw compressor plant.
- The desired outcome of this research was to develop a tool for everyday use by engineers and other specialists to identify and study the unsteady behaviour of real screw compressor plant.

3.2. Contribution to Science and Engineering

As a result of the work described in this thesis the following original contributions have been made to the modelling of compressor plant when operating under unsteady conditions:

- Development of a finite difference model, based on the differential equations of the conservation of internal energy and mass continuity of a complex compressor plant which consists of a screw compressor, low pressure and high pressure tanks and communications between them and auxiliary equipment, like valves or pumps. It is, up to now, the only model available in the open

published literature, which describes the whole compressor plant, including a detailed screw compressor model.

This was done by combining the full compressor model with the finite difference description of a lumped tank and tube process. The difference of this approach, to that of the classical tank and tube, was in its ability to acquire dynamic characteristics of the compressor plant. Moreover, since the plant time constant was far larger than the compressor time constant, these two dynamic processes were coupled together by two independent time scales, the compressor, solved in its time, fully converges within one plant time step. This then marches with the compressor results as boundary conditions. An application of this type is not known to have been published for any kind of compressor.

- The model was verified by tests on an experimental compressor plant, during unsteady operation, using both oil-injected and oil-free screw compressors. This included startup, speed and pressure variation. A variety of experimental data for different compressor types, different speeds and different startup scenarios is available, on request, for further analysis. The data acquisition system was modified to register dynamic changes within the plant, which required a new time scale to be introduced compared with previous measurements. Apart from that, the screw compressor startup process was measured. This has not been found in other publications.

- Sample cases, and how they vary in the different scenarios that may occur in compressor plant, were calculated, together with a comprehensive study of the plant response in each case.

The developed model has a wide range of applications within the screw compressor field including both oil-injected and oil-free types. It can be used in compressed air plant, process plant or refrigeration plant, with different types of working fluid, such as gas or refrigerant or a gas-liquid mixture. In addition, the effects of water or refrigerant injection can be considered; and, finally, all operating parameters can be

varied in this model to predict plant performance during non-steady modes of operation.

The results of the investigation performed in this thesis will reside at the Compressor Centre as an engineering design tool to help those who wish to include unsteady aspects of complex plant behaviour in their performance and design calculations.

4. Experimental Studies

To investigate and identify the parameters, which are significant for transient performance analysis, experimental studies were carried out prior to the mathematical model development. These have already been described by Chukanova et al (2012). Further experimental work was then done in order to verify the mathematical model after its development. This chapter describes the equipment used and an overview of the parameters tested. Four sets of tests were carried out over a period of 3 years. All were performed on the air compressor test rig in the Compressor Centre Laboratory. This is shown in Figure 3. Two startup investigations and two speed variation tests were performed.

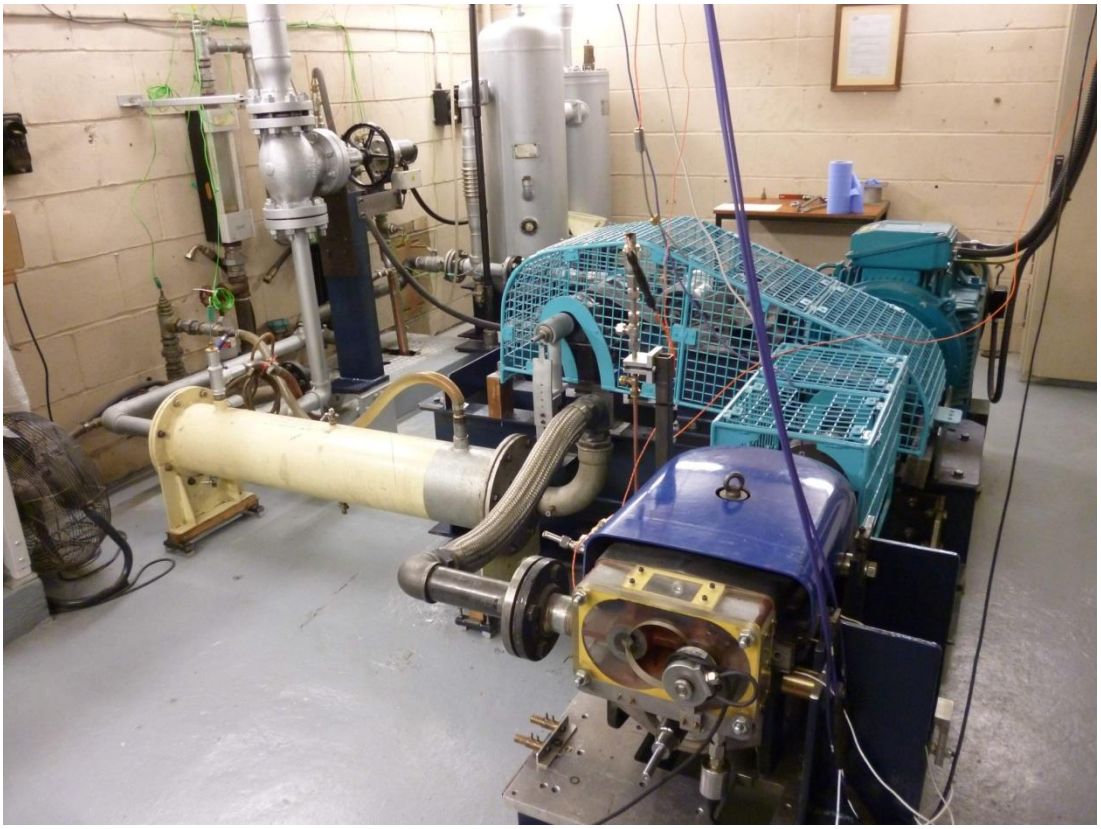

Figure 3: Laboratory Air Compressor Test Rig for both oil-free and oil-injected machines

4.1. Test Rig Description

Two air compressor test rigs with some common shared facilities were available, so that it is possible to test either oil-injected or oil-free air compressors. In both cases atmospheric air is induced externally through a common flue pipe. Accordingly, it was possible to check both types of compressor plant. All the pressure transducers and the torque meter were recalibrated for the tests and the calibration results were input to the data acquisition software. More details of the rig and its instrumentation are given in Appendices 2 and 3.

4.1.1. Oil-Injected Air Compressor Plant

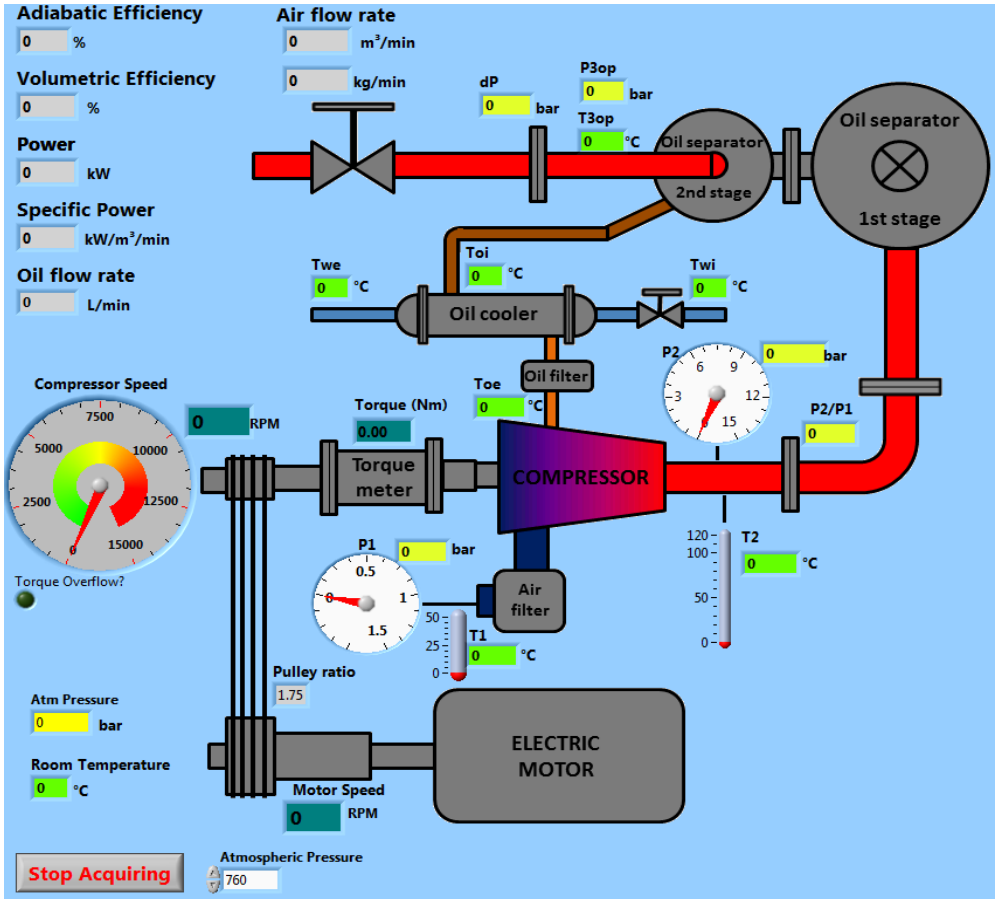

Figure 4: Schematic view of oil-injected compressor test rig – Computer screen

A schematic layout of the oil-injected air compressor test plant is shown in Figure 4. The compressor is driven by a six-band belt drive coupled to a 75 kW electric motor. The speed is controlled by a frequency inverter. The two stage oil separator, shown in Figure 4, consists of two separator tanks, which are limited to operate at a maximum

working pressure of 15 bars. The combined volume of the two tanks is 325 cubic litres. The oil cooler is a water cooled shell and tube heat exchanger. This system does not have a pump, the oil is injected into the compressor by means of the pressure difference between the oil separator and compressor working chamber. A motor driven throttle valve, after the oil separator, controls the air pressure inside the oil separator.

The compressor tested is shown in Figure 5. It has a 4/5 lobe configuration (4 male rotor lobes and 5 female rotor lobes). The main rotor diameter is d=128mm, while the length to diameter ratio, L/d=1.55.

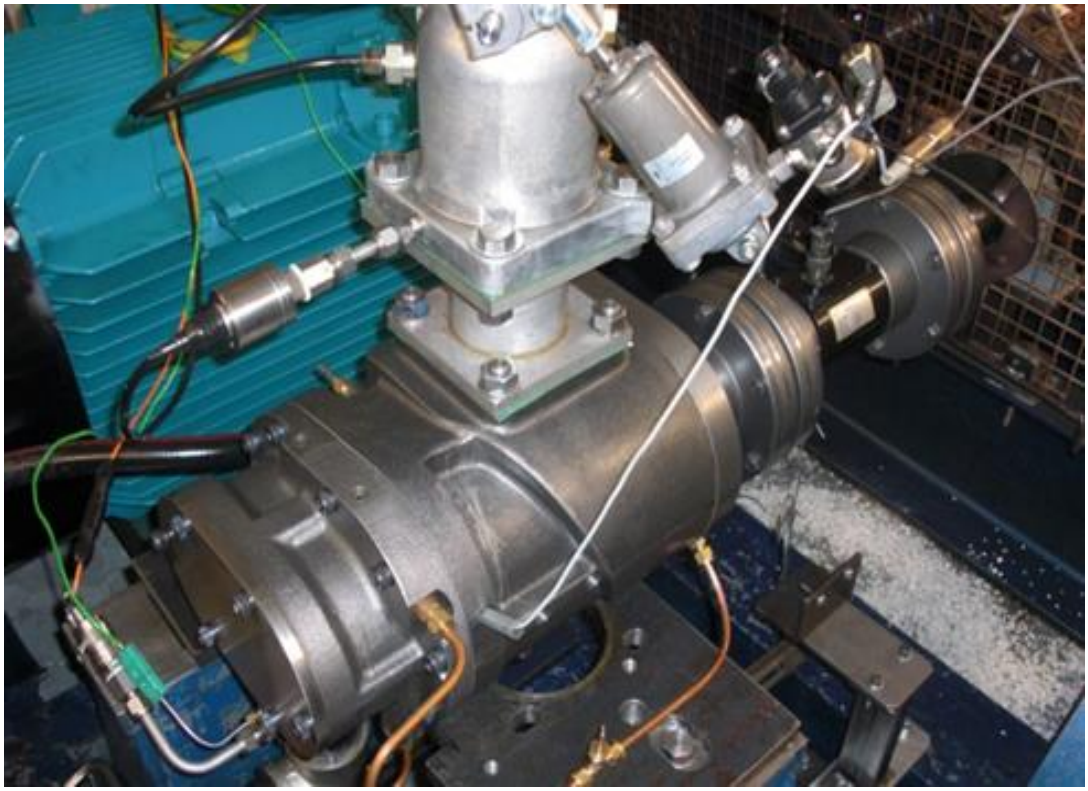

Figure 5: Oil-injected screw compressor tested

The first tests were concerned with a study of the plant during startup, when the rotational speed changes, during the first few seconds, from zero to 3,000rpm, before attaining steady conditions. Details of the tests carried out, together with an analysis of their results are given in Chapter 6.

On completion of the startup tests, a study was carried out on the effects of speed variation, while maintaining a fixed starting pressure of 4 bar. Step changes in speed of 1000rpm, were made between 2000rpm and 5000rpm. A time interval of 60

seconds was made between tests in order to enable the pressure to stabilise after each speed change. Table 2 shows the final pressures achieved for each selected speed.

Table 2: Oil-injected compressor experimental plan: Initial pressure and speed values are not highlighted. Experimentally obtained pressure values are highlighted in grey

№	Pressure, bar	Shaft Speed, rpm
1	4	2000
2	6.0	3000
3	7.8	4000
4	9.3	5000
5	7.8	4000
6	6.0	3000
7	4	2000

4.1.2. Oil-Free Air Compressor Test Plant

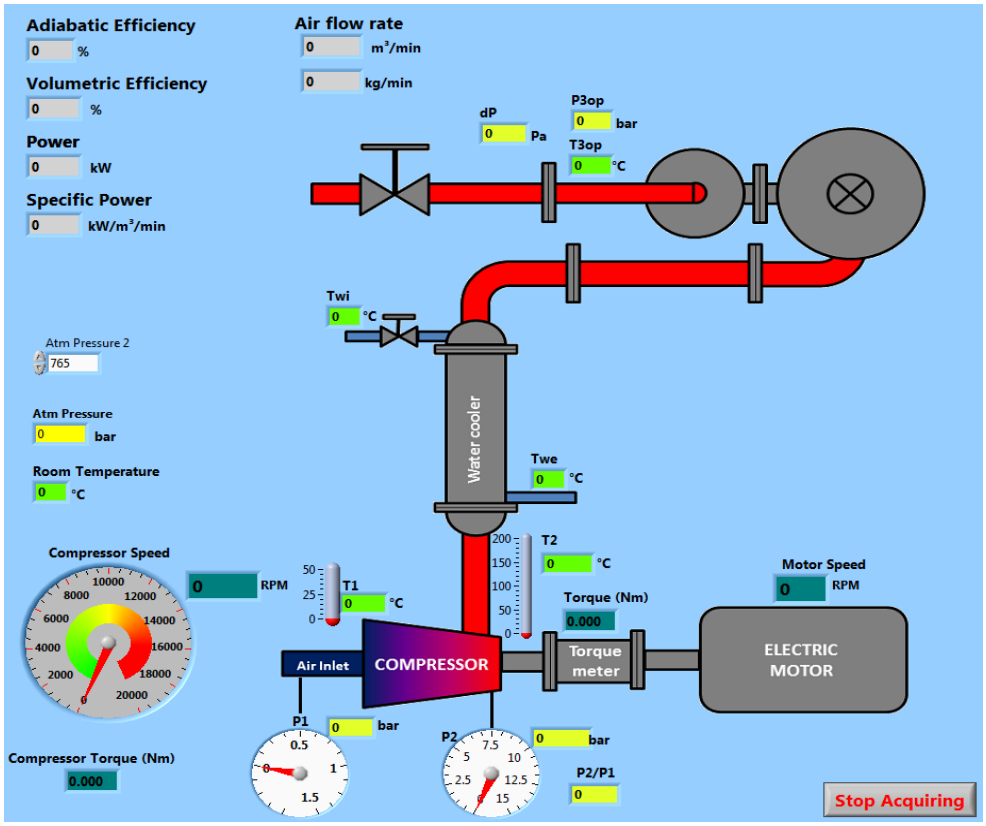

Figure 6: Schematic view of oil-free compressor test rig – Computer screen

The experimental test rig for an oil-free compressor, as shown in Figure 6, has many parts in common with the oil-injected compressor test rig, but the oil-free compressor is driven through a gearbox. There is no oil supply or oil cooler but an air cooler is included to reduce the temperature of the discharged air.

The compressor tested is shown in Figure 7. This has a 3/5 lobe configuration. The main rotor diameter is d=127mm, while the length to diameter ratio is L/d=1.6.

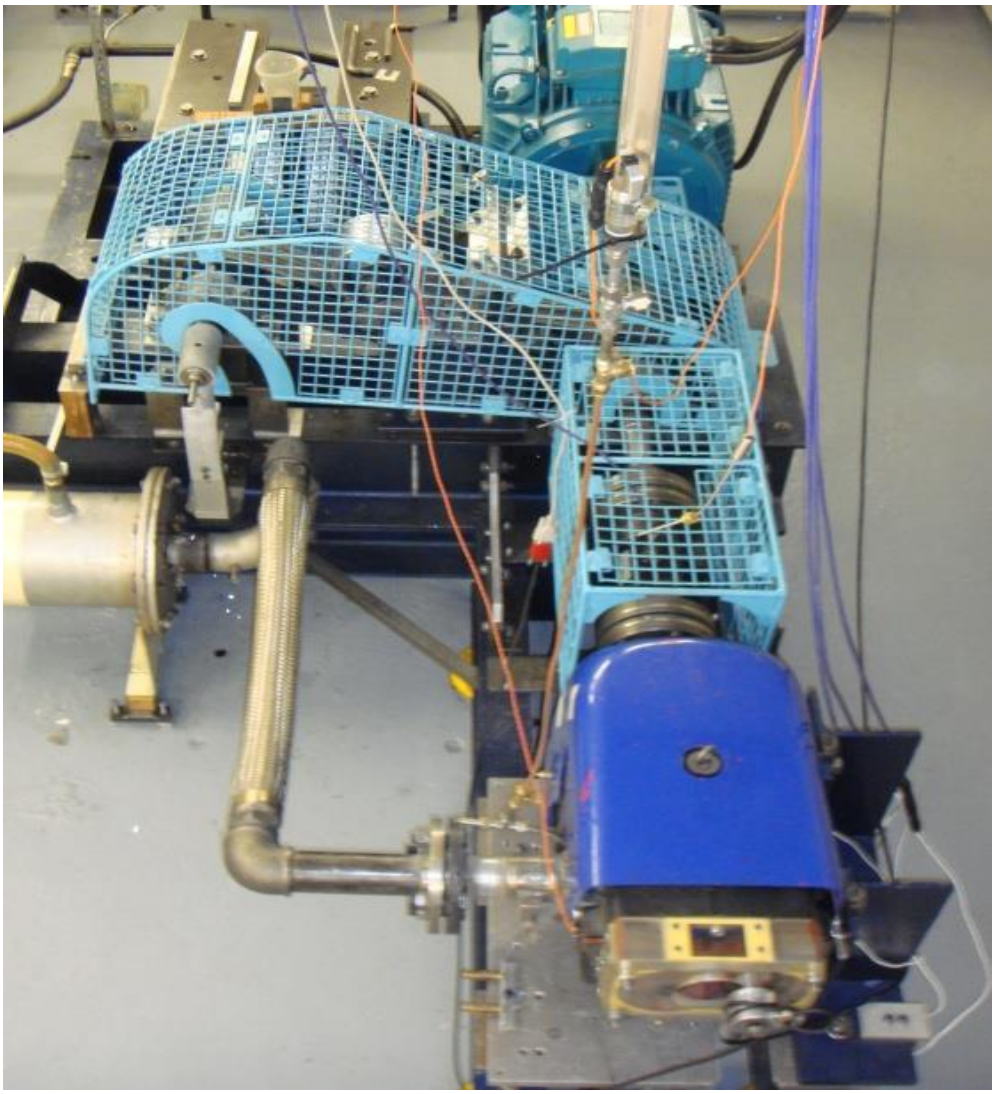

Figure 7: Tested oil-free machine

Tests were carried out, varying the speed of the male rotor between 3000 rpm and 8500rpm with a time interval of 30 seconds between tests. The results of the tests are shown in Table 3, where the intial values are not highlighetd but the final pressures obtained, as a result of the change in speed are highlighted grey.

Table 3: Oil-free compressor experimental plan: Initial pressure and speed values are not highlighted. The final obtained pressures are highlighted in grey

№	Pressure, bar	Shaft Speed, rpm
1	1.2	3000
2	1.45	5000
3	1.85	7000
4	2.2	8500
5	1.85	7000
6	1.45	5000
7	1.2	3000

5. Mathematical Model of the Screw Compressor Plant

The previous chapter described the experimental work which was done to verify the model developed for analysing unsteady screw compressor plant operation. The mathematical approach used in this model is explained in this chapter, and describes separately a model for the compressor itself and a model for the whole plant.

The algorithm of the thermodynamics and flow processes in a screw compressor, described by Stosic et al (2005), is based on a mathematical model, defined by a set of differential equations, which describe the physics of the complete process in a compressor. The equation set consists of the equations for the conservation of energy and mass continuity together with a number of algebraic equations defining the flow phenomena in the fluid suction, compression and discharge processes. Also included are differential kinematic relationships, which describe the instantaneous operating volume and its change with the shaft rotation angle or time. The model accounts for a number of 'real-life' effects, which may influence the final performance of a compressor and validate it for a wider range of applications. Any gas or liquid-gas mixture of known properties can be used as a working fluid. The model takes account of heat transfer, between the gas and the compressor rotors and its casings, and leakage between rotor-to-rotor and rotor-to-casing.

5.1 Equations governing the screw compressor process

The working chamber of a screw machine, together with the suction and discharge plenums, can be described as a flow system in which the mass flow varies with time and for which the differential equations of conservation laws for energy and mass are derived using Reynolds Transport Theorem. More details are given in Appendix 4.

The following are the simplifications that were made:

- Fluid flow in the model is assumed to be quasi one-dimensional;
- Kinetic energy changes of the working fluid within the working chamber are negligible compared to internal energy changes;
- Gas or gas-liquid inflow to and outflow from the compressor ports is assumed to be isentropic;

- Leakage flow of the fluid through the clearances is assumed to be adiabatic.

A feature of the model is to use the unsteady flow energy equation to compute the effect of variation of influential parameters upon the thermodynamic and flow processes in a screw machine in terms of rotational angle, or time.

The following conservation equations have been employed in the model.

The conservation of internal energy:

$$\omega\left(\frac{dU}{d\theta}\right) = \dot{m}_{in}h_{in} - \dot{m}_{out}h_{out} + \dot{Q} - \omega p\frac{dV}{d\theta} \tag{1}$$

Where θ is angle of rotation of the main rotor, *h=h(θ)* is specific enthalpy, $\dot{m} = \dot{m}(\theta)$ is mass flow rate, *p=p(θ)* is fluid pressure in the working chamber control volume, $\dot{Q} = \dot{Q}(\theta)$ is heat transfer between the fluid and the compressor surrounding and $V = V(\theta)$ is local volume of the compressor working chamber. Flow through the suction and discharge ports is calculated from the continuity equation:

$$\omega\frac{dm}{d\theta} = \dot{m}_{in} - \dot{m}_{out} \tag{2}$$

The suction and discharge port fluid velocities are obtained through the isentropic flow equation. The computer code also accounts for reverse flow. This is calculated through equation 3:

$$w = \mu\sqrt{2(h_2 - h_1)} \tag{3}$$

Leakage in a screw machine is an important part of the total flow rate and affects the compressor delivery, i.e. the volumetric and adiabatic efficiencies; the gain and loss leakages are considered separately. The gain leakages come from the discharge plenum and from the neighbouring working chamber with a higher pressure. The loss leakages leave the chamber towards the suction plenum and to the neighbouring chamber with a lower pressure.

An idealized clearance gap is assumed to have a rectangular shape and the mass flow of leaking fluid is expressed by the continuity equation:

$$\dot{m}_l = \mu_l \rho_l w_l A_g \tag{4}$$

where ρ and w are density and velocity of the leaking gas, $A_g = l_g.\delta_g$ is the clearance gap cross-sectional area, l_g is the leakage clearance length, δ_g is the leakage clearance width or gap and μ=μ(Re,Ma) is the leakage flow discharge coefficient.

The leakage velocity through the clearances is considered to be adiabatic Fanno-flow through an idealized clearance gap of rectangular shape and the mass flow of leaking fluid is calculated from the continuity equation. The effect of fluid-wall friction is accounted for by the momentum equation with the friction and drag coefficients expressed in terms of the Reynolds and Mach numbers for each type of clearance:

$$w_l dw_l + \frac{dp}{\rho} + f\,\frac{w_l^2}{2}\frac{dx}{D_g} = 0 \tag{5}$$

where f(Re,Ma) is the friction coefficient which is dependent on the Reynolds and Mach numbers, D_g is the effective diameter of the clearance gap, $D_g \approx 2\delta_g$ and *dx* is the length increment.

The injection of oil or other liquids for lubrication, cooling or sealing purposes, modifies the thermodynamic process substantially. The same procedure can be used to estimate the effects of injecting any liquid but the effects of gas or its condensate mixing and dissolving in the injected fluid or vice versa should be accounted for separately.

The solution of the droplet energy equation in parallel with the momentum equation yields the amount of heat exchange with the surrounding gas.

The equations of energy and continuity are solved to obtain U(θ) and m(θ). Together with V(θ), the specific internal energy and specific volume u=U/m and v=V/m are now known. T and p, or x can then be calculated. All the remaining thermodynamic and fluid properties within the machine cycle are derived from the pressure, temperature and volume directly. Computation is repeated until the solution converges.

For an ideal gas, the internal thermal energy of the gas-oil mixture is given by:

$$U = (mu)_{gas} + (mu)_{oil} = \frac{mRT}{\gamma - 1} + (mc_{oil}T)_{oil} \tag{6}$$

Hence, the pressure or temperature of the fluid in the compressor working chamber can be explicitly calculated by the equation for the oil temperature T_{oil}.

In the case of a real gas the situation is more complex, because the temperature and pressure cannot be calculated explicitly. However, since the equation of state $p=f_1(T,V)$ and the equation for specific internal energy $u=f_2(T,V)$ are decoupled, the temperature can be calculated numerically from the known specific internal energy and the specific volume obtained from the solution of differential equations, the pressure can then be calculated explicitly from the temperature and the specific volume by means of the equation of state.

These equations are in the same form for any kind of fluid, and they are essentially simpler than any others in derived form. In addition, the inclusion of any additional phenomena into the differential equations of internal energy and continuity is straightforward. A full account of the compressor model used in this work can be found in Stosic et al (2005).

5.2 The unsteady process in a lumped volume of the plant reservoirs and connecting pipes

The screw compressor plant model is represented in Figure 8. The detailed screw compressor model, described in section 5.1, is shown within the small red rectangle. The whole plant program, described in this section, is shown in the large red rectangle.

All connecting pipes in the compressor plant are considered to be short enough, for their volumes, together with the reservoir volumes, to be summed up into one lump tank volume. This assumes that all the thermodynamic properties are uniform within such a control volume. Thus the conservation equations of continuity and energy already used in equation (1) for the compressor model may be utilized for the tank calculations.

$$\omega\left(\frac{dU}{d\theta}\right) = \dot{m}_{in}h_{in} - \dot{m}_{out}h_{out} + \dot{Q} - \omega p\frac{dV}{d\theta}$$

Since the heat transfer $\dot{Q}$ and the compressor work $\omega p \frac{dV}{d\theta}$ do not exist in the tank system, this equation now takes the following form:

$$\omega\left(\frac{dU}{d\theta}\right) = \dot{m}_{in} h_{in} - \dot{m}_{out} h_{out}$$

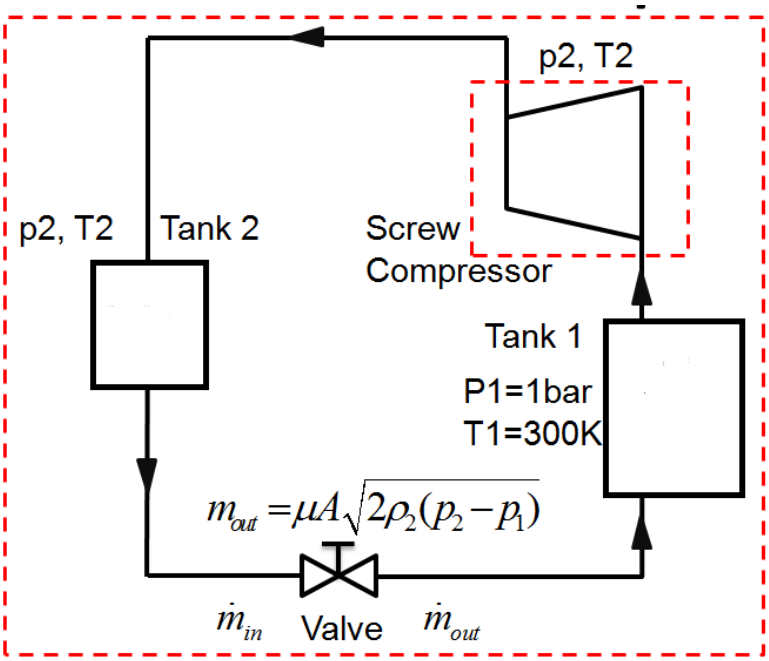

Figure 8: Screw compressor plant model used for transient analysis

The tank filling/emptying equations for that analysis derived from equations (1) and (2) in the form of finite differences are now as follows:

$$\begin{aligned} m_2 u_2 - m_1 u_1 &= \left(\dot{m}_{in} h_{in} - \dot{m}_{out} h_{out}\right)\Delta t \\ m_2 - m_1 &= \left(\dot{m}_{in} - \dot{m}_{out}\right)\Delta t \end{aligned} \tag{7}$$

where indices 1 and 2 denote the start and end times of filling/emptying respectively and Δt is the time difference between them.

The ideal gas case may serve as an illustration in which the finite difference equations of thermodynamic and flow parameters can be written as:

$$p_2 = p_1 + \frac{\gamma R \Delta t}{V}\left(\dot{m}_{in} T_{in} - \dot{m}_{out} T_{out}\right) \tag{8}$$

$$\dot{m}_{out} = \mu A \sqrt{2\rho_2 (p_2 - p_0)} \qquad \rho_2 = \frac{m_2}{V} \qquad T_2 = \frac{p_2}{R\rho_2} \tag{9}$$

To estimate the unsteady behaviour of a compressor plant system, the tank equations are coupled with the compressor model equations and solved in sequence to obtain a series of results for each time step.

The algorithm used in the developed program is presented in Figure 9. When the pressure p_2 in the tank at each time step is known, the flow and temperature m_{in} and T_{in}, at the compressor discharge, can be calculated. These derived values are then taken as the input parameters for the next time step. When the tank pressure p_2 is calculated, m_{out} is either known, or calculated, as for the flow through the exit throttle valve to pressure $p_{0,}$ and T_2 becomes T_{out} in the next time step. The calculation is repeated until the final time is reached.

Mass inflow and outflow are calculated as pipe flow with restrictions which comprise both line and local losses, thereby defining pressure drops within the plant connections. Since the tanks are of far greater volume than the connections, which results in far lower gas velocities within them, the losses in the tanks are far lower than the pipe losses and can be neglected.

Two levels of programming were applied. Firstly the compressor and plant processes were solved separately. The compressor process was calculated through the software suite which simulates the screw compressor process. The results from the compressor program were used as inputs to the plant program allowing the plant process to be calculated. The results were presented in tabular and graphical form by the use of Excel, with mutual interchange of their input and output data. This speeded the calculation, allowing the bulk estimation of the unsteady behaviour of a screw compressor plant under various scenarios.

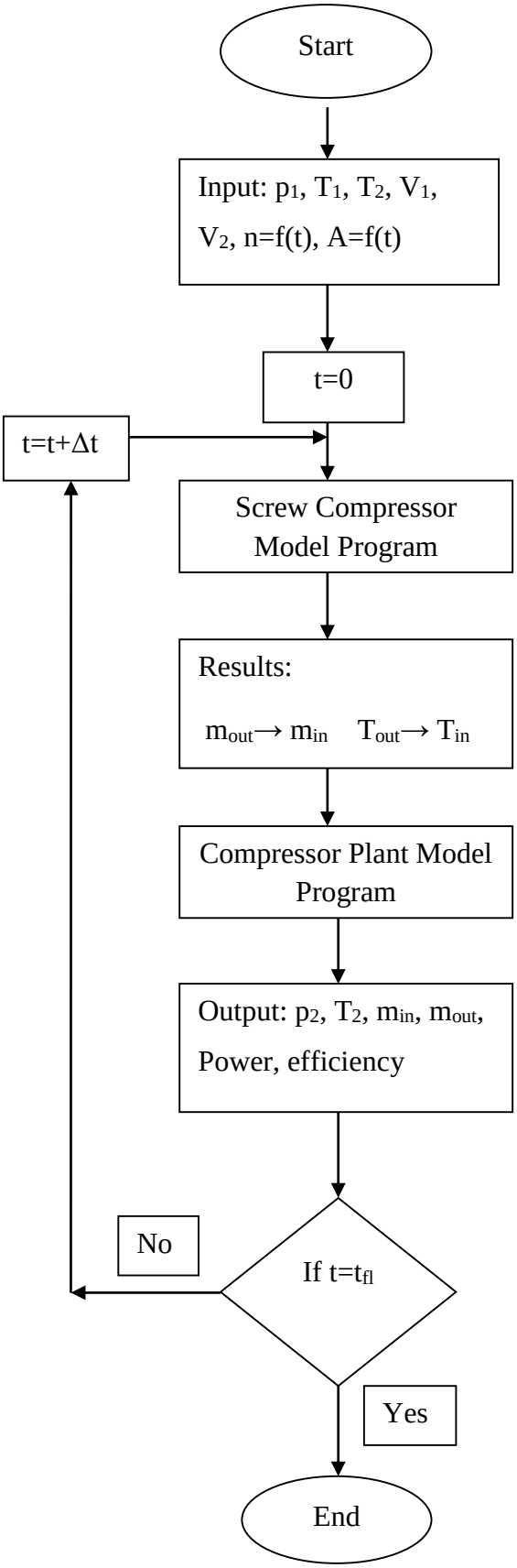

Figure 9: Flow Chart of transient screw compressor plant program

6. Startup Test Results and Data Analysis

The first tests were to investigate the startup characteristics of air oil-injected screw compressor plant as a transient process in order to verify the utilisation of the simple filling tank program as a first step in the development of a more advanced model in the future.

6.1 Verification of Filling Tank Simulation

The simulation process of the tests was straightforward, because the discharge valve was closed and the analytical model was very simple, while the full model is presented in Chapter 5. As shown in Figure 10 and Figure 11, the simulated and measured results agree closely.

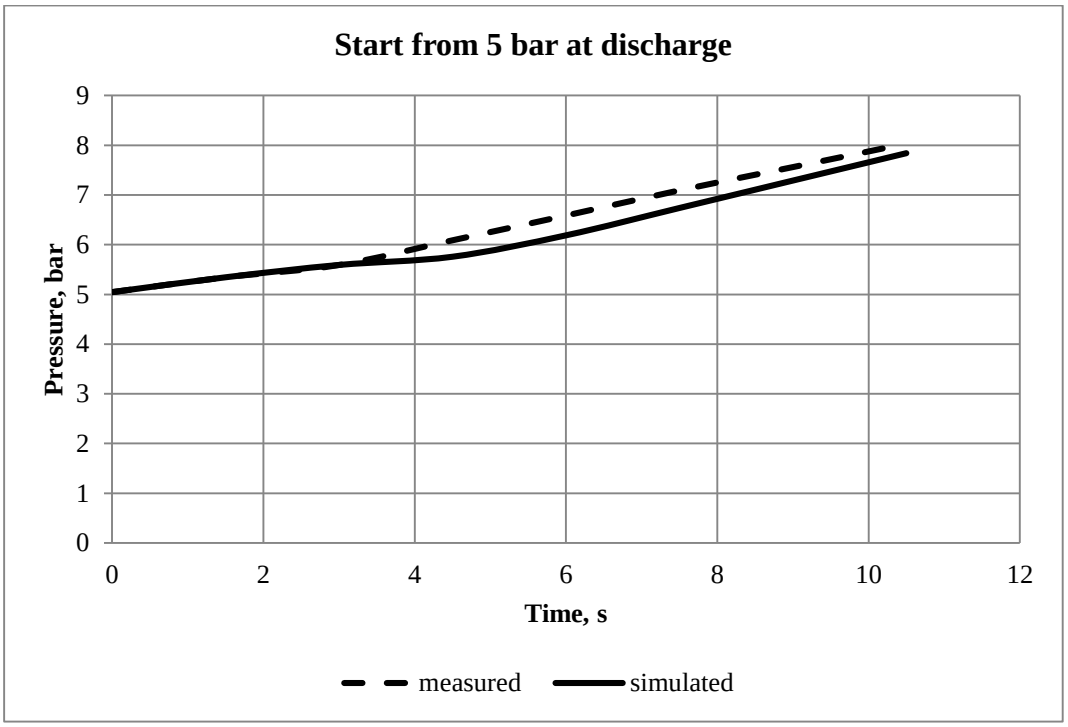

Figure 10: Measured and predicted rates of pressure rise in the tank during compressor startup when the starting pressure is 5 bar

This indicated that the model could be used to simulate the compressor startup and shutdown. The next step was to use this program to simulate some interesting situations during the startup as, for example, rapid change of shaft speed, and variation of pressure or change in the tank volume. This gave an insight into what happens to the system pressure immediately after the parameters are changed.

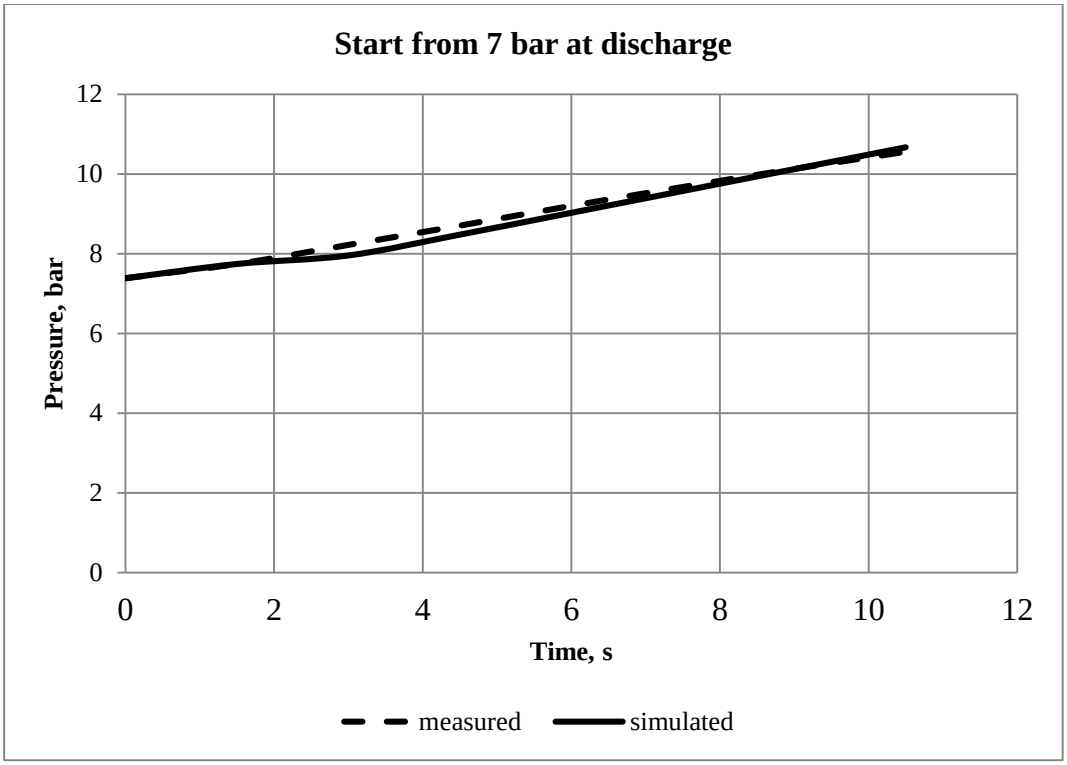

Figure 11: Measured and predicted rates of pressure rise in the tank during compressor startup when the starting pressure is 7 bar

6.2. Data Analysis

As already stated, the aim of these tests was to determine the behaviour of the compressor before oil injection started. It was expected that, during startup, the temperature would rise quickly before the oil enters the working chamber. This might result in damage to the rotor surfaces. Frequent start-stop operation may, therefore, lead to wear and a rapid decrease in the compressor performance.

It can be seen from Figure 12 that when the compressor started from atmospheric pressure, the temperature increases from 55 up to 100^{o}C and after 8 seconds it decreases to 90^{o}C due to the development of oil injection. It needed some time for the pressure to build-up in the oil reservoir and for oil to enter the compressor as a result of the pressure difference.

The situation is different when the compressor starts with its discharge pressure higher than the inlet pressure, as shown in Figure 13. In this case, when the compressor stops, oil flows into the compressor due to the pressure difference, but since the rotors are not revolving, the compressor will fill with oil. So, when it starts to rotate, again, the

oil within it will flow out through the compressor discharge port and the temperature will immediately decrease. Soon afterwards, it stabilises. However, as shown in Figure 12 and Figure 13 when the compressor stops at atmospheric discharge pressure, the discharge port is open and all the oil flows out of it. As a consequence, when the compressor starts, it contains no oil and there is no pressure difference to promote its flow. This period of dry contact between the rotors, can be reduced by closing both, the compressor suction and discharge during the start. When the compressor starts, a pressure difference develops immediately due to the pressure drop in the compressor suction.

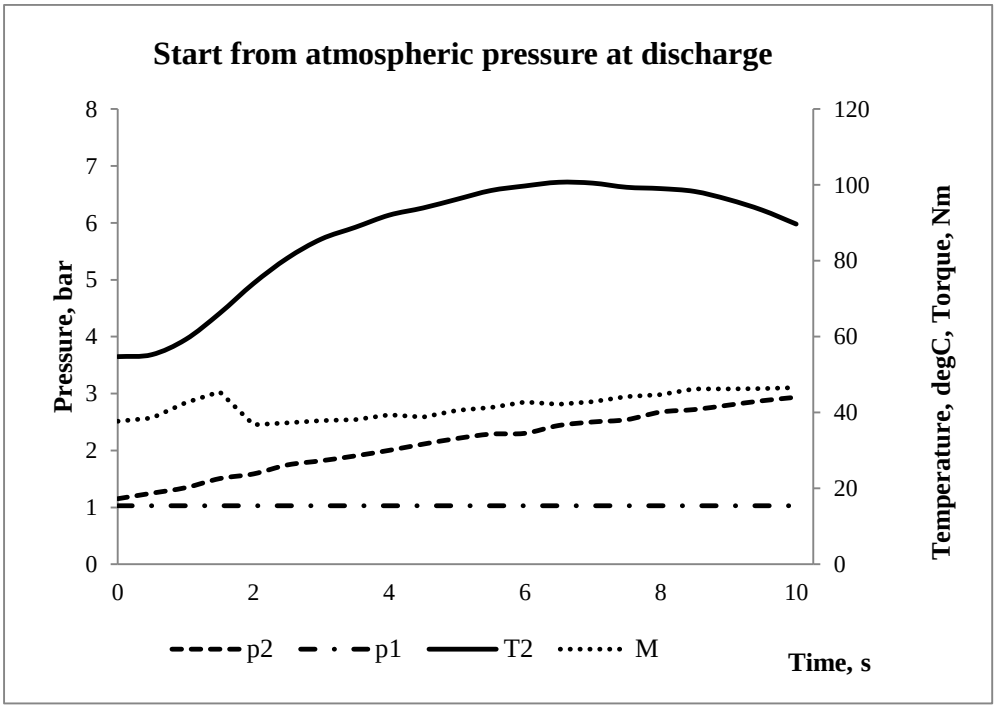

Figure 12: Oil-injected air compressor startup characteristics when discharging at atmospheric pressure

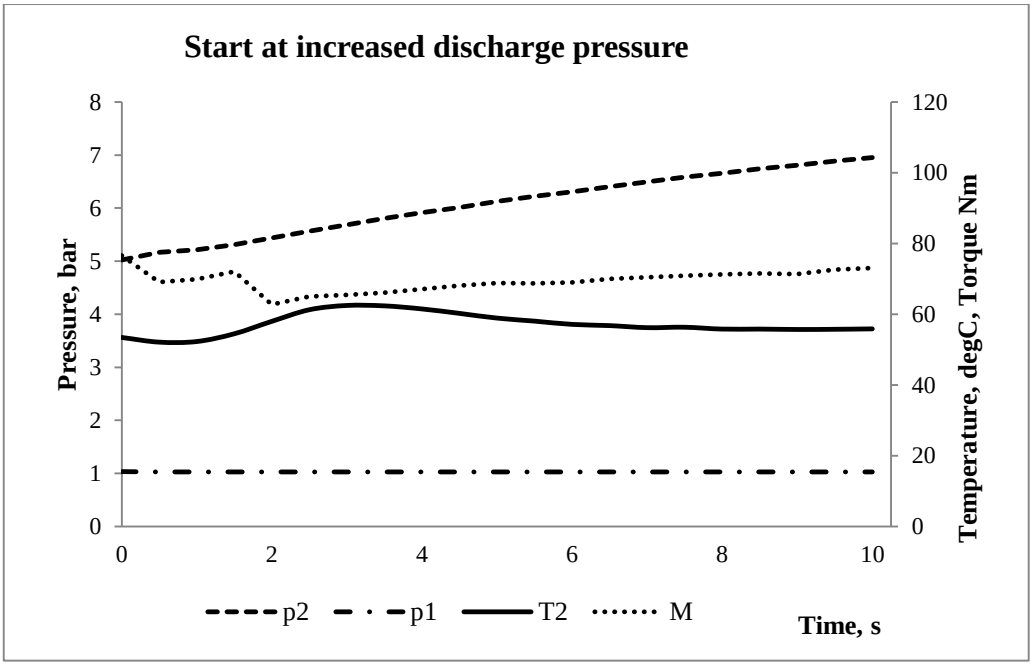

Figure 13: Oil-injected air compressor startup at increased discharge pressure. Decrease of torque between 1.7 and 2 s is due to the improved lubrication after the oil flow was established

The effect of closed suction is shown in Figure 14. This creates a significant temperature rise from 50°C up to 90°C in the first 2 seconds due to the high compressor pressure ratio caused by low suction pressure. When the pressure difference reaches the required level, oil flows in and the temperature decreases. The non-lubricated period is decreased from 8 seconds for an ordinary start, as shown in Figure 12, down to only 2 seconds when starting with closed suction. After a period of, 32 seconds, as shown in Figure 14, the suction was opened manually and the temperature rose again. The reason for this second temperature increase is that by opening the suction, the gas inflow was increased and the oil flow was insufficient to keep the air temperature at the same level. The temperature then increased during the next 2 seconds until the pressure difference built-up for enough oil to be injected. The second increase is less significant than the first, because the temperature only increased from 55°C up to 70°C during this phase.

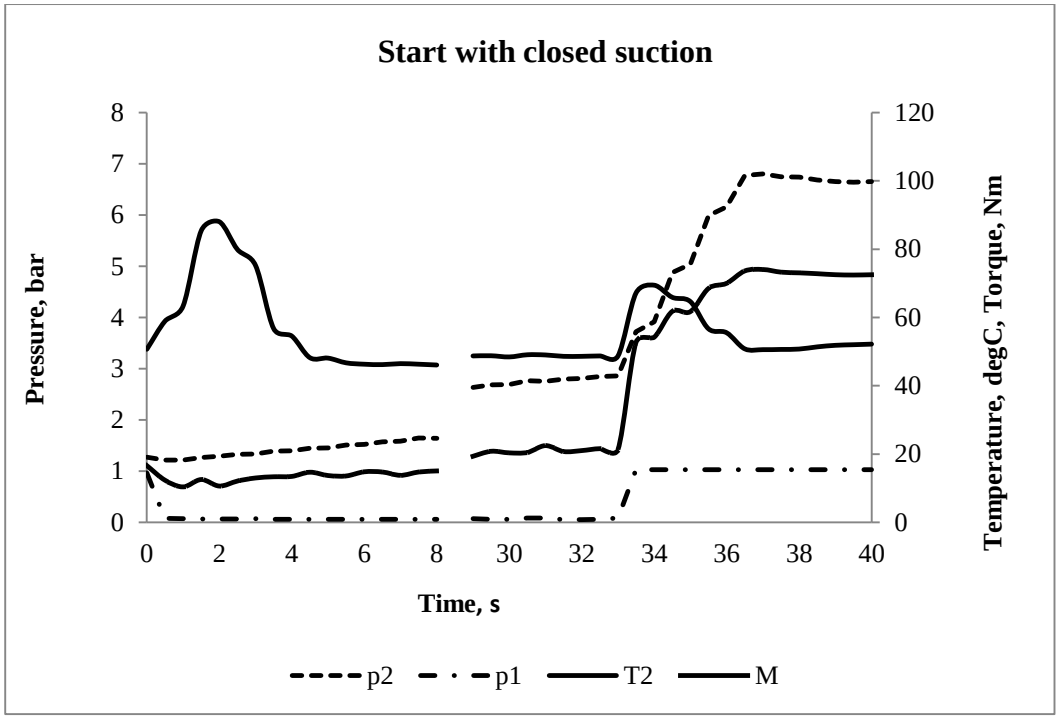

Figure 14**:** Oil-injected air compressor start with closed suction

There are other advantages to starting the compressor with closed suction because, as the compressor starts in this manner, the suction pressure decreases below atmospheric pressure and the air flow is almost zero. However, the discharge pressure will be equal to the atmospheric pressure, as in the case when the discharge is open. As can be seen in Figure 15, where the starting torque required is compared to the case shown in Figure 12, and that in Figure 14, it follows that due to the small pressure difference between inlet and discharge pressures, the peak torque is approximately one third lower than during start with open suction, while the starting torque is approximately four times less. As a consequence, this will result in a safer start, lower power consumption and, less noise. This procedure is applied by many screw compressor manufactures.

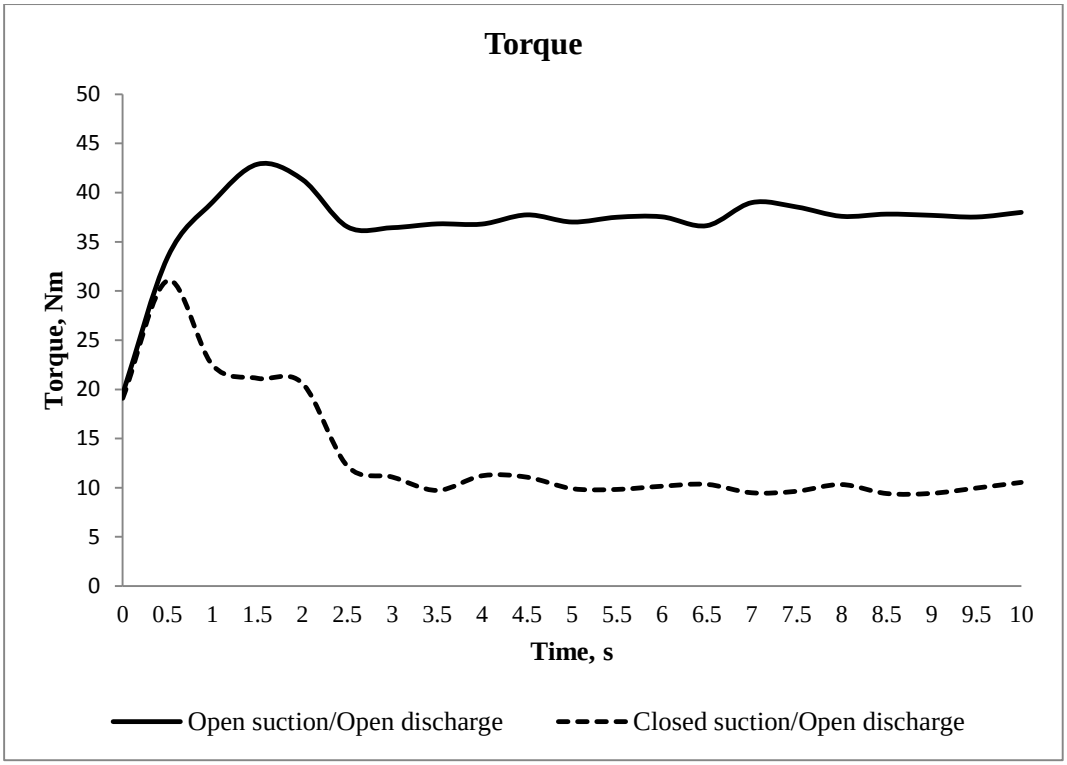

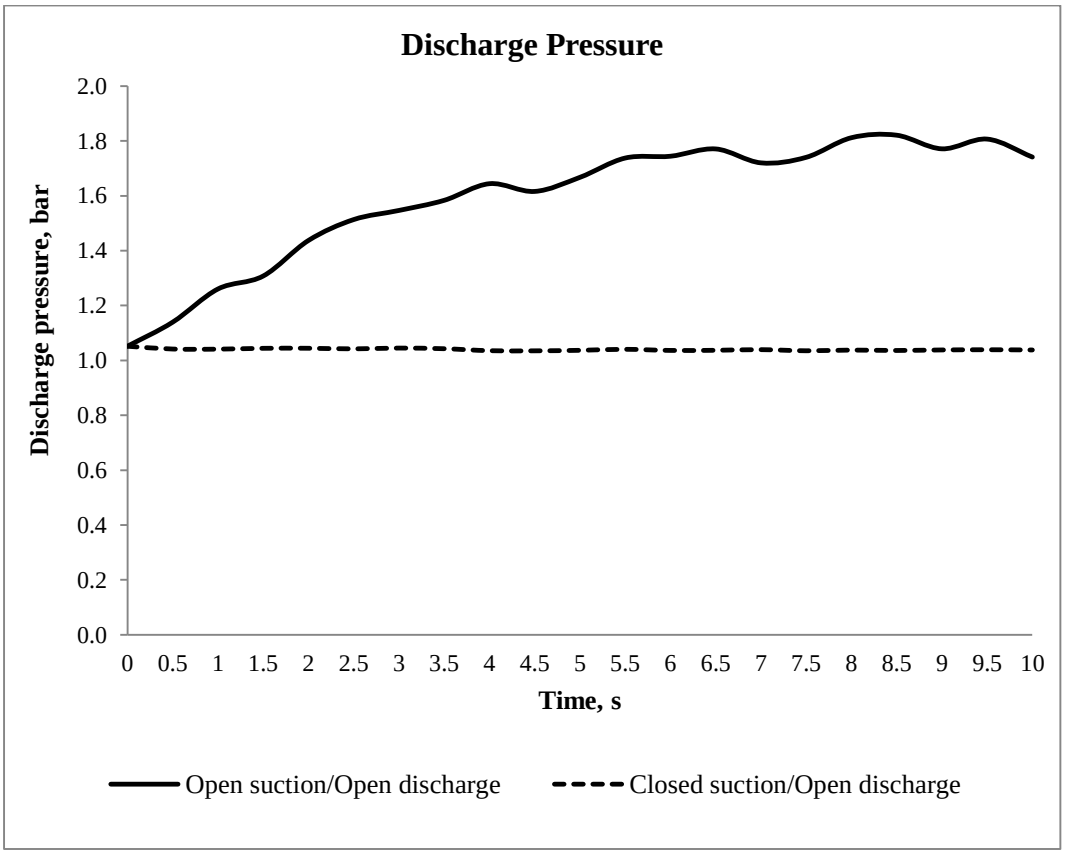

Figure 15: Comparison of startup with open and closed suction for oil-injected air compressor, Upper graph shows Torque, Lower graph shows discharge pressure

It was found, from further startup tests with closed suction, that it took a longer time to reach 3000rpm as the discharge pressure was increased, as shown in Figure 16 and Figure 17. It is clear that the slowest start and the lowest acceleration were achieved at 7 bar discharge, which was the highest pressure achieved. It was not possible to start the compressor at discharge pressures above this value, due to limitation of the motor current.

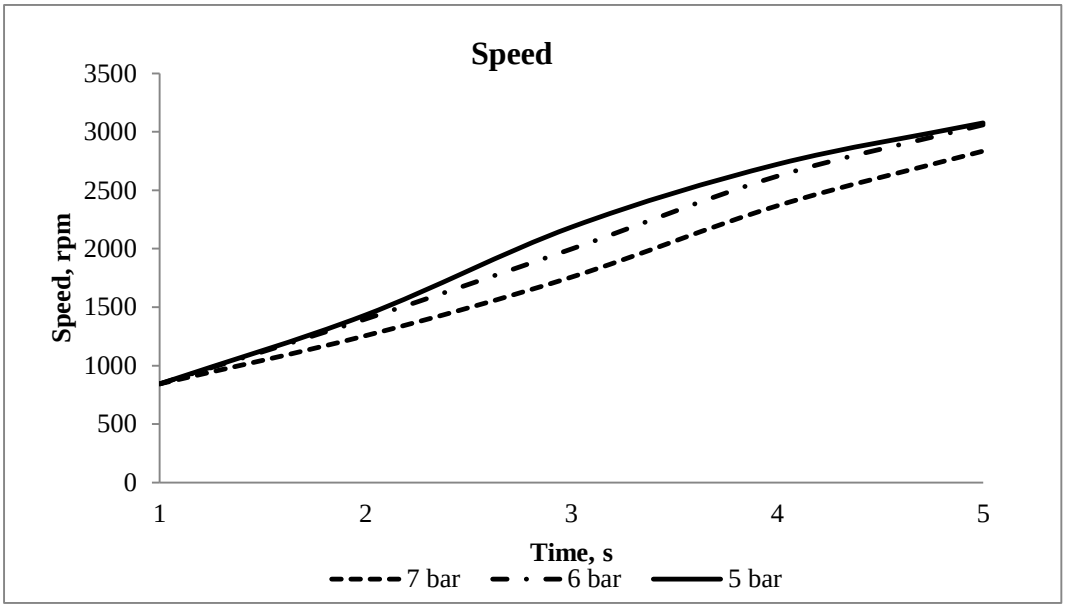

Figure 16: Startup times for oil-injected air compressor at different discharge pressures, for clarity, the same starting point is assumed fo all cases

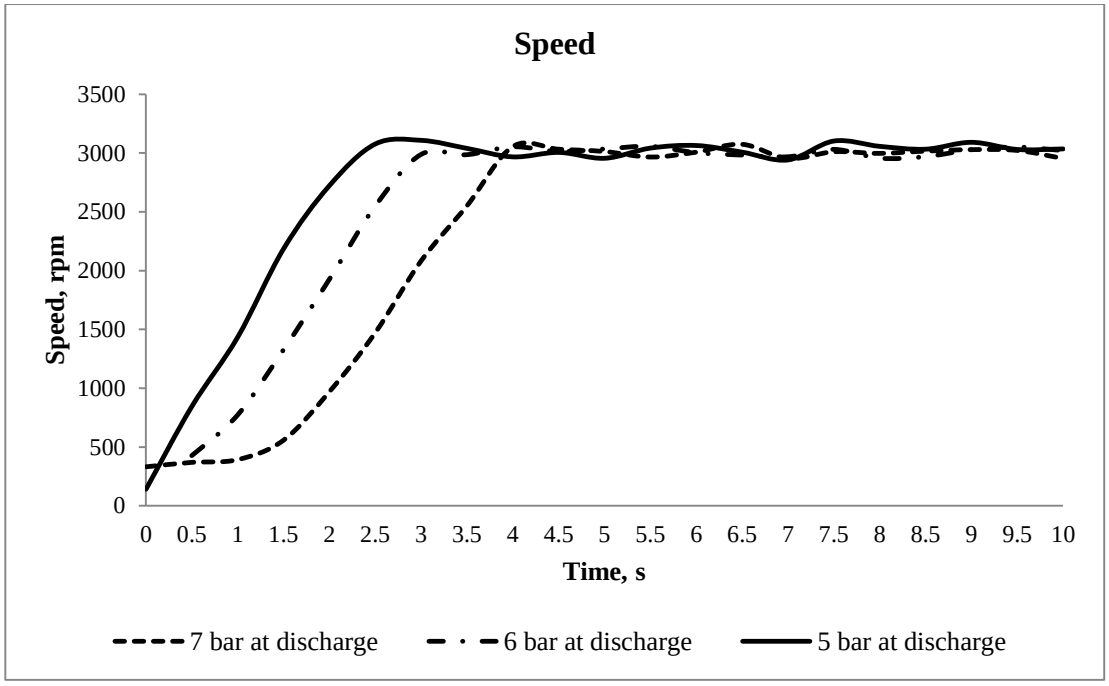

Figure 17: Startup times for oil-injected air compressor at different discharge pressures

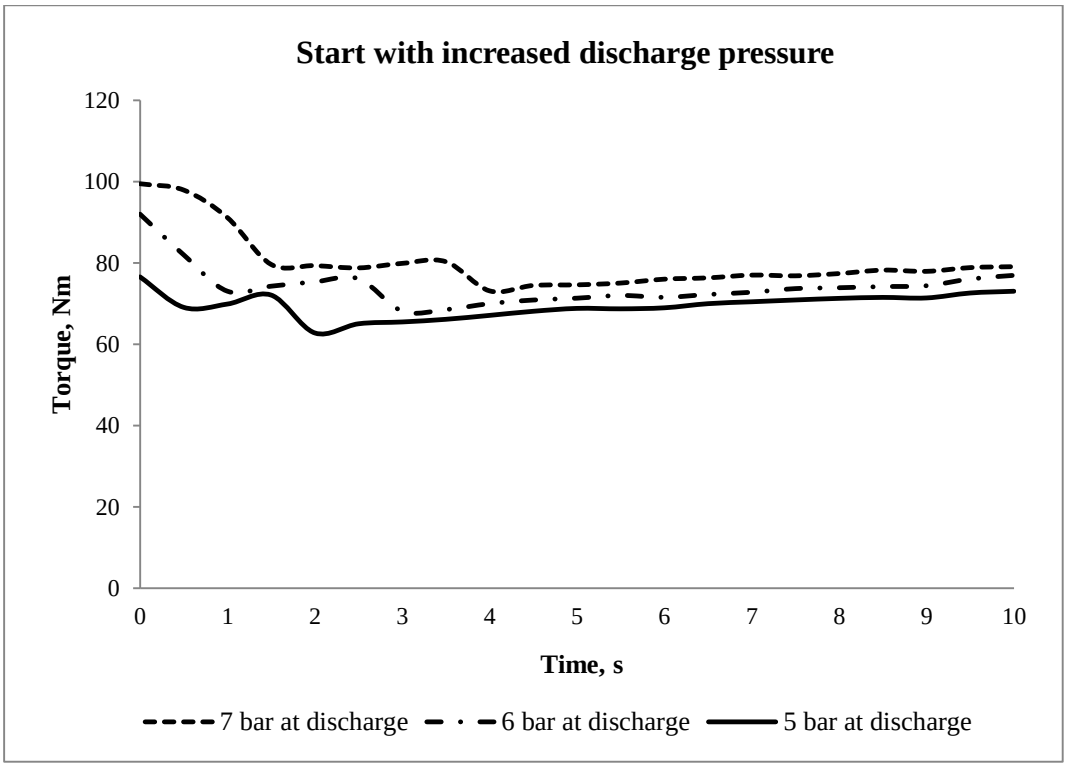

Figure 18: Startup torque variation with discharge pressure for oil-injected air compressor

As shown in Figure 18, the torque variation, during startup, follows a similar trend, with the demand increasing as the discharge pressure is raised with the initial value,

at rest, falling. However, as shown in, there is a reversal in the trend of the startup discharge pressure, which rises, immediately at 5 bar, but which falls initially at 6 bar and 7 bar, before starting to rise.

This follows because the internal discharge pressure of compressor is 4.7 bar but the pressure in the pipe was measured straight after the discharge and is shown in Figure 19. Accordingly, as soon as compressor started running and the discharge port was opened, there was a pressure drop when the pressure in the pipe was 6 and 7 bar. However, when pressure in the pipe was 5 bar, it started to increase immediately.

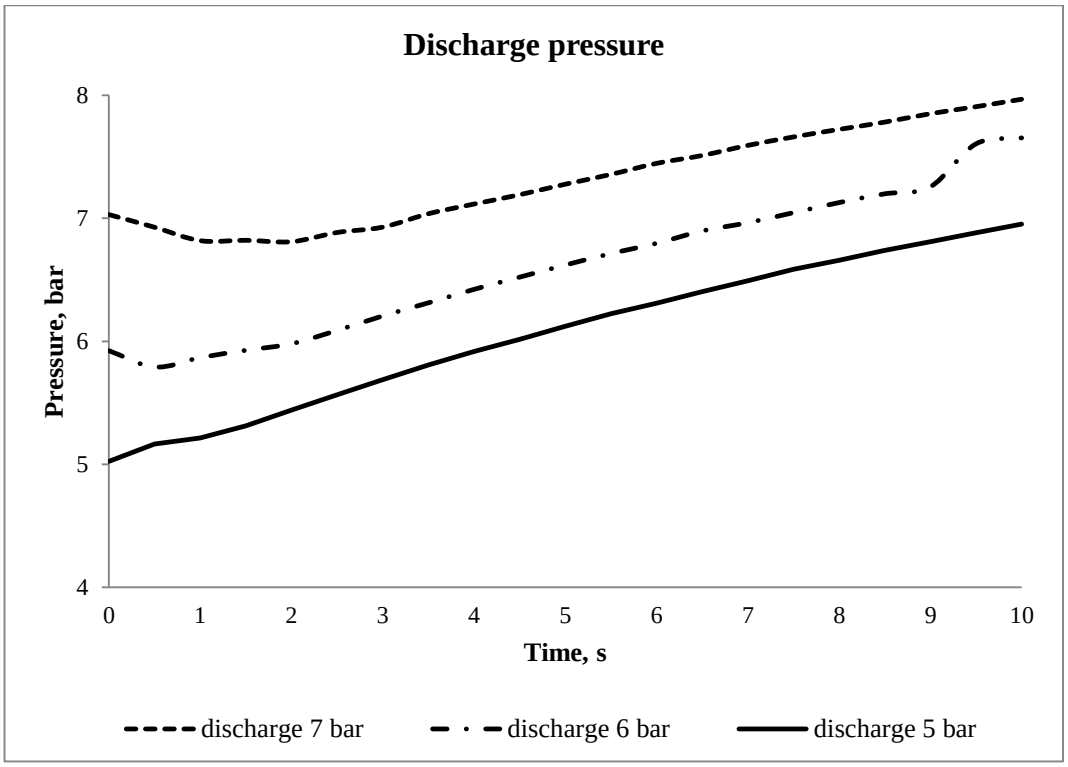

Figure 19: Discharge pressure curves for oil-injected air compressor startups at different pressures

6.3. Torque Classification and Moment of Inertia Quantification

The thermodynamic process, the pressure forces acting on the rotors and the shaft torque were all estimated using DISCO, the proprietary software package for the analysis of screw compressor performance, prepared in house, of which some details are already given in Chapter 5. This was written to predict compressor behaviour

during steady state operation, but was used here, in a sequence of calculations, to derive values at each discreet time, and thus, to simulate unsteady behaviour and to quantify inertial effects during the compressor startup.

The simulation results obtained from the thermodynamic model are different to those obtained from the test data, as shown in Figure 20 for the case of the compressor starting at a discharge pressure of 7 bar.

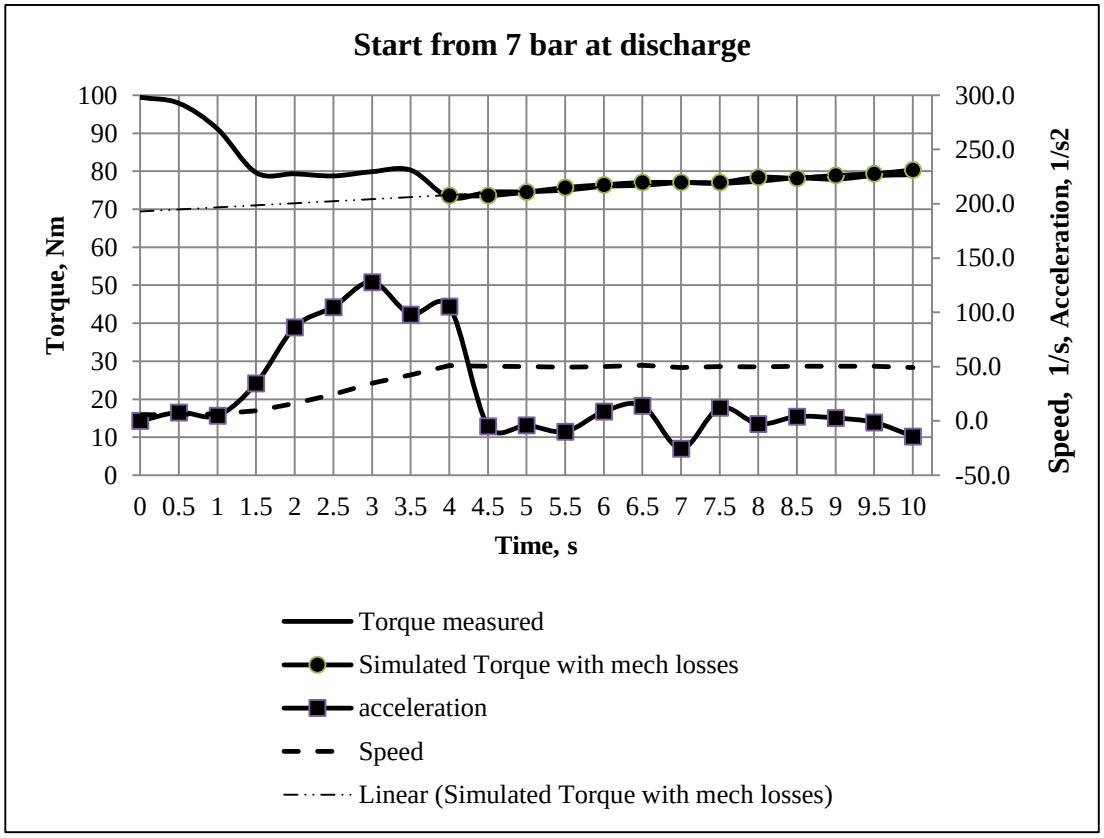

Figure 20: Comparison between simulated and measured Speed and Torque changes for oil-injected air compressor at a discharge pressure of 7 bar

The difference between the simulated torque, with mechanical losses taken into account, as extrapolated, and the measured values, during the first 4 seconds can be explained as due to rotor inertia in the period between 0.5s and 4s and the increased friction torque in the period between 0s and 0.5s. The simulation did not function at speeds below 1000 rpm.

Diagrams for the compressor starting at both atmospheric pressure and increased pressure at discharge are presented in Figure 21 and 22.

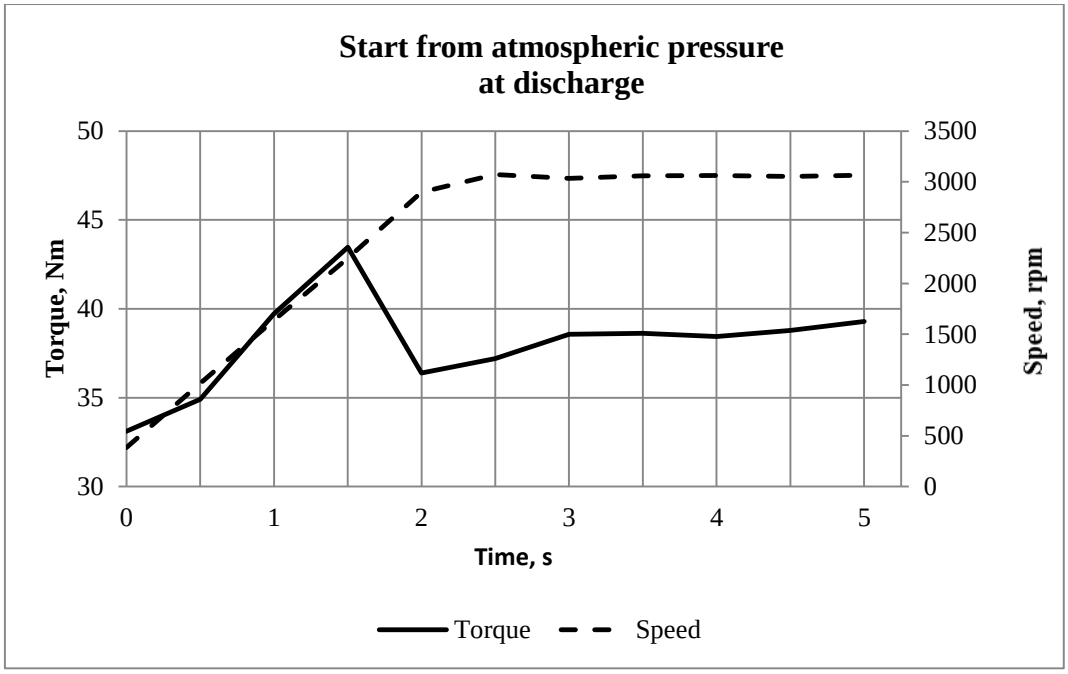

Figure 21: Starting torque diagrams for an oil-injected air compressor discharging at atmospheric pressure

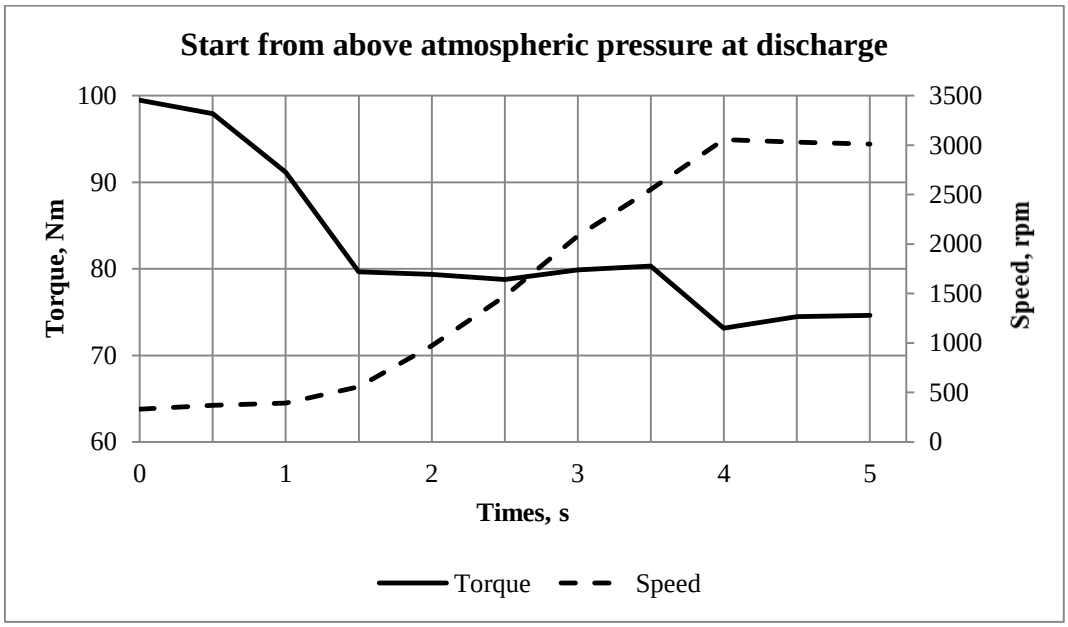

Figure 22: Starting torque diagrams for an oil-injected air compressor discharging at above atmospheric pressure

Pressure torque could be estimated by the DISCO software and friction torque can be estimated from the assumed mechanical efficiency but inertia torque can only be derived from the difference between the measured and predicted values.

A qualitative analysis of starting torque curves, based on Figure 21 and Figure 22 is given below, where the torque curves were analysed assuming the following:

Total torque = Pressure torque plus Friction torque plus Inertial torque

Table 4: Torque effects during oil-injected air compressor startup

	Start from Atmospheric Pressure at Discharge	**Start from Increased Pressure at Discharge**
Pressure Torque	Pressure torque increases constantly until maximum discharge pressure is achieved.	Pressure torque is high since compressor starts rotating. Pressure forces, which affect torque, might be even higher in the first fraction of a second since compressor is full of oil during high pressure start.
Friction Torque	Inertia of moving parts affects total torque at the very beginning.	Inertia of moving parts affects total torque at the very beginning. Again, as compressor is flooded with oil, friction torque may also increase.
Inertia Torque	Inertia forces act while compressor accelerates and inertia torque tends to zero when 3000 rpm is achieved, torque drops after 2 seconds on diagram.	Since compressor overcomes friction, torque drops after 1.5s on the diagram, and machine starts accelerating, inertia forces affect total torque. Inertia torque tends to zero after compressor achieves 3000 rpm, torque drop between 3.5s and 4s.

7. Screw Compressor Plant Model Validation

Following the initial tests on the transient behaviour of screw compressor systems, the development of a software simulation model and initial comparisons between measured and predicted system performance, this chapter contains a fuller comparison between them. As was described in Chapter 4, both oil-free and oil-injected air compressor plants were modelled and measured. Plant parameters, such as compressor speed and starting pressure and temperature were used as initial conditions for simulation studies. When the working fluid was assumed to be an ideal gas, one full set of 300-800s of real compressor operating time required 5-10 minutes of computer calculation time, using a PC with an Intel Core2 Duo CPU 2.33GHz, with 4 GB of RAM. When the working fluid was assumed to be a real gas the calculation time took eight to ten times longer.

7.1. Oil-injected compressor

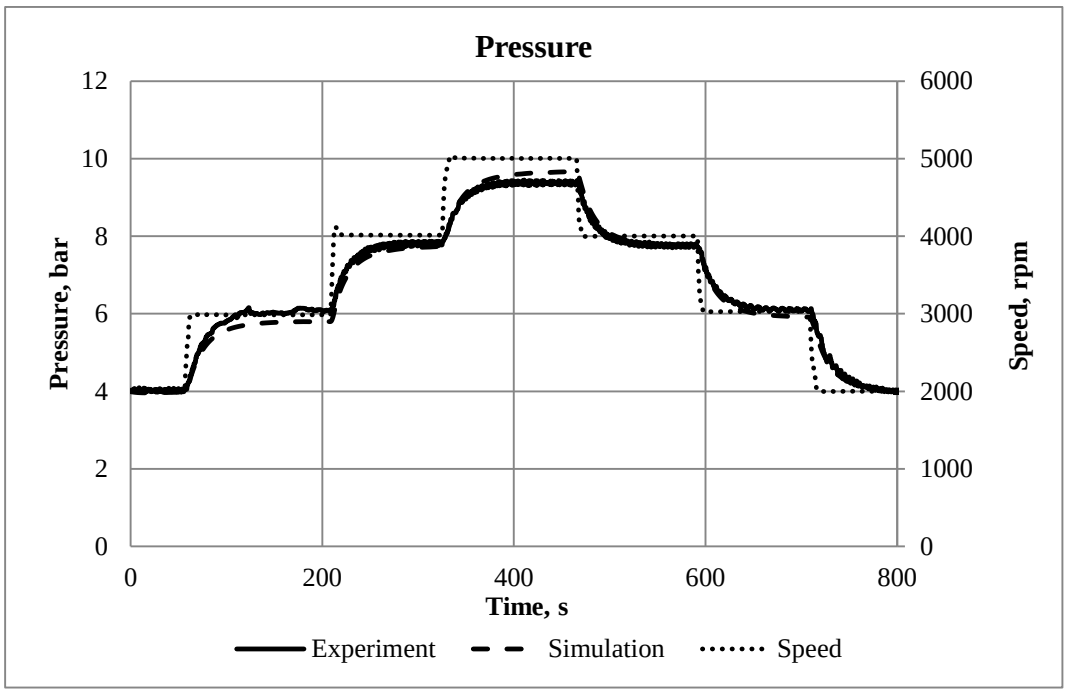

Figure 23: Comparison of estimated and measured pressure changes in oil-injected air screw compressor plant. Differences < 5%

During the experiment the compressor speed was varied from 2000 up to 5000 rpm, and back, in step changes of 1000 rpm, each within a time interval of 60 seconds, which was sufficient time for the pressure to stabilise after the speed was changed.

Variation of the main parameters with time is presented in following diagrams and shows good agreement between experimental and simulated results.

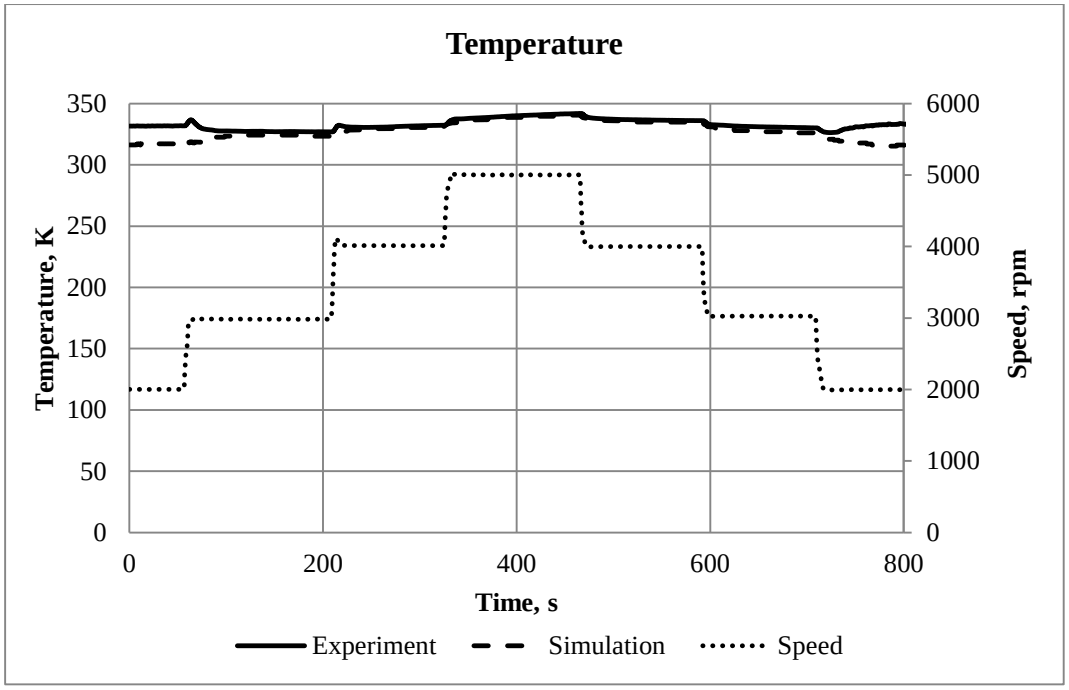

Figure 24: Comparison of estimated and measured temperature changes in oil-injected air screw compressor plant. Differences < 5%

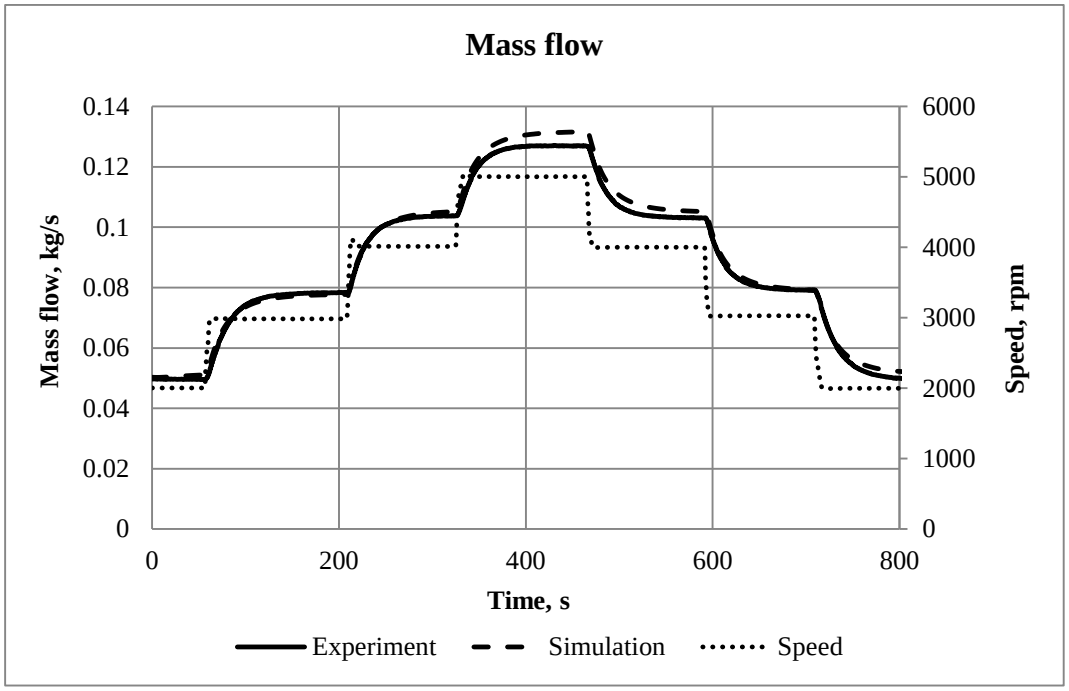

Figure 25: Comparison of estimated and measured mass flow rate changes in oil-injected air screw compressor plant. Differences < 5%

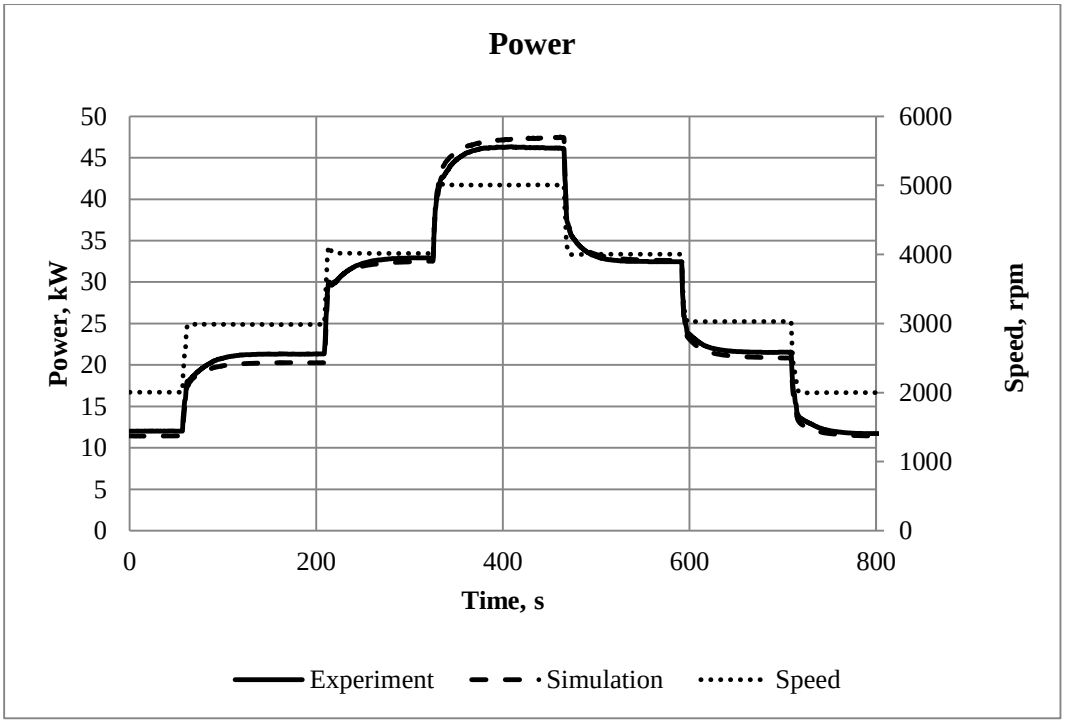

Figure 26: Comparison of estimated and measured input power changes in oil-injected air screw compressor plant. Differences < 5%

A comparison between the measured and simulated performance of an oil-injected compressor plant is shown in Figure 23 to 26, when increasing and decreasing the rotational speed between 2000 rpm and 5000 rpm. The difference between the measured and predicted values of pressure, mass flow, power and temperature, are less than 5% of the absolute values, in all cases. This indicates the basic suitability of the predictive model for further development The greatest discrepancy was in the estimated and measured temperature at a rotational speed of 2000 rpm, when the difference was approximately 15ºC. A possible reason for this is the low compressor speed. This strongly affects leakage and could therefore have a substantial influence on the temperature.

A further case is demonstrated in Figure 27 to 30, where the compressor speed was increased directly from 3000 rpm to 5000 rpm and back. Even better agreement was obtained for the same parameters in this case.

.

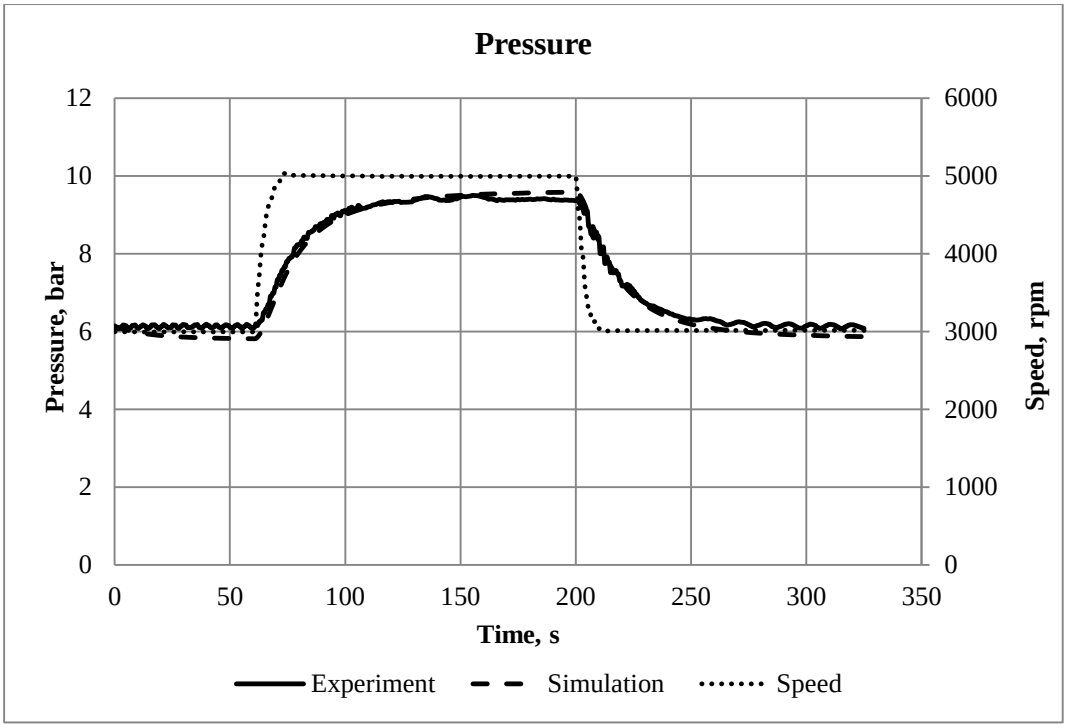

Figure 27: Comparison of estimated and measured pressure changes in oil-injected air screw compressor plant. Differences < 5%

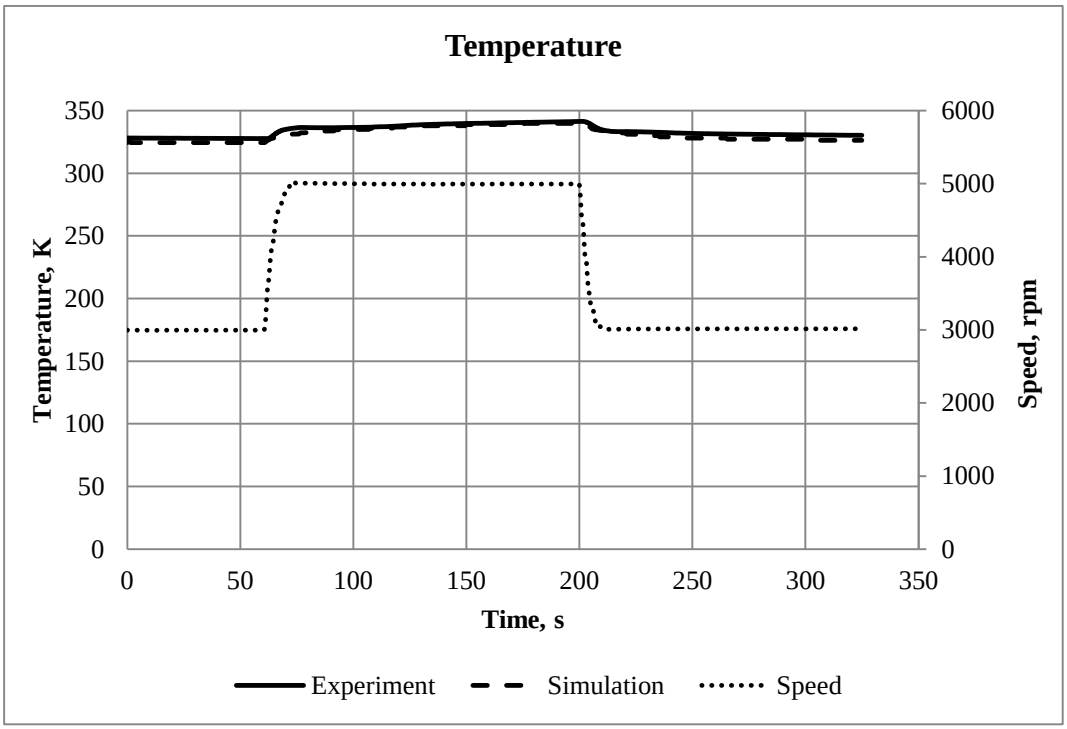

Figure 28: Comparison of estimated and measured temperature changes in oil-injected air screw compressor plant. Differences < 5%

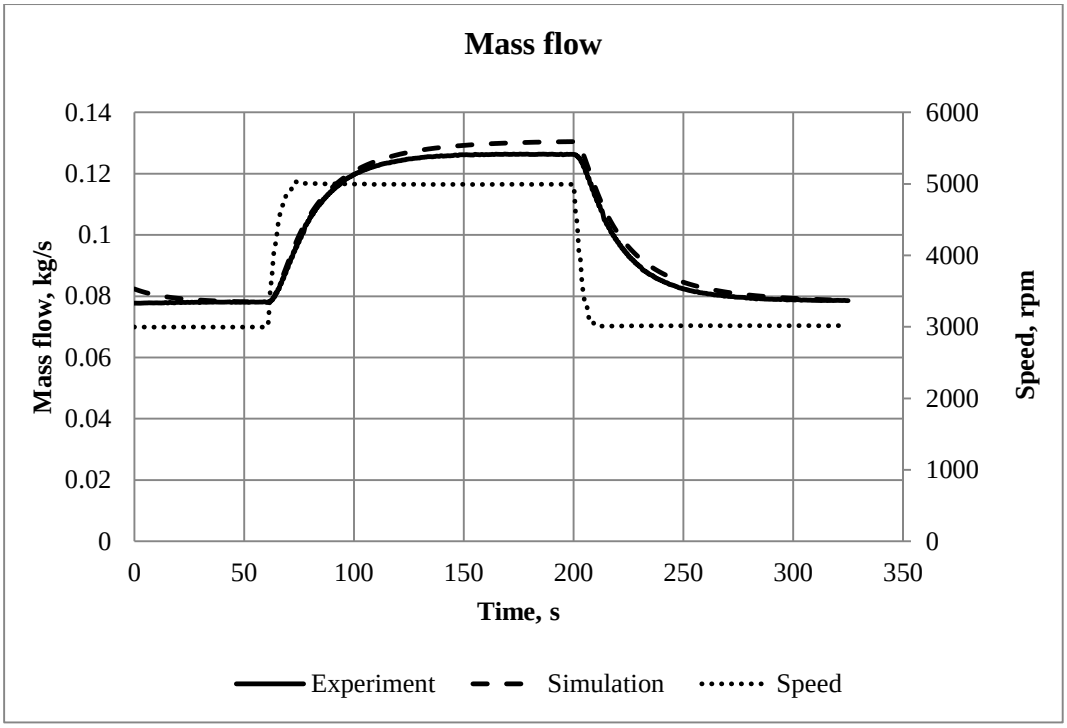

Figure 29: Comparison of estimated and measured mass flow rate changes in oil-injected air screw compressor plant. Differences < 5%

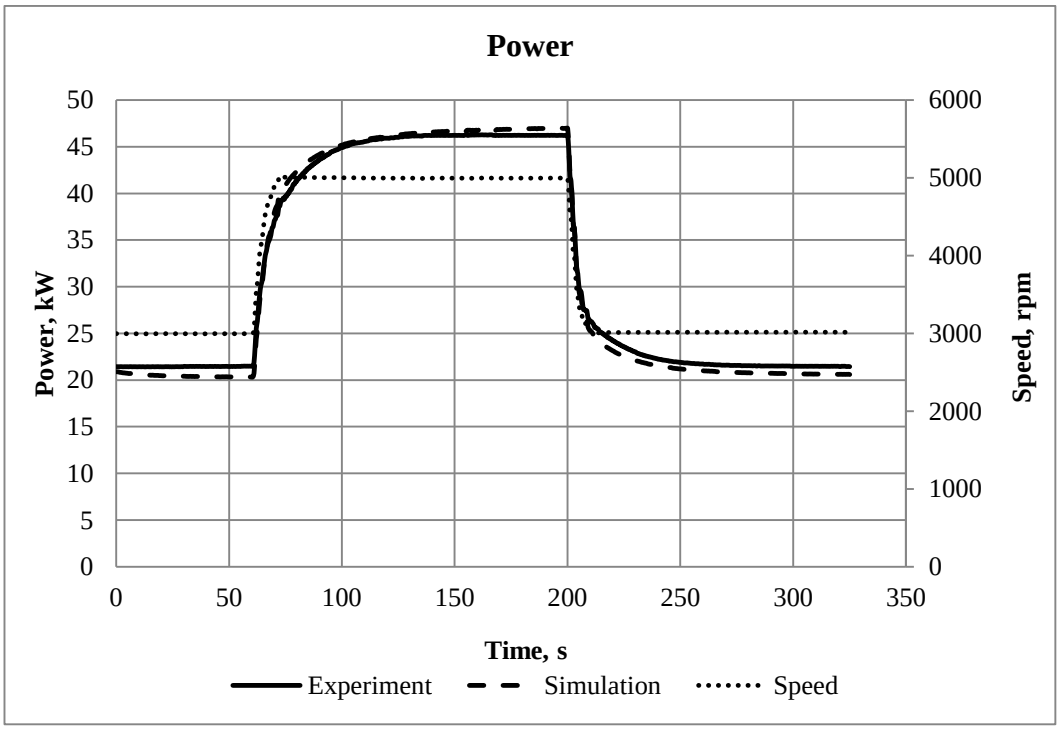

Figure 30: Comparison of estimated and measured input power changes in oil-injected air screw compressor plant. Differences < 5%

7.2. Oil-Free Compressor

A comparison between the measured and predicted performance of an oil-free air screw compressor plant is shown in Figure 31 to Figure 34. The compressor speed was chosen as a variable parameter for transient analysis and it was varied from 3000 rpm up to 9000 rpm and then back in steps of 2000 rpm and time intervals of approximately 30 seconds. This was sufficient time for the pressure to stabilise after the speed was changed. As can be seen, the pressure in the oil-free compressor changed almost immediately after the speed was changed, while the pressure in the oil-injected changed gradually. The lag in Figure 23, may be due to the oil thickness which creates some inertia effect.

All the parameters shown in Figure 31 to Figure 34 are within acceptable 5% difference of their absolute values, although the temperature discrepancy shown in Figure 32, is present again, as in the case of the oil-injected machine.

It can be seen from Figure 32, that the calculated values of temperature are 'symmetric', i.e. the acceleration and deceleration values are similar after some time spent at a given speed. However, the experimental air temperature values are higher for deceleration than for acceleration, because it is necessary to heat the tank and pipes up during acceleration. This requires time, therefore, the air is cooled during that process and it will show a lower temperature than it would be if there were` no heat transfer between the air and the pipes. During deceleration however, the higher temperature of the recently heated pipes causes the air to be heated up during that process and thus it shows higher temperature values if compared with acceleration. This confirms, once again, that the model is working properly and can be used by other investigators.

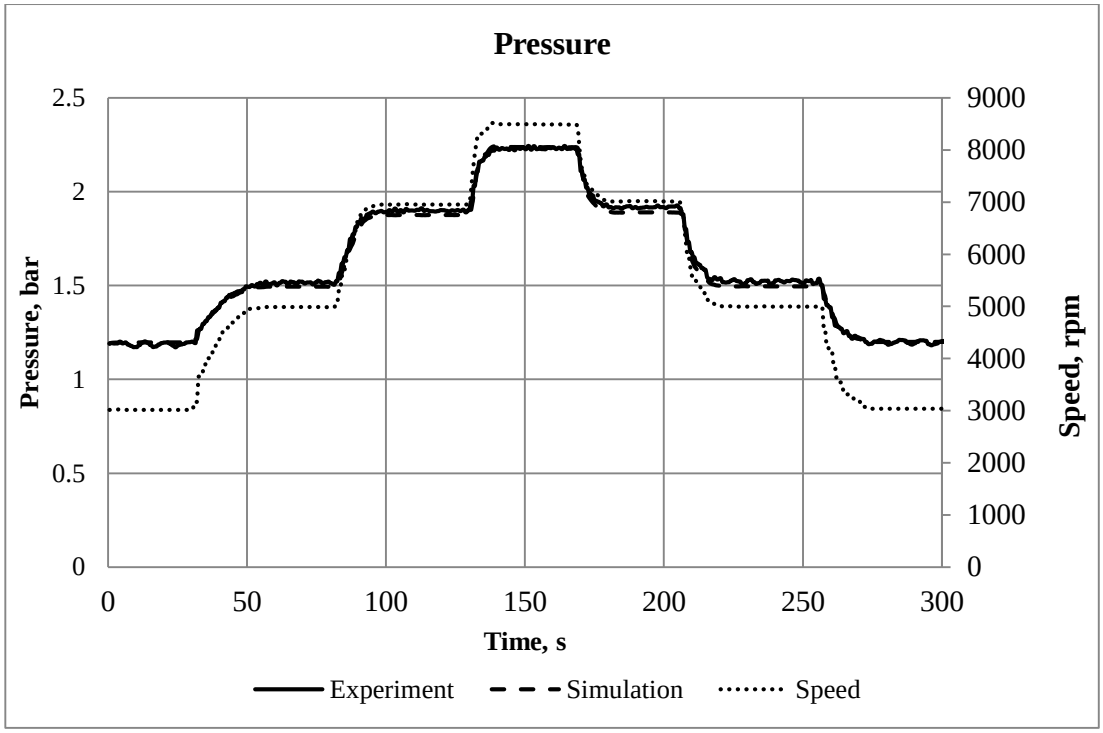

Figure 31: Comparison of estimated and measured pressure changes in oil free air screw compressor plant. Differences < 5%

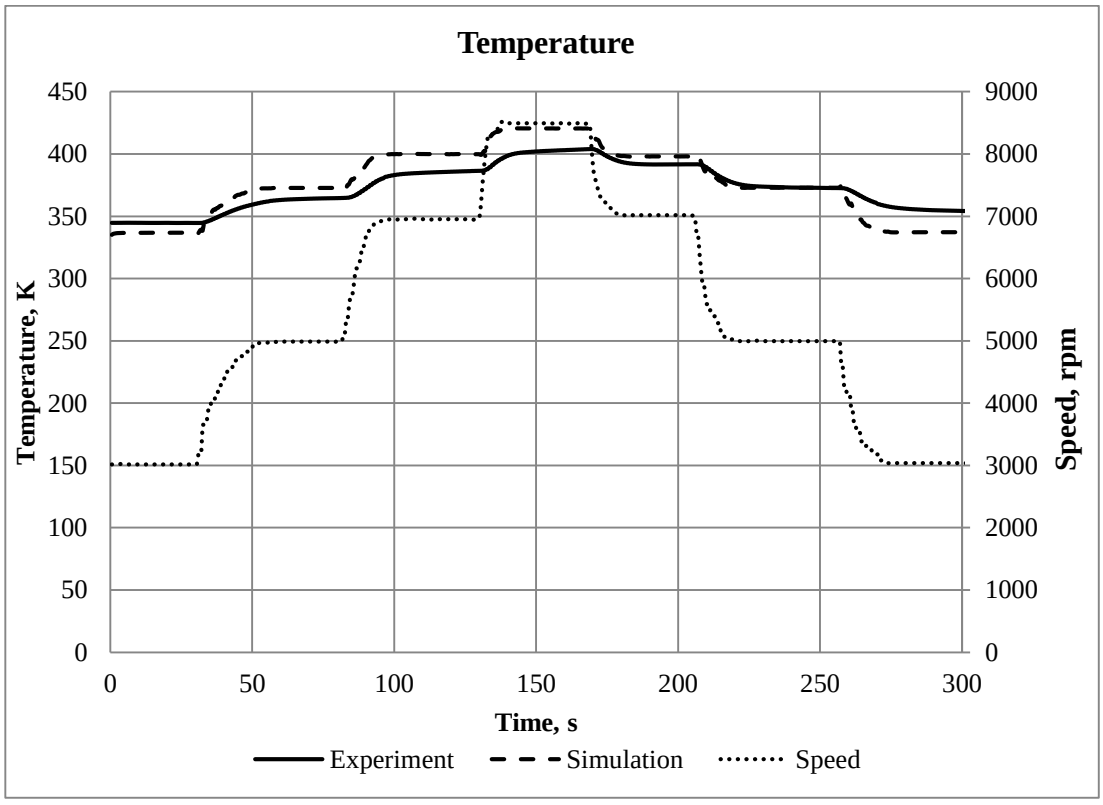

Figure 32: Comparison of estimated and measured temperature changes in oil free air screw compressor plant. Differences < 5%

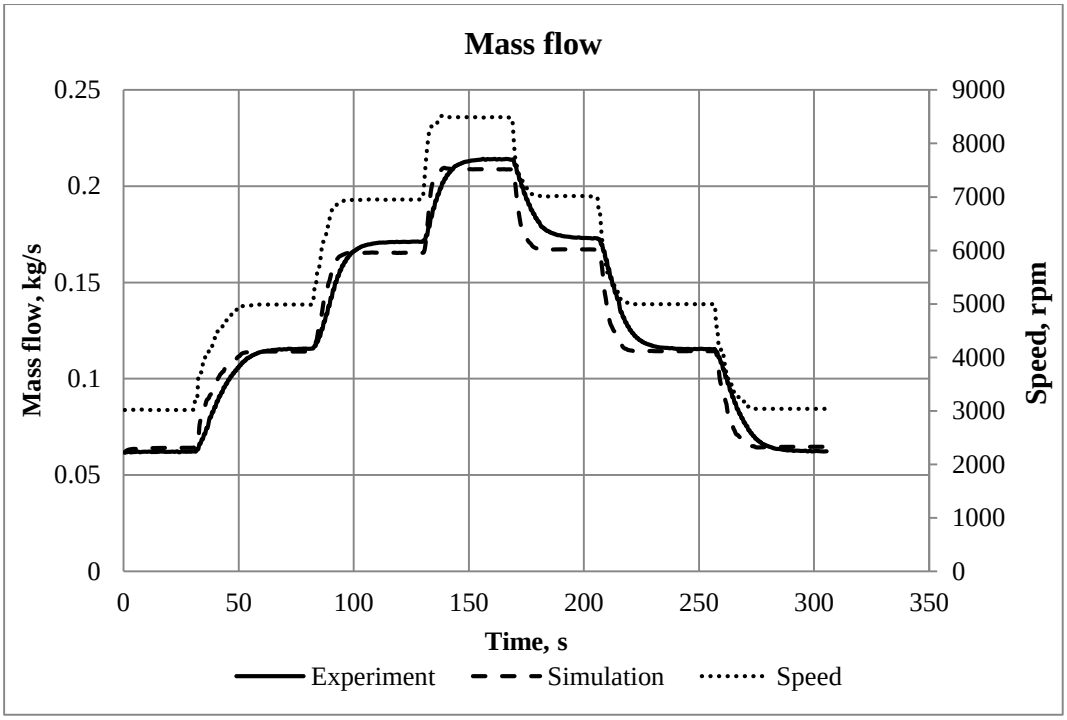

Figure 33: Comparison of estimated and measured mass flow changes in oil free air screw compressor plant. Differences < 5%

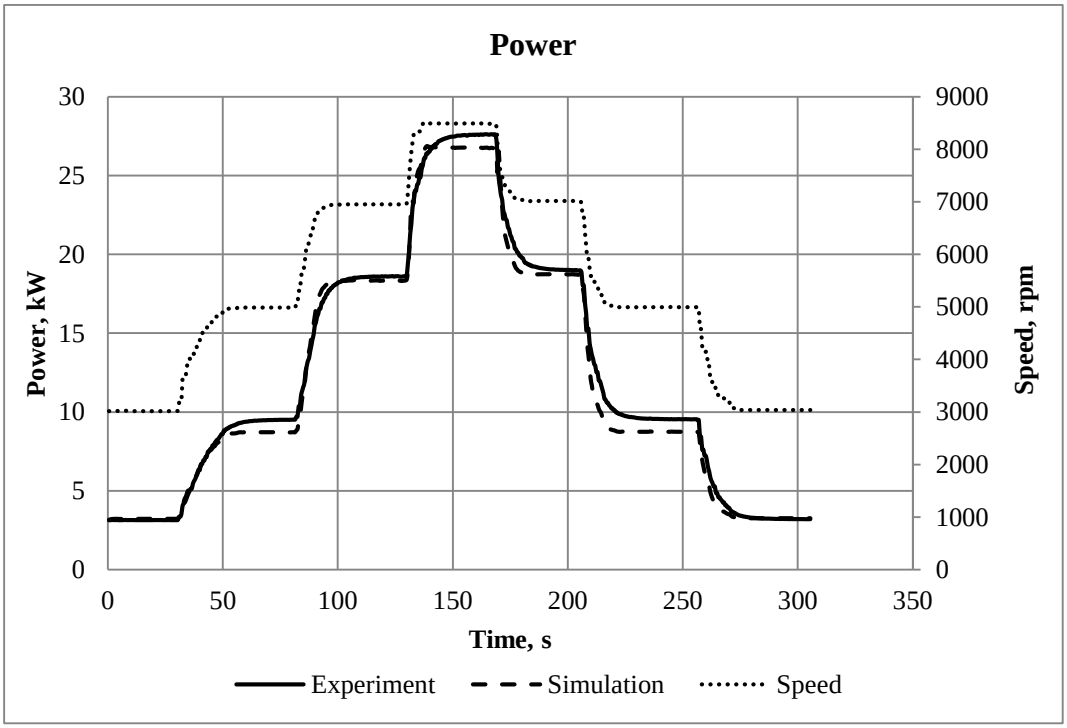

Figure 34: Comparison of estimated and measured power input changes in oil free air screw compressor plant. Differences < 5%

8. Screw Compressor Plant Simulation Cases

As stated in Chapter 3, the aims of this research included the derivation of a simulation model to predict the effects of changes of design parameters on both the final steady state and transient operating conditions of a complete compressor system Examples are given of how the developed software was used to predict the final steady state conditions and response time of a complete system as a result of changes in pressure, tank volume and, valve area. This is followed by the effects of sudden changes in valve area and speed.

8.1. The Effects of Plant Parameter Variation in Oil-Injected Air Screw Compressor Systems on Response times and Final Steady Flow Conditions

The first simulations were carried out on air oil-injected screw compressor plant by varying such parameters as valve area, tank volume and tank pressure. All other parameters were maintained constant with time. Answers to such questions as "what happens if..."could then be obtained from them.

8.1.1. Variation of Valve Area

From the diagrams on Figure 35 it can be seen how pressure and temperature change for different valve areas. For example, with the valve closed, the pressure in the tank reaches 33 bar in less than 2 minutes and the air temperature increases from 350K (77°C) to 450K (177°C) in just 10 seconds. If the valve is slightly open, the air temperature reaches its peak of 400-450K in 10 seconds and then stabilises together with the tank pressure. Actually, controlling the valve area is a means of influencing the pipe discharge pressure.

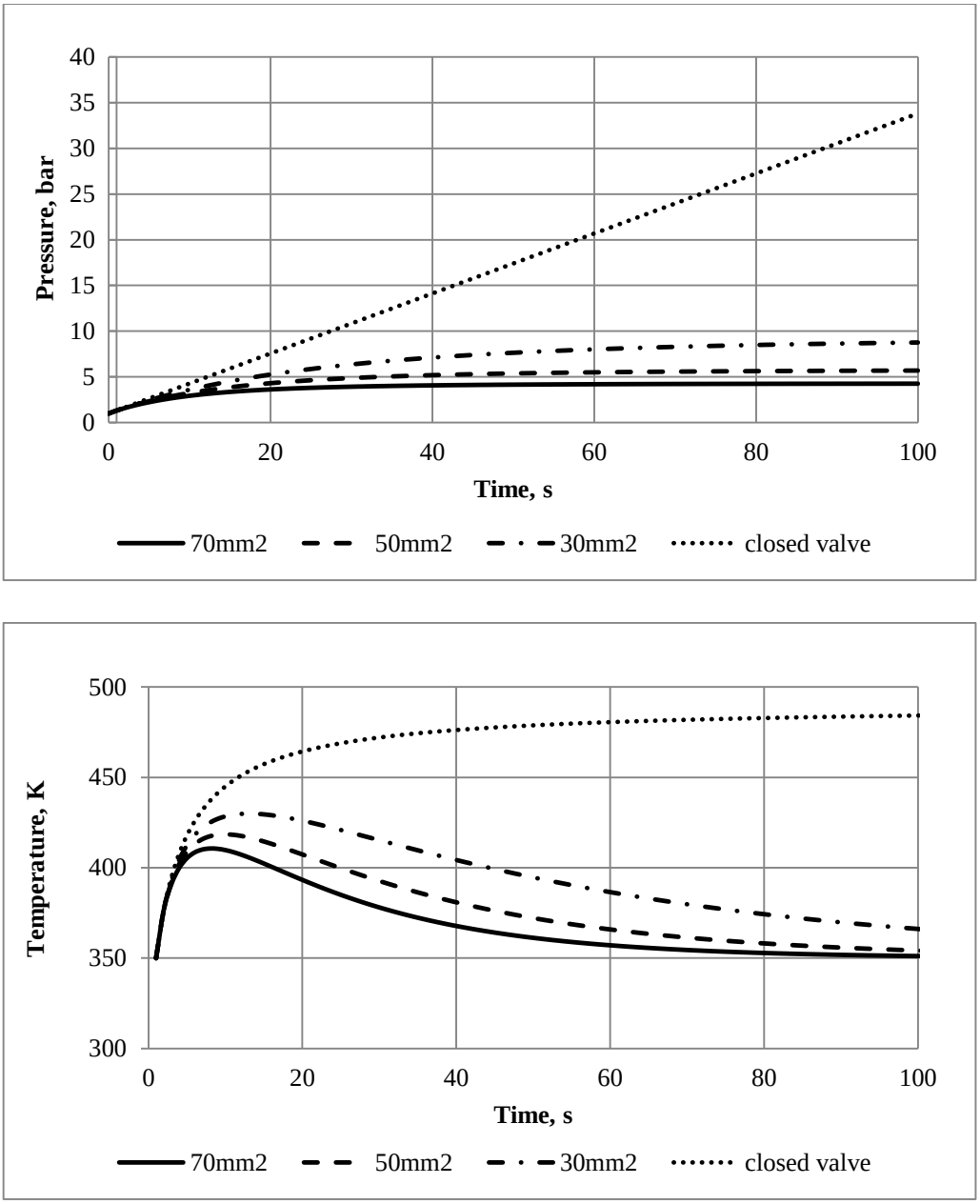

Figure 35: The effect of varying the valve area in an oil-injected air screw compressor plant. The upper graph shows the Tank Pressure, and the lower graph shows the Temperature

8.1.2. Varying the Tank Volume

It is evident from the diagram in Figure 36 that, for a given throttle valve area, the final discharge pressure will be independent of the tank volume and changes in the latter will only affect the time required to reach steady stage conditions. Thus with a

30 litre tanks steady conditions are attained in 2 seconds, but for a 600 litre tank the time taken is about 2 minutes. A similar situation happens with the temperature: when its peak value of 420-450K is attained more rapidly with a smaller volume, before returnings to the initial value of 350K.

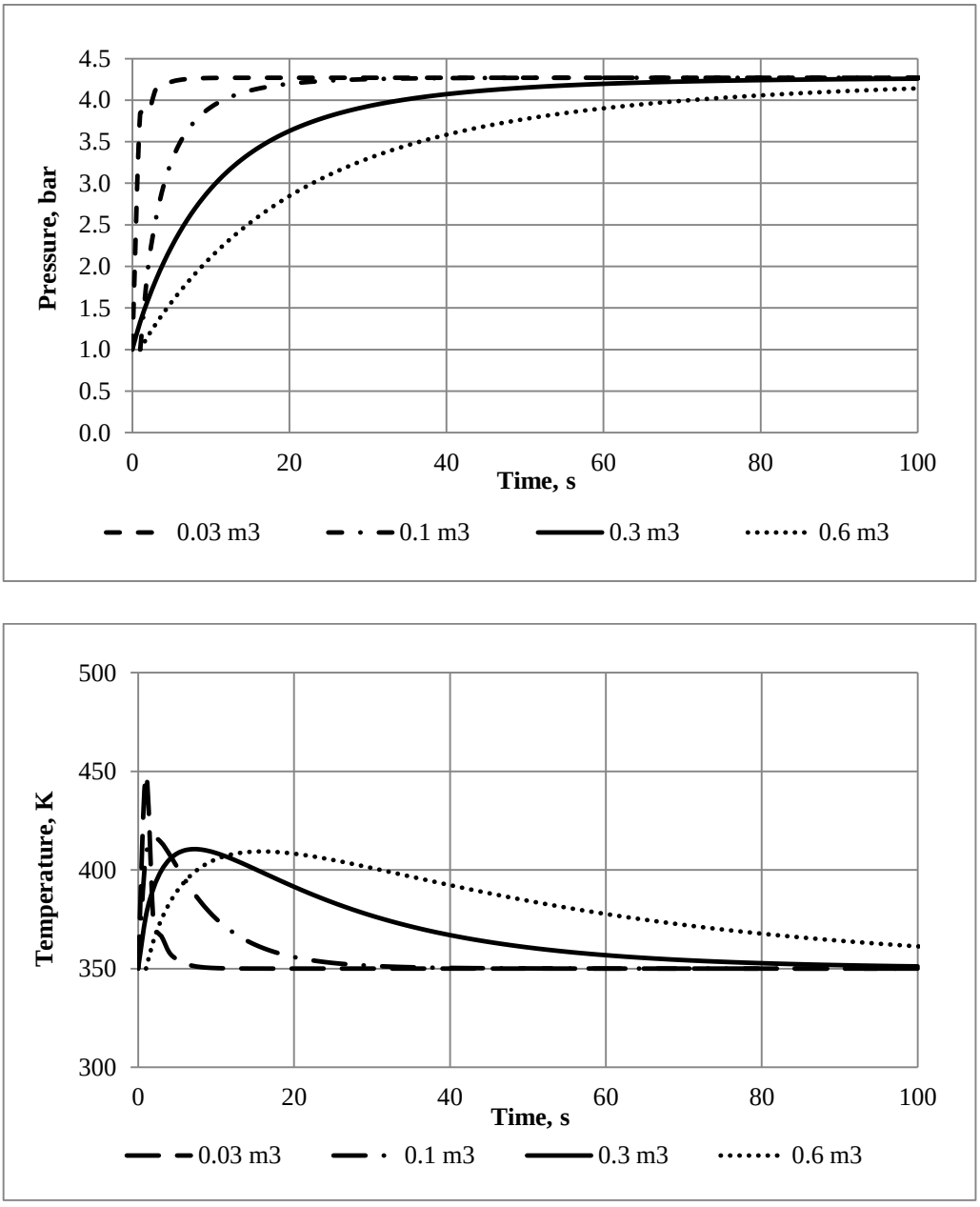

Figure 36: The effect of varying the tank volume in an oil-injected air screw compressor plant. The upper graph shows the Tank Pressure, and the lower graph shows the Temperature

8.1.3. Varying the Tank Pressure

As shown in Figure 37, regardless of its initial value, the final pressure achieved in the tank is determined by the valve area. Thus, as already shown in Figure 36, the final discharge conditions in the pipe are a pressure of 4.2 bar and a temperature of 350K, whether the initial pressure is higher or lower than this value.

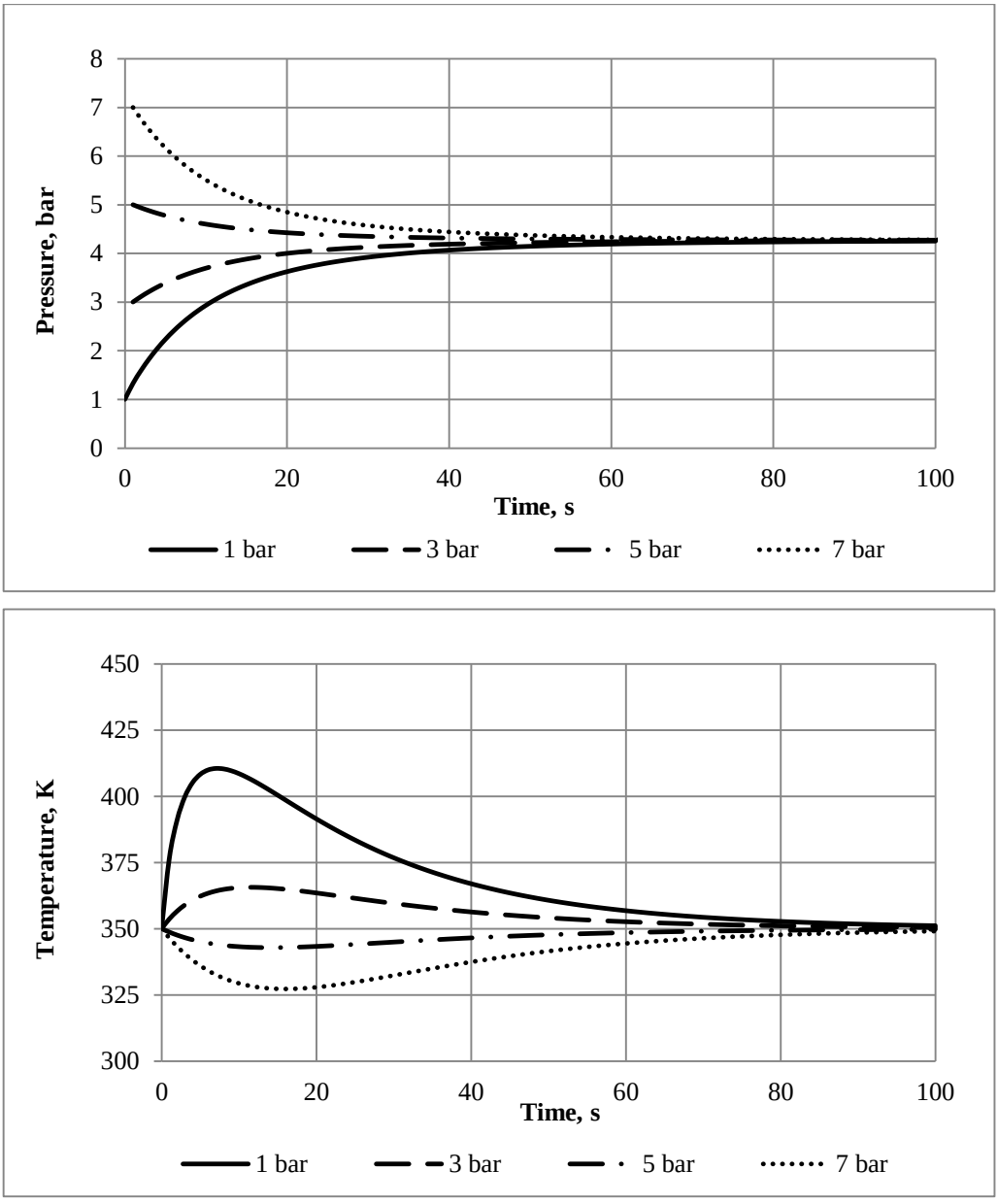

Figure 37: The effect of varying the initial tank pressure in an oil-injected air screw compressor plant. The upper graph shows the Tank Pressure, and the lower graph shows the Temperature

As can be seen from all the given diagrams, the results, obtained from the compressor plant model, agree with the laws of Physics and provide a solid basis for extending its use for unsteady plant simulation in more complex applications.

8.2. Closed loop Screw Compressor Plant Simulations

The single tank model in an open plant system can be adapted to simulate a compressor system containing two tanks operating in a closed loop, with gases, refrigerants or air as the contained working fluid.

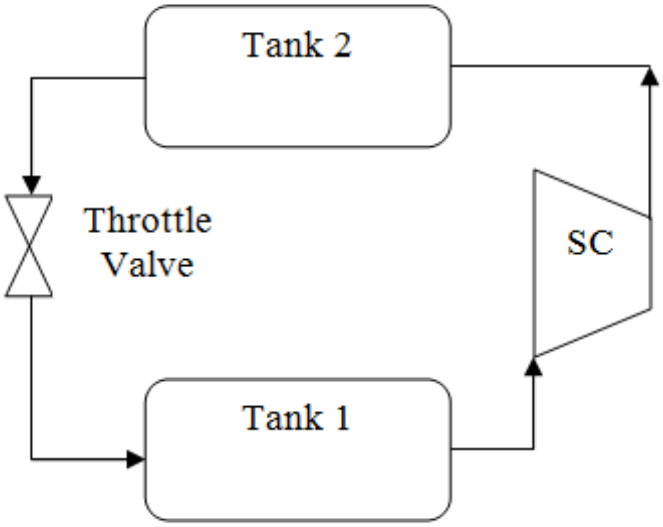

Figure 38: Two tank closed loop screw compressor plant system

As shown in Figure 38, air, or any other gas, leaves Tank 1 to enter the screw compressor, from which it is discharged into Tank 2, to return to Tank1, via a throttle valve. It is assumed, for this and all further simulations, that the volume of Tank 1 is much larger than that of Tank 2.

For a given compressor speed, the steady state pressures in the two tanks, attained after startup, are determined by the valve area. Thus, reducing the valve area, decreases the flow into Tank 1 and then into Tank2, thereby resulting in a lower preessure in Tank 1. Conversely, opening the valve will increase the pressure in Tank 1 after the compressor starts, but in both cases, for a fixed valve area, the system will stabilise to maintain constant pressure in both tanks.

8.2.1. Varying the Compressor Shaft Speed in a Closed Loop System

The effect of varying the compressor rotational speed, for a fixed starting pressure is shown in Figure 39. As can be seen, because Tank 1 is much larger than Tank 2, the pressure remains constant for shaft speed 4500 rpm and it converges to a higher or lower value if the speed is increased or decreased.

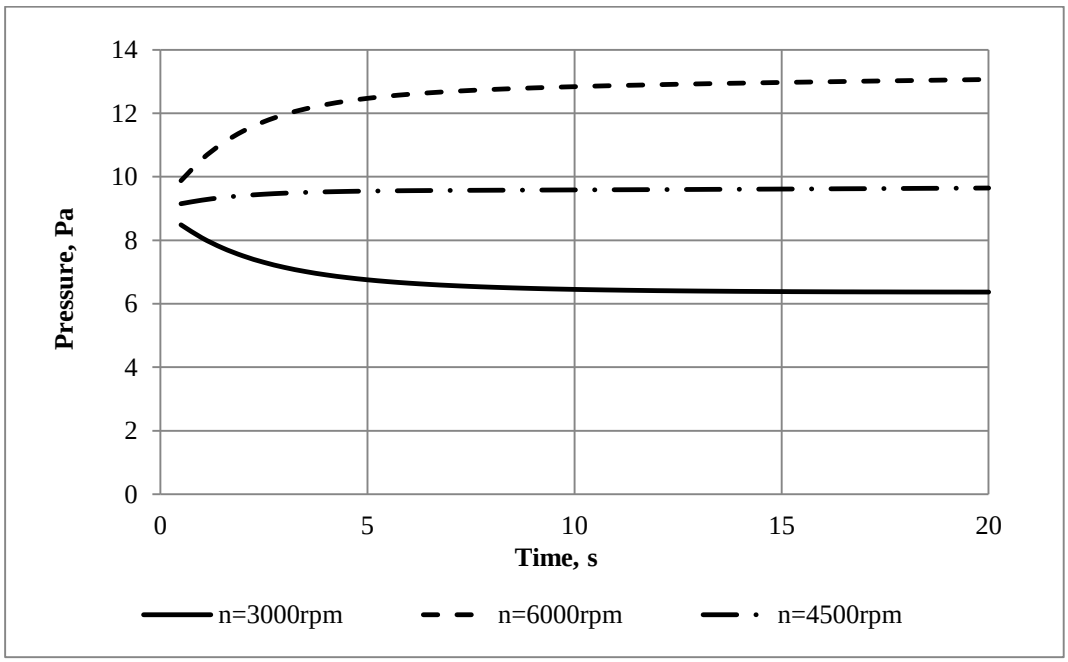

Figure 39: Pressure variation in the discharge Tank, as a result of speed changes in a closed loop air screw compressor plant

At constant speed, the mass flow into the discharge tank (Tank 2) remains constant, but as the speed is increased, it may be seen that for the steady case at n=4500 rpm, as shown in Figure 39 and Figure 40, as the speed is increased, the mass flow into Tank 1 rises. Conversely, when the shaft speed is decreased, the mass flow entering Tank1 decreases until it equals the mass flow into the Tank2, resulting in a rise in pressure in Tank 1 and a fall in pressure in Tank 2.

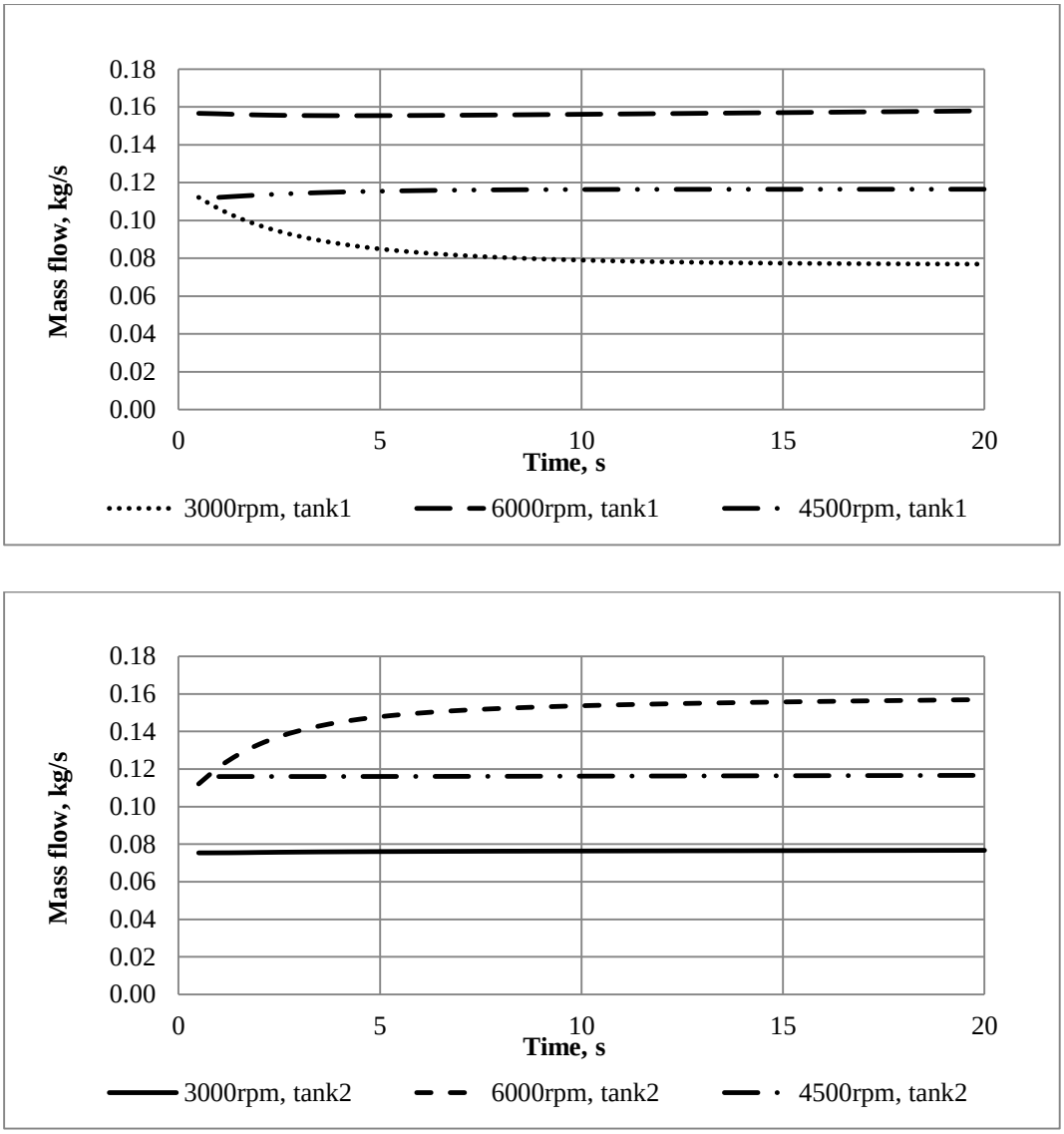

Figure 40: Mass flow going to both tanks at different shaft speeds

8.2.2. Variation of Shaft Speed during Compressor Operation in a Closed Loop System

The next simulation case was to determine the effects of a sudden change in the compressor speed while the system was in operation. The result is shown in Figure 41. As soon as the speed increased from 3000 rpm to 6000rpm, the pressure in Tank2 started to increase slowly but the pressure in Tank 1 remained constant because the volume of Tank 1 is much larger than that of Tank 2. However, as shown in Figure 42, the mass flow into the Tank 2 is doubled immediately because the inflow is proportional to the shaft speed, but it took about 10 seconds for flow into Tank1 to reach to the same value.

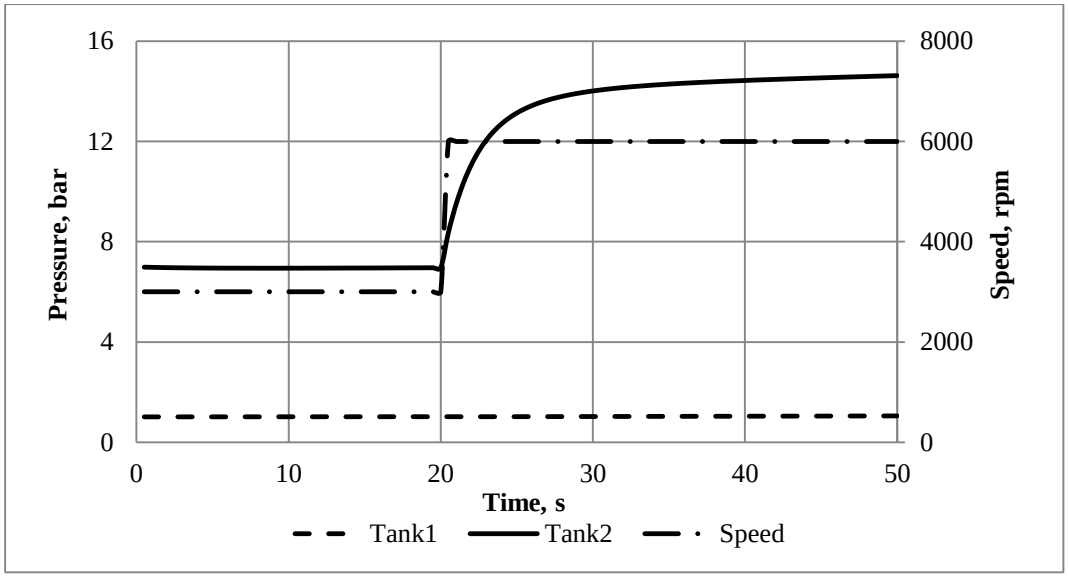

Figure 41: The effect of sudden speed variation on discharge pressure, when changing speed from 3000 to 6000rpm

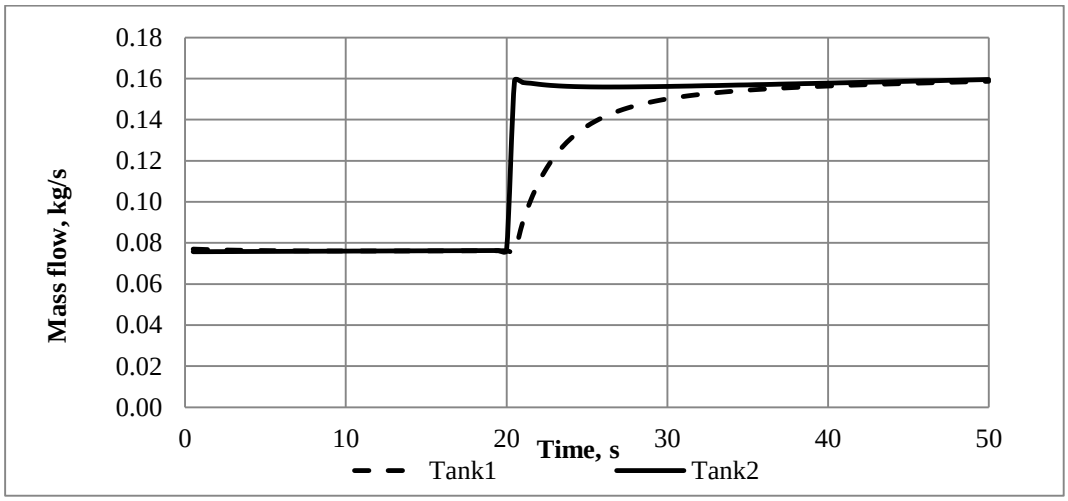

Figure 42: The effect of sudden variation of speed from 3000 to 6000 rpm on the Mass flow in and out

Very interesting results may be seen in Figure 43. It might be expected that as soon as the speed is increased, the mass of air in both tanks would increases slowly in both tanks. But as it can be seen, due to the pressure rise in Tank 2 and the corresponding decrease in pressure in Tank 1, the mass of air contained in Tank 2 is increased, while that in Tank 1 is decreased.

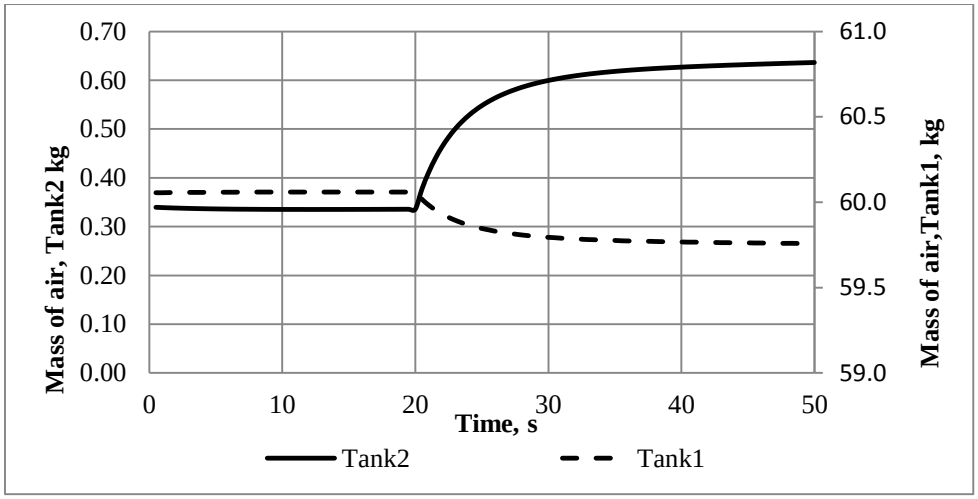

Figure 43: Change of mass of air in both tanks, as a result of changing speed from 3000 to 6000rpm

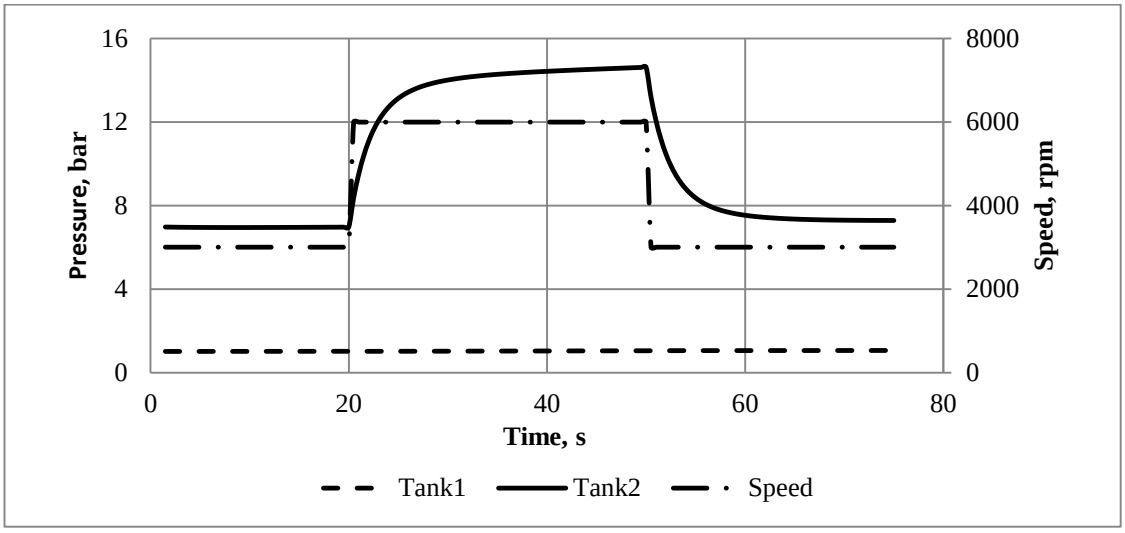

Figure 44: Pressure changes in both tanks, resulting from speed changes from 3000 to 6000rpm and back to 3000

Another example is presented in Figure 44 where the compressor speed is suddenly increased from 3000 rpm to 6000 rpm and subsequently, suddenly reduced back to 3000 rpm. The pressure in Tank1 will not change substantially because its volume is much larger than of Tank 2. The pressure in Tank 2 increases gradually as soon as the speed is increased and returns back to the same pressure of 7 bar when the speed returns to 3000rpm.

8.3. Simulation of Multiple Tank Screw Compressor Plant

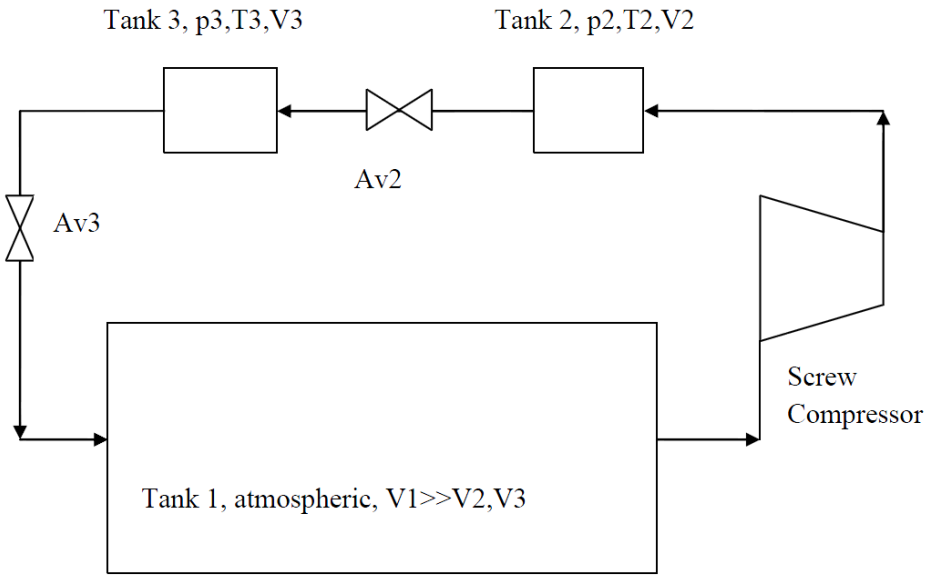

Figure 45: Compressor plant layout for multiple tank configuration

As has been stated before, the model may be used to simulate all types of configuration and consequent unsteady conditions which may be found in real plant. An example of a multiple tank configuration is shown in Figure 45, where there are three tanks. This was also investigated assuming the same initial values of starting pressure p_1=1bar, discharge pressure p_2=5bar, and starting temperature T=303K. The possibilities considered are presented in Table 5 and examples given for each case.

Table 5: Scenarios plan

Scenario 1	Scenario 2	Scenario 3
$V_2=V_3$	$V_2=V_3$	$V_2\neq V_3$
$\Delta t\neq const$	$A_{v2}\neq A_{v3}$	$A_{v2}\neq A_{v3}$

8.3.1. Scenario 1: Time Variation

As shown in Figure 45, Tank1 is much bigger than others, while the volumes of Tank2 and Tank3 are equal, as well as the valve areas Av2 and Av3. For Case1, the compressor speed varies from 3000 rpm to 6000 rpm and back for successive periods of 25s in Case1, 50s in Case2 and 100s in Case3.

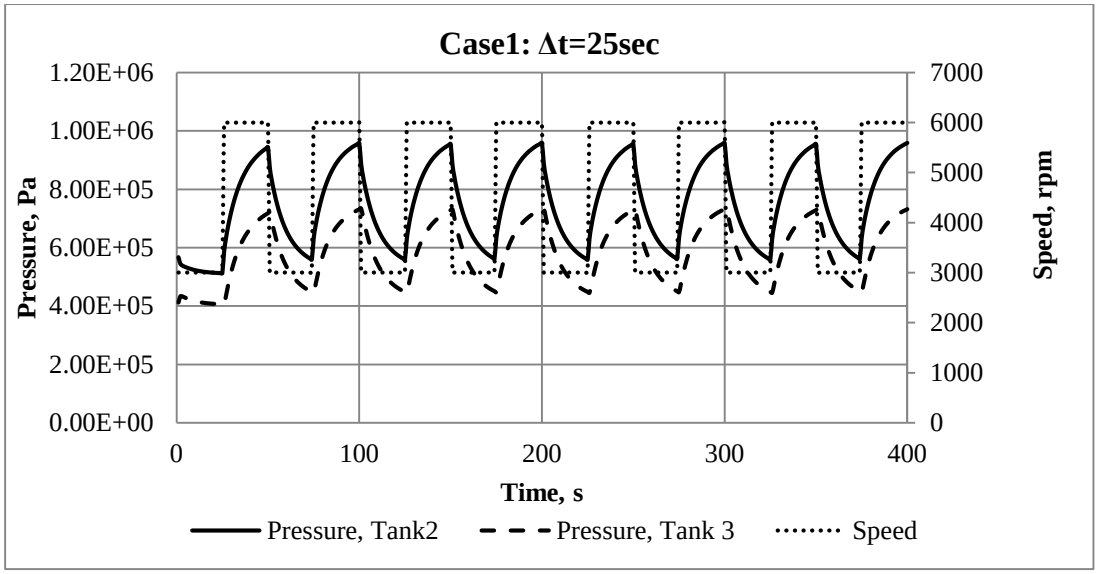

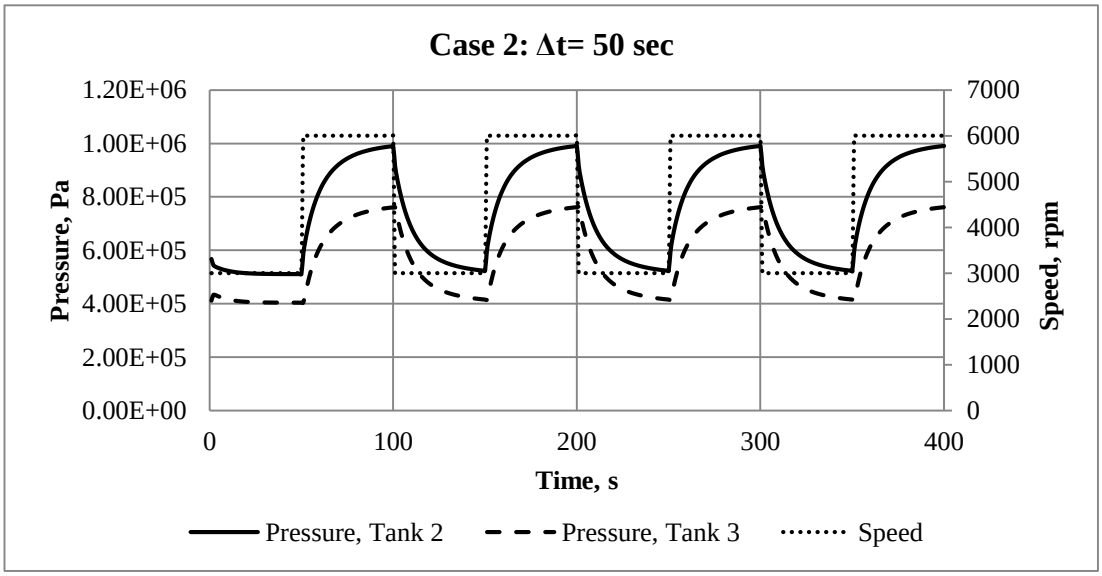

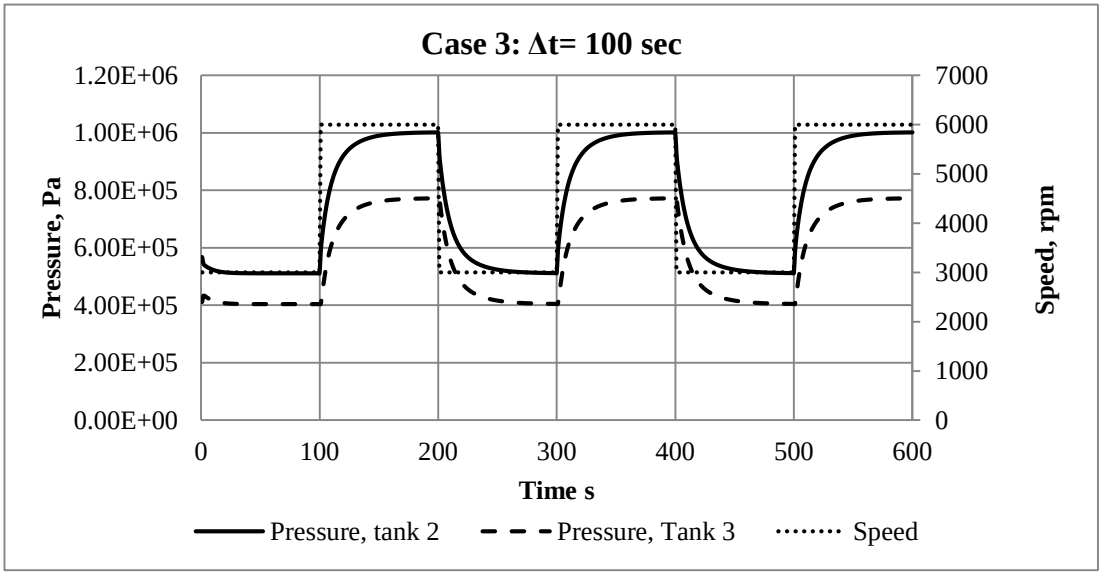

Figure 46: Pressure variation in Tank 2 and Tank 3 for different cycle time Intervals

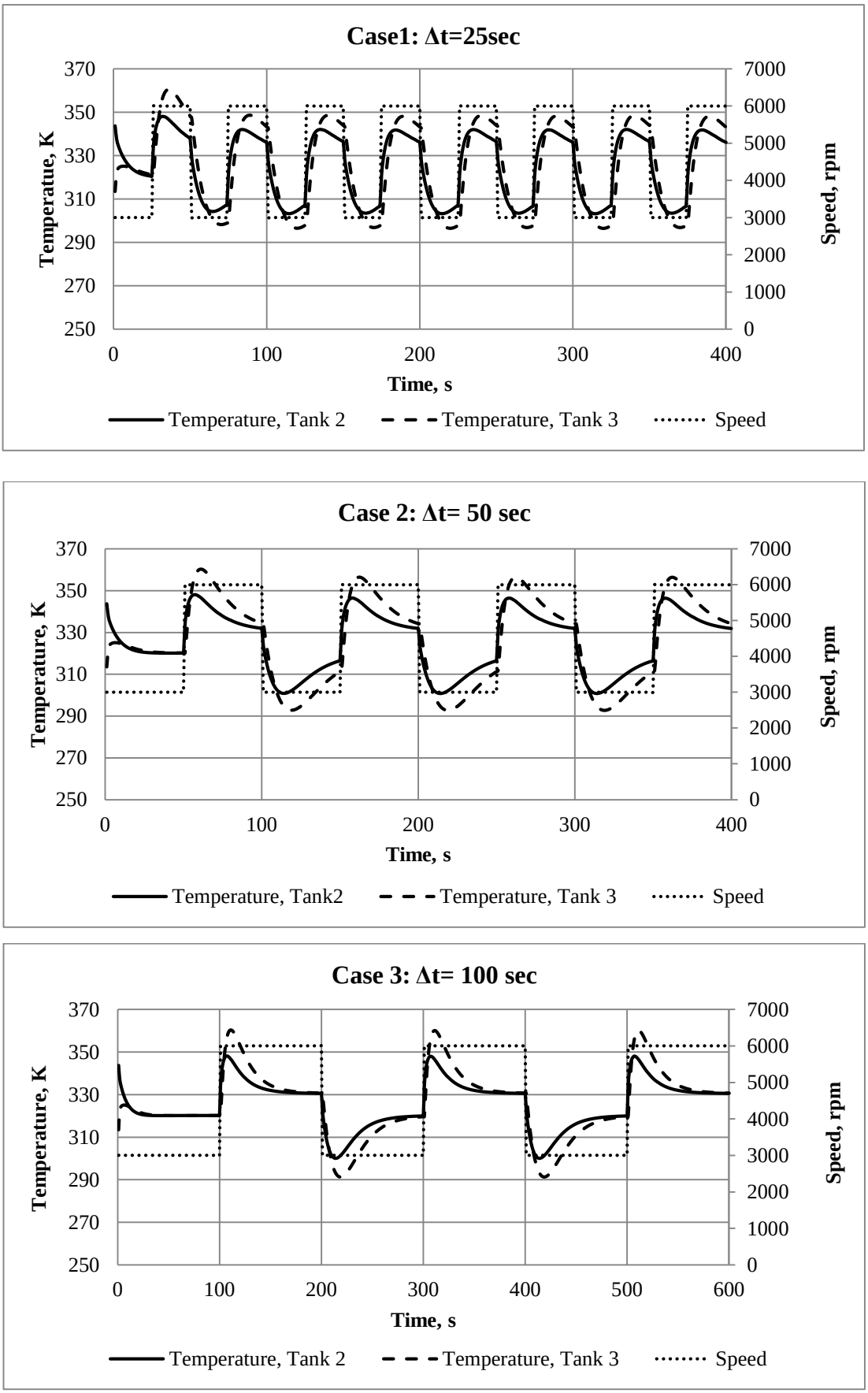

Figure 47: Temperature variation in Tank2 and Tank3 for different cycle time intervals

Tank2 and Tank3 are downstream of the compressor and it can be seen from Figure 46 and Figure 47 how the pressure and temperature vary for each of the three cycle times. If Tank2 is considered, it can be seen that pressure would rise further in Case1 if Δt were longer, but it attains a maximum of 10 bar for Case2 and Case3. Although the pressure rose from 5 to 10 bar in both cases 2 and 3, the larger time interval between cycles, in Case3, enabled steady conditions to be maintained for a longer period . The temperature changes shown in Figure 47 confirm the same trends, namely, the maximum and the minimum values are the same for all three cases but the larger cycle times enable steady conditions to be attained for longer periods with sharper peaks. This is another illustration of the advantages of a dynamic model rather than estimating the extreme conditions, using a steady state model.

8.3.2. Scenario 2: Valve Area Variation

Scenario 2 includes 5 cases: valve areas are equal in the beginning but then valves A_{v2} or A_{v3} can be varied, as given in Table 6.
Cases 1-2-3 and Cases 1-4-5 are considered separately.
Table 6: Valve area variation cases

Case №	A_{v2}	A_{v3}
Case 1	1.2	1.2
Case 2	1.2	0.8
Case 3	1.2	1.6
Case 4	0.8	1.2
Case 5	1.6	1.2

The pressure and power for these cases are given in Figure 48. As soon as valve A_{v3} is closed in Case 2, the power input increases from 62 to 70 kW when the compressor speed n=6000 rpm, the pressure in Tank 2 rises from 8 to 10.3bar and in Tank 3 – from 5.3 to 7.8 bar. The power does not change so significantly when the speed is 3000 rpm. When valve A_{v3} is closed, air starts to accumulate in both tanks and causes both the pressure and the input power to rise. When valve A_{v3} is opened, in Case 3, it can be seen that the pressure and power decrease.

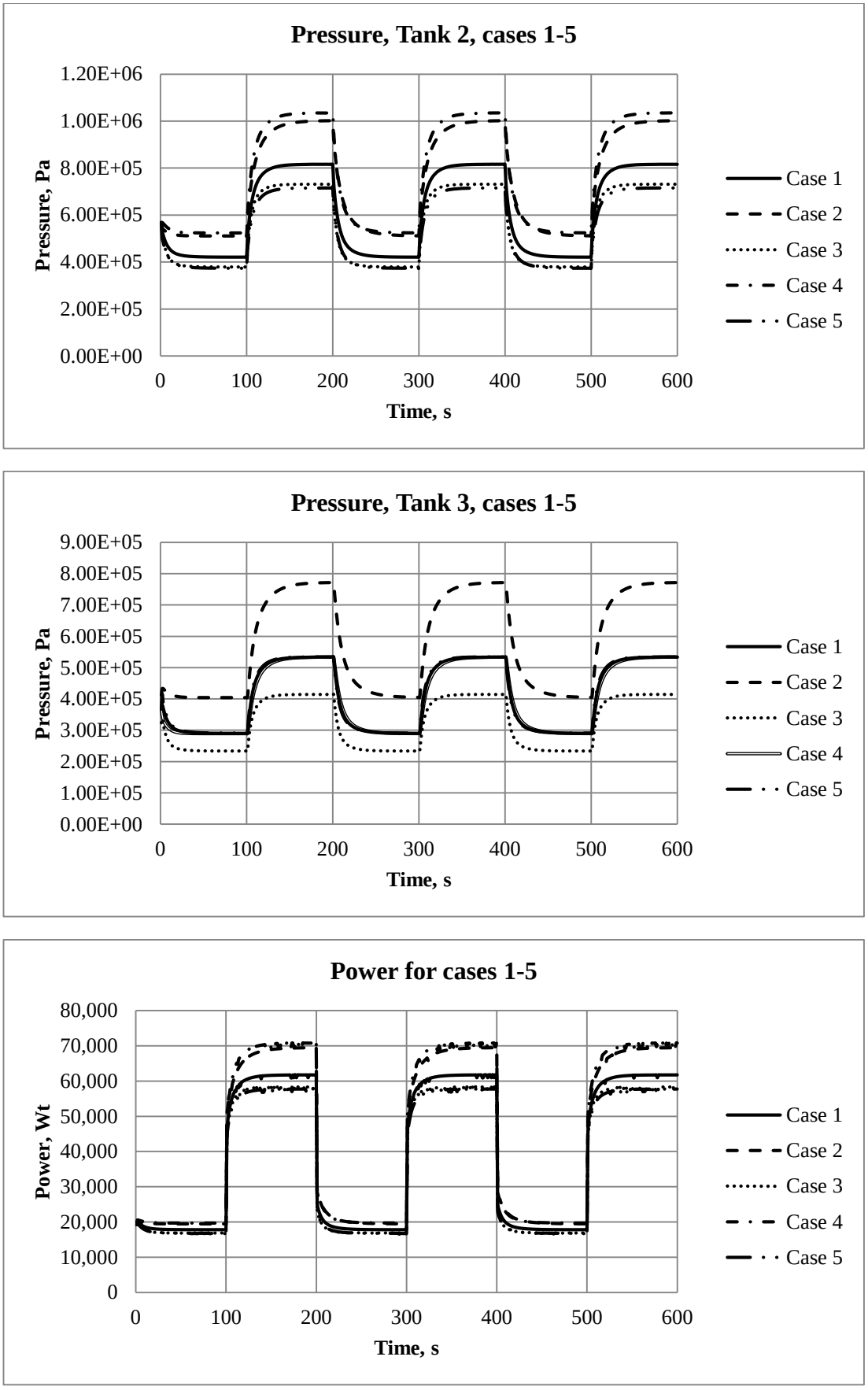

Figure 48: Pressure in Tank2 and Tank3 and input power for cases 1-5

When valve A_{v2} is closed, air starts to accumulate in Tank 2 and this causes the pressure in it to rise from 8 to 10.3 bar at compressor speed 6000rpm and from 4 to 5 bar at 3000rpm, power rises at high speed only, from 62kW to 70kW, although pressure in the Tank3 is similar. Diagrams show that pressure and power drop down when valve A_{v2} open.

8.3.3. Scenario 3: Valve Area and Tank Volume Variation

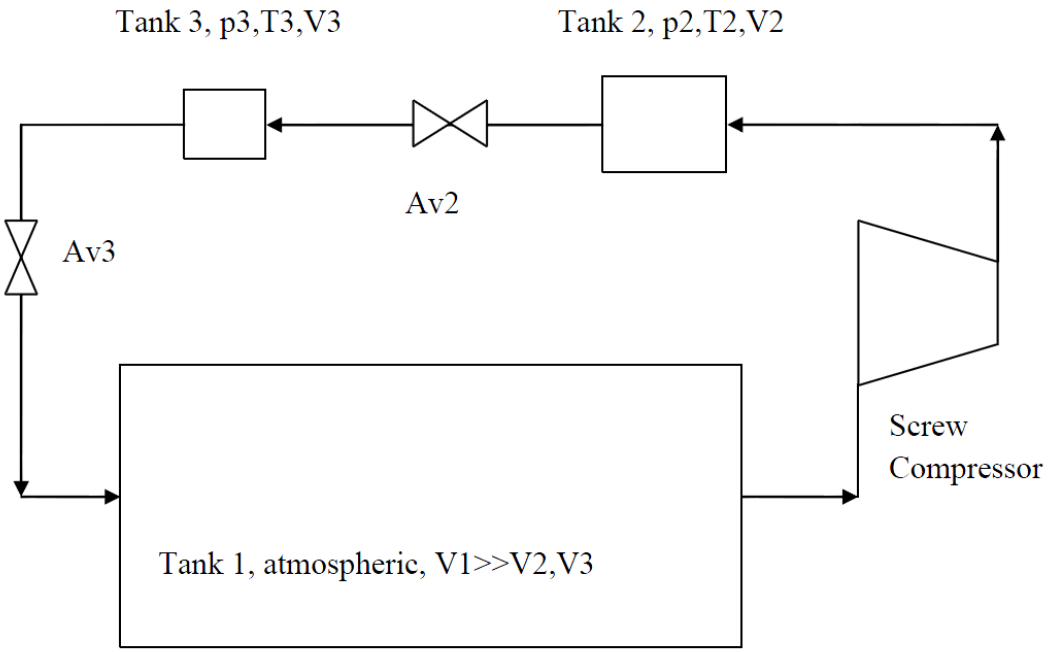

Figure 49: Compressor plant layout for multiple tank configuration

The multiple tank system presented in Figure 49 is similar to that in Figure 45, but the volume of Tank2 is twice that of Tank3, i.e.$V_2=2V_3$. Three different cases were considered, when the valve area between the tanks varies; namely: $A_{v2}=A_{v3}$ in Case1, $A_{v2}=2A_{v3}$ in Case2 and $A_{v3}=1.5A_{v2}$ in Case3. The initial temperatures and pressures are the same as in the previous cases. Again, it can be clearly seen that the pressure rise varies for different valve areas, namely: the more the valve is open, the faster the pressure rise, as shown in Figure 50. So, it is important to understand plant dynamics properly when the system performance is analysed. For Case2, when the second valve has a small opening area, the pressure difference between the tanks is the least, at 1-2 bar, and the final pressure is the highest at 10-12 bar, because air accumulates in the tanks due to the small area of A_{v3}. Temperature dynamic is shown in Figure 51.

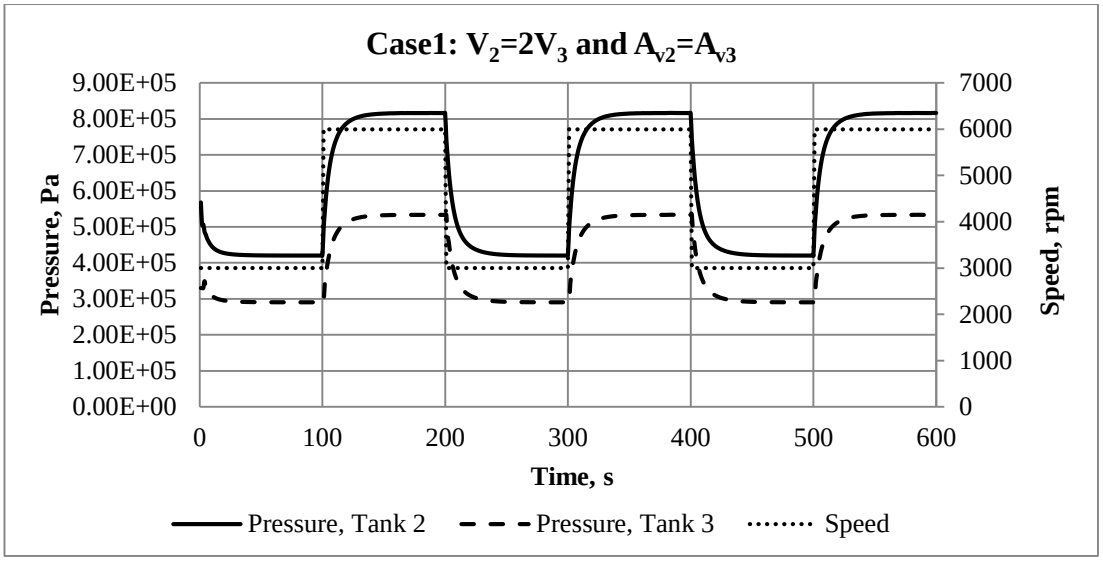

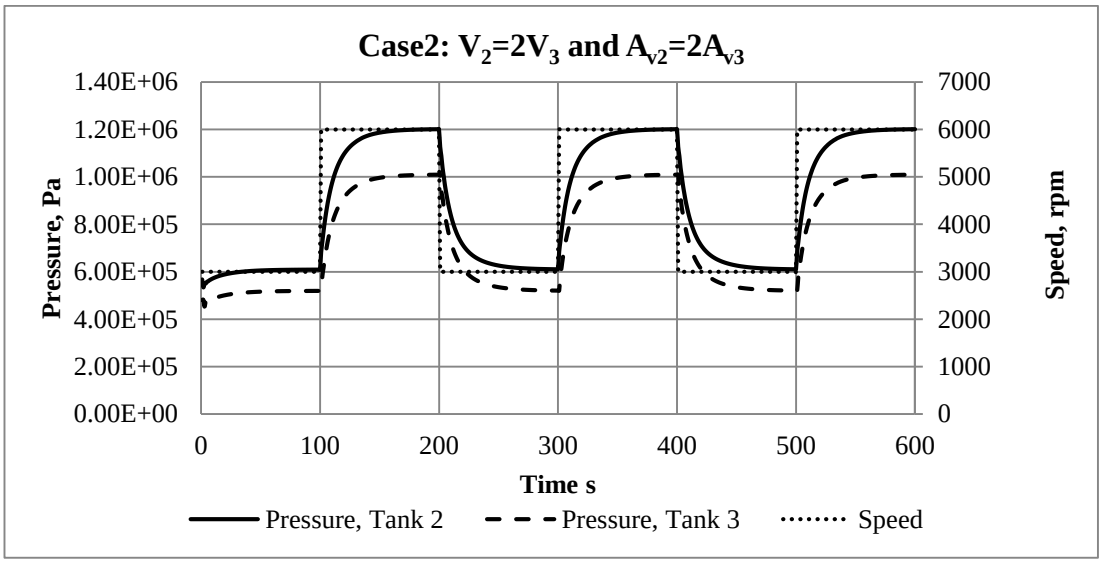

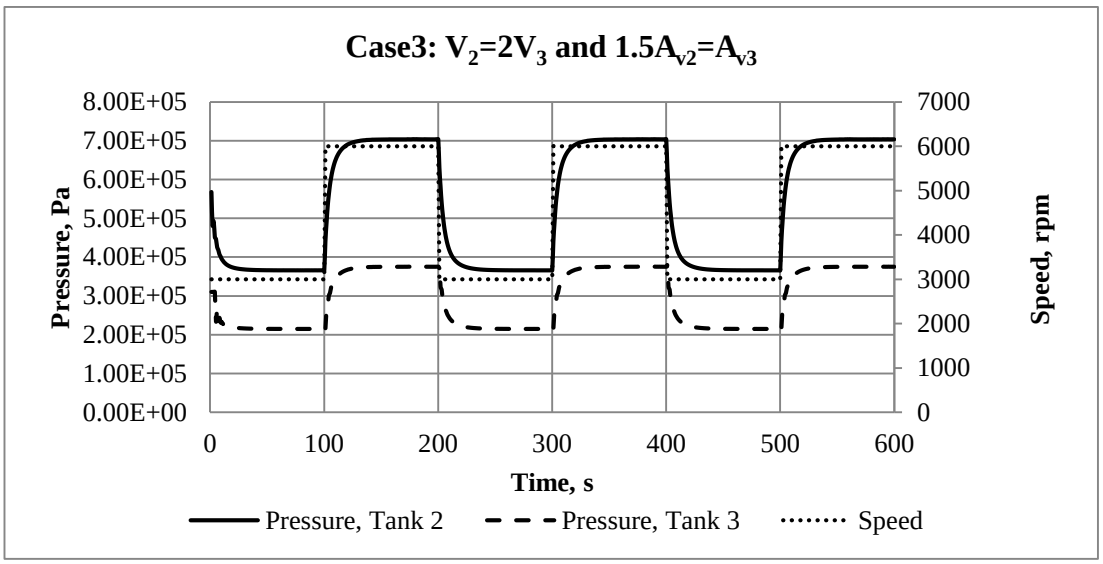

Figure 50: Rates of pressure change in Tank2 and Tank3 for varying valve areas and tank capacities

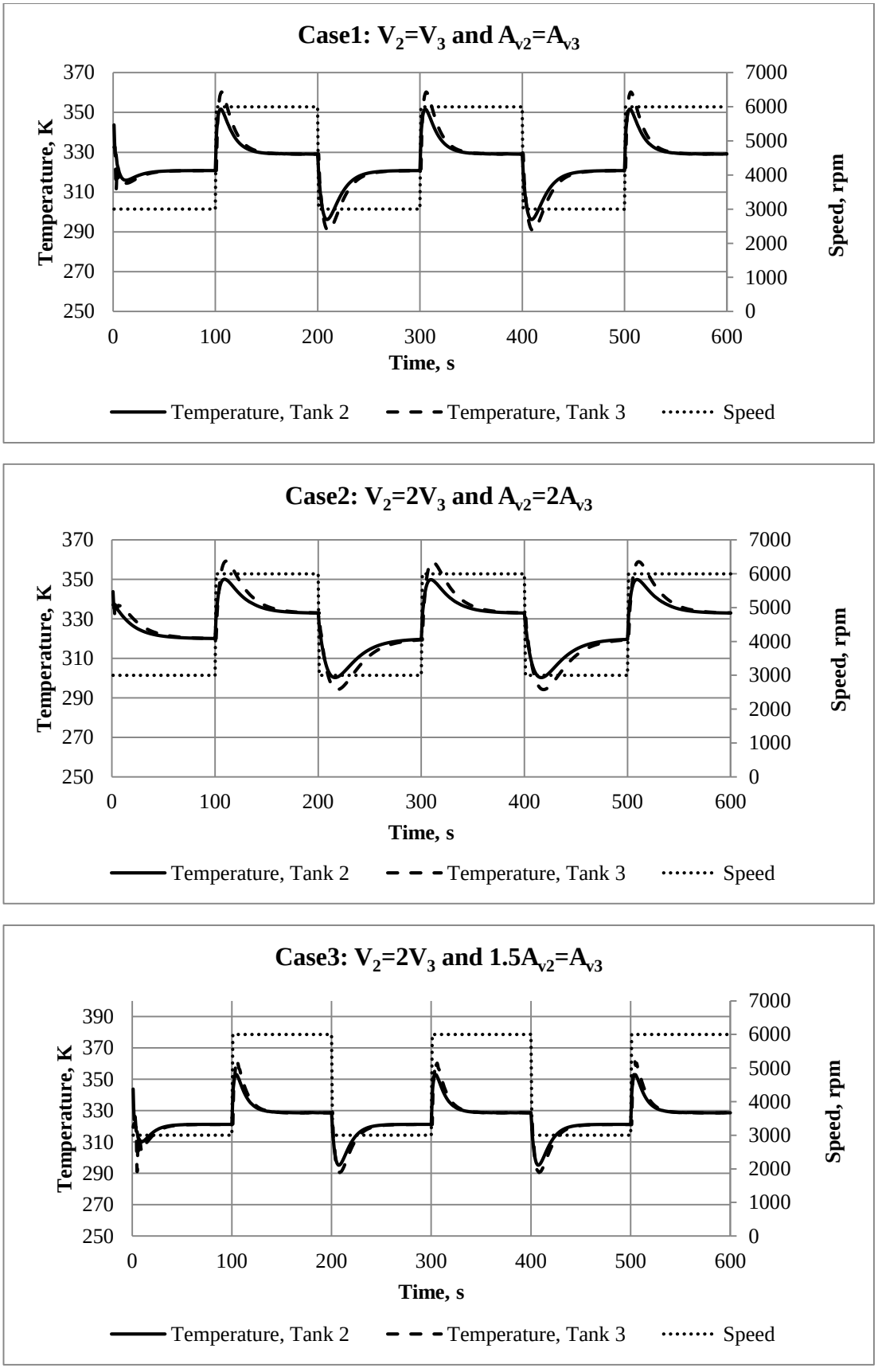

Figure 51: Rates of temperature change in Tank2 and Tank3 for varying valve areas and tank capacities

8.3.4. Scenario 4: Four Tank Compressor Plant

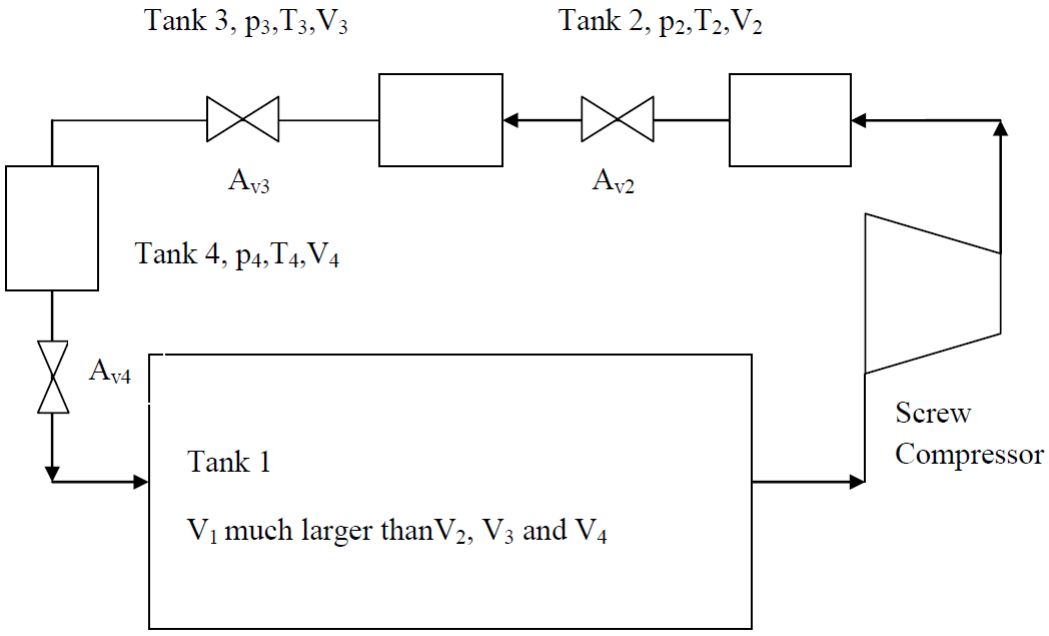

Figure 52: Four tank compressor plant configuration

A Further analysis was carried out for a four tank system, as shown in Figure 52 and a comparison of the response rates with different numbers of tanks is given in Figure 53 and 54. As can be seen, the discharge pressure from the compressor increases with the number of tanks in the system.

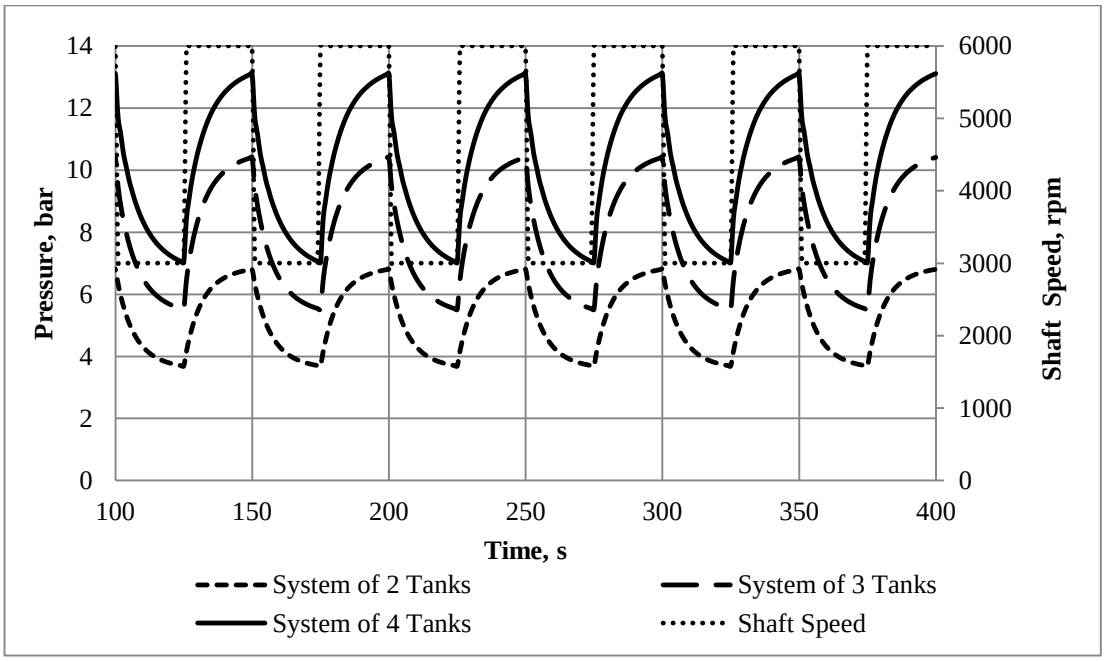

Figure 53: Pressure in the tank after compressor for 2-, 3- and 4-tank systems

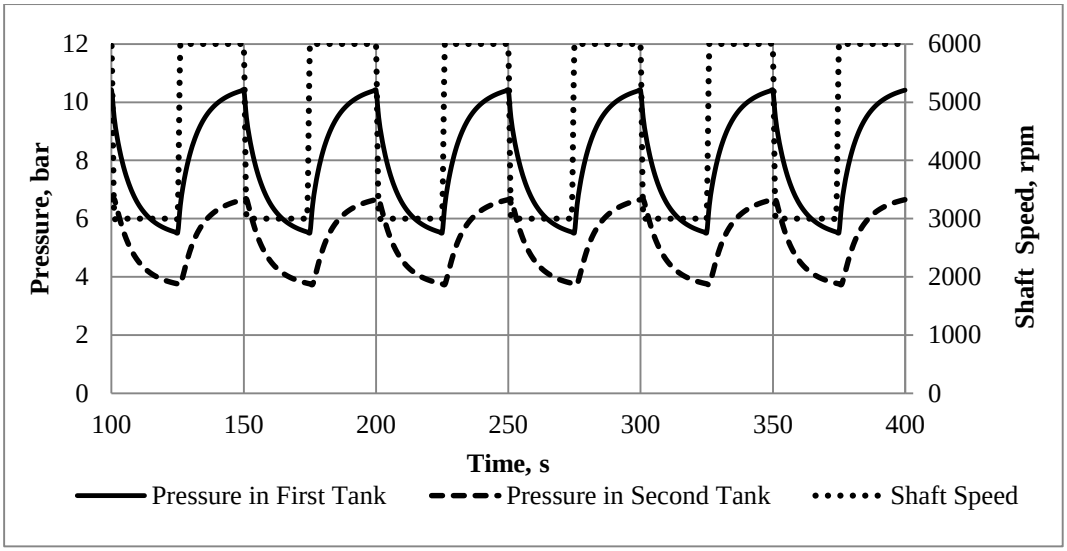

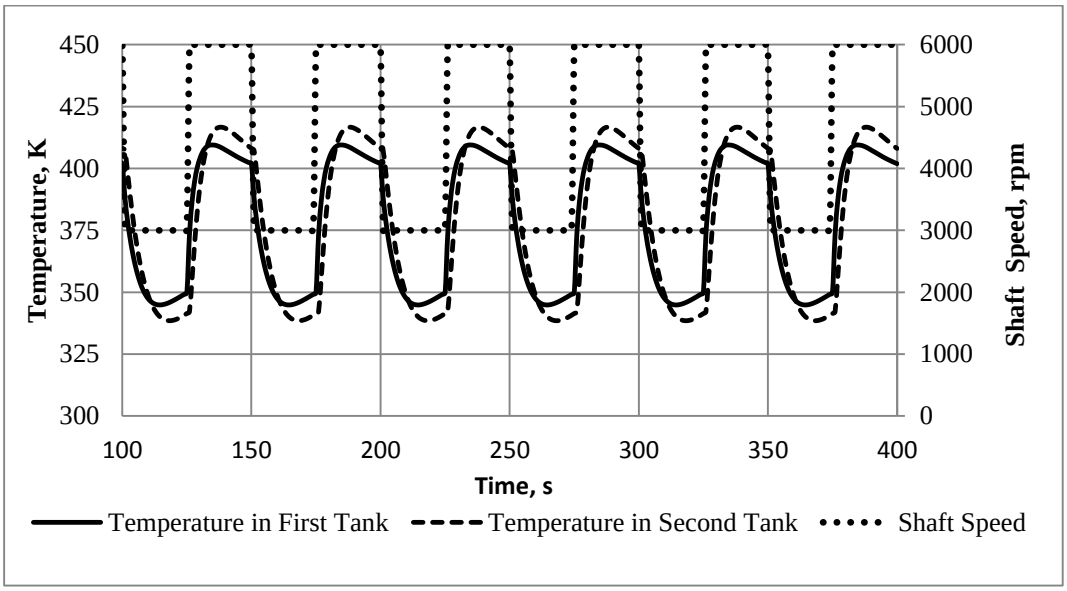

Figure 54: Variation of pressure, above, and temperature, below, in three tank compressor plant model depending on speed changes

Pressure and temperature changes in a three tank compressor plant, resulting from speed changes, are shown in Figure 54. Although the speed was decreased before the pressure stabilised, it can be seen that cycles are repetitive.

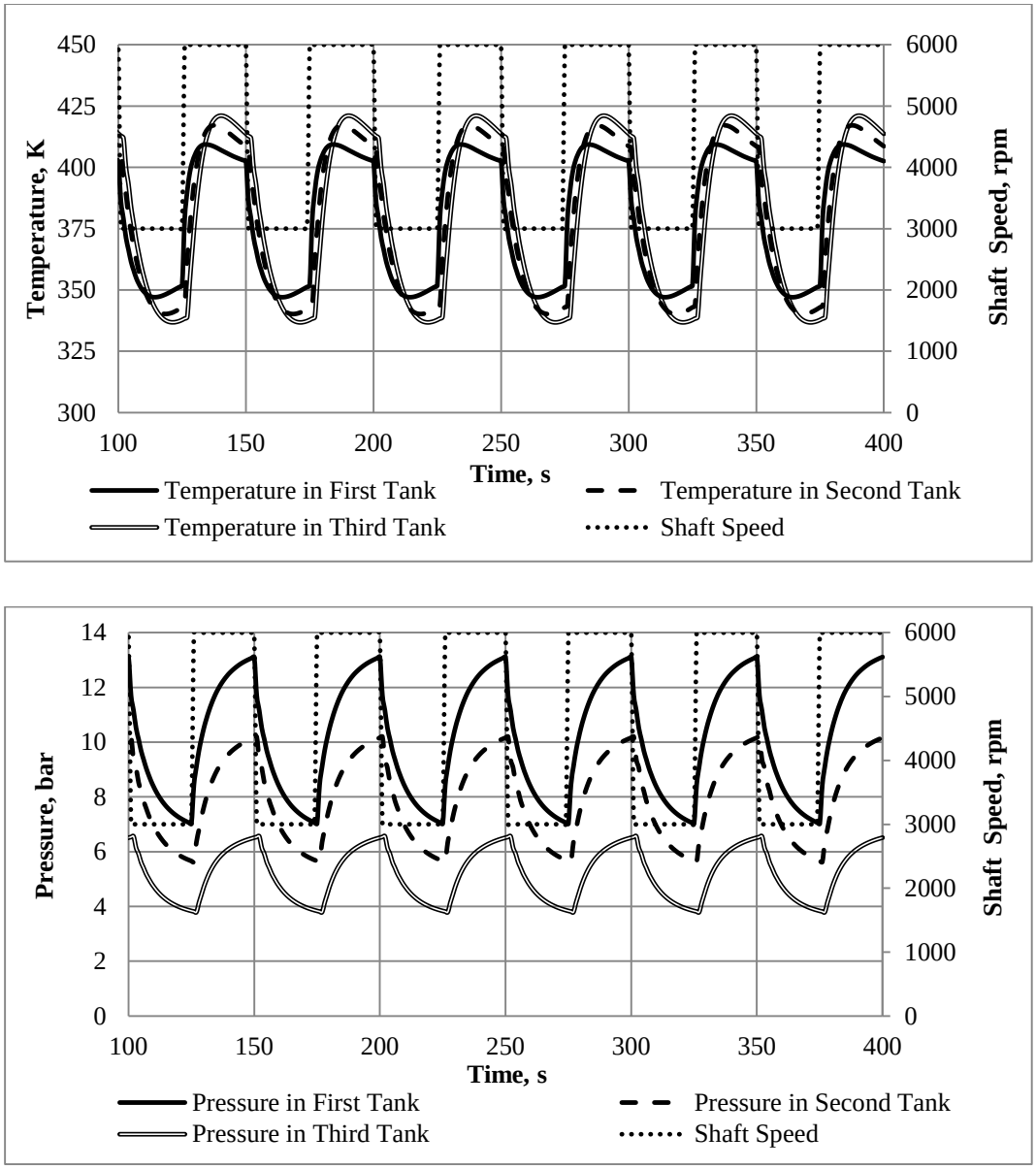

Figure 55: Variation of pressure and temperature in a four tank compressor plant model resulting from step changes in speed.

An example of speed induced pressure fluctuation in a four tank model is shown in Figure 55.

8.3.5. Scenario 5: Simulation of a Plant where the Tanks are widely separated

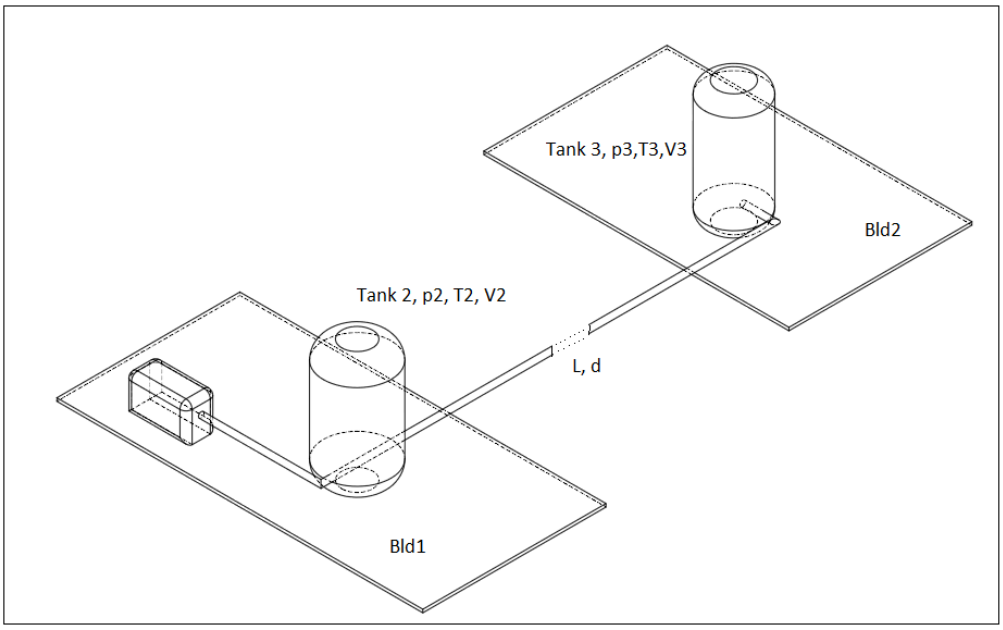

Figure 56: Screw compressor plant with widely spaced tanks

Scenario 5 does not present any comparison, but give an example of real factory case where dynamic program can be used to get any parameter value at any time. The developed program is useful for complex facilities with air distribution systems. An example of such plant can be illustrated as follows. Compressor and Tank2 are located in building 1. There is need for pneumatic instruments in another building 2 where Tank3 is located at distance L from building 1, as shown in Figure 56. The model enables the dynamic response to parameter changes in both tanks to be investigated.

If pressure in Tank3 is at its required level and the compressor performance is defined, the effects of possible variation in the pipe length L and its diameter d_h can be calculated. For example, if the compressor provides 5 bar at discharge, while the required pressure, for instrumentation, is 4 bar and the distance between building 1 and building 2 is 15m. Using initial calculation results, a pipe diameter d_h=25mm is defined. This pipe can be replaced with a valve, across which the pressure drop is equal to pressure drop in the pipe 1" and 15m length. Varying parameters of pressures, tank volume, pipe and diameter length, compressor speed, it can be concluded how

these changes affect all parts of the system. Mass flow and pressure responses to speed changes are shown in Figure 57.

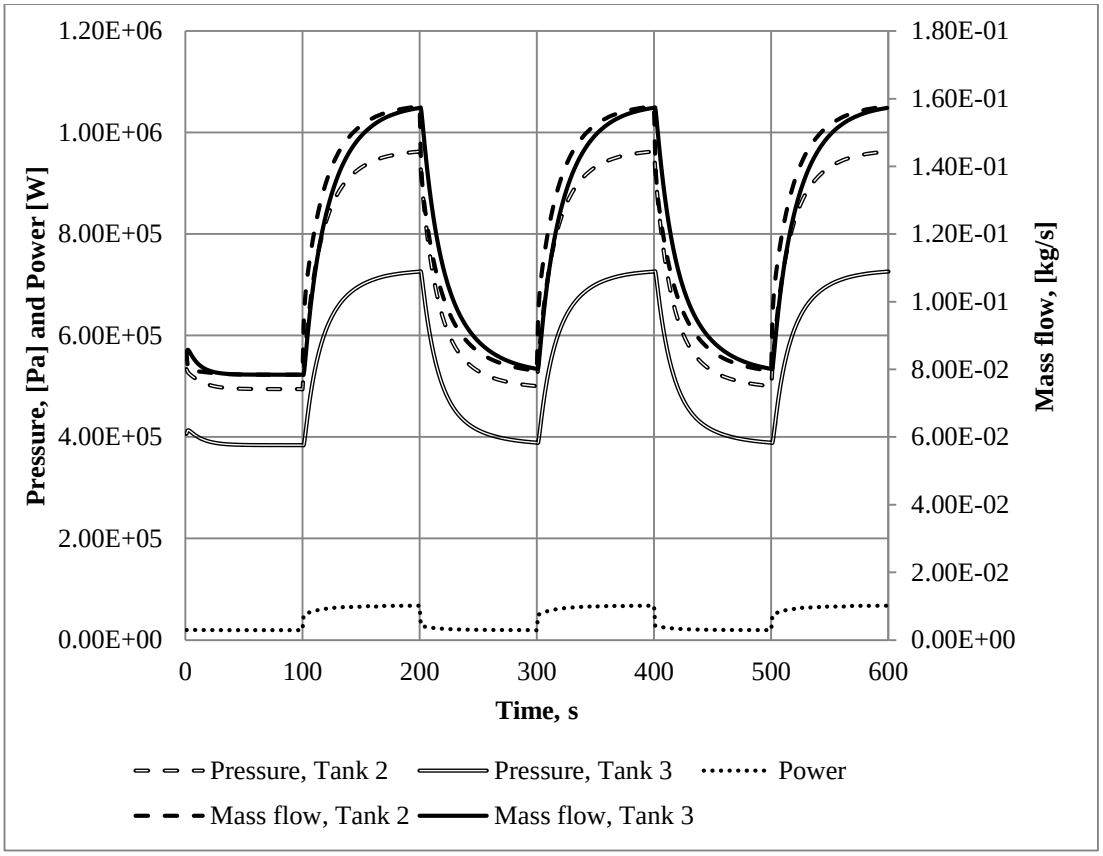

Figure 57**:** Rates of pressure and mass flow change in a widely spaced tank system

Sample Calculation of the effects of pipe diameter change.

p_2=5 bar, p_3=4bar → Δp=1bar

then air velocity in a pipe is calculated:

$$w = \frac{Q}{A}$$

where Q is volume flow, m^3/s, A – area of the pipe, m^2

Chosen pipe diameter is 25mm, volumetric flow is taken from results file of the program

$$w = \frac{4.035 \;\; 4}{60\pi 0.025^2}$$

$$w = 137 m/s$$

Then Reynolds number is calculated:

$$Re = \frac{wd}{v}$$

where kinematic viscosity is taken from the table for dry air and temperature 325K, $v = 1.807 \times 10^{-5} \mathrm{m}^2/\mathrm{s}$

$$Re = 1.9\ 10^5$$

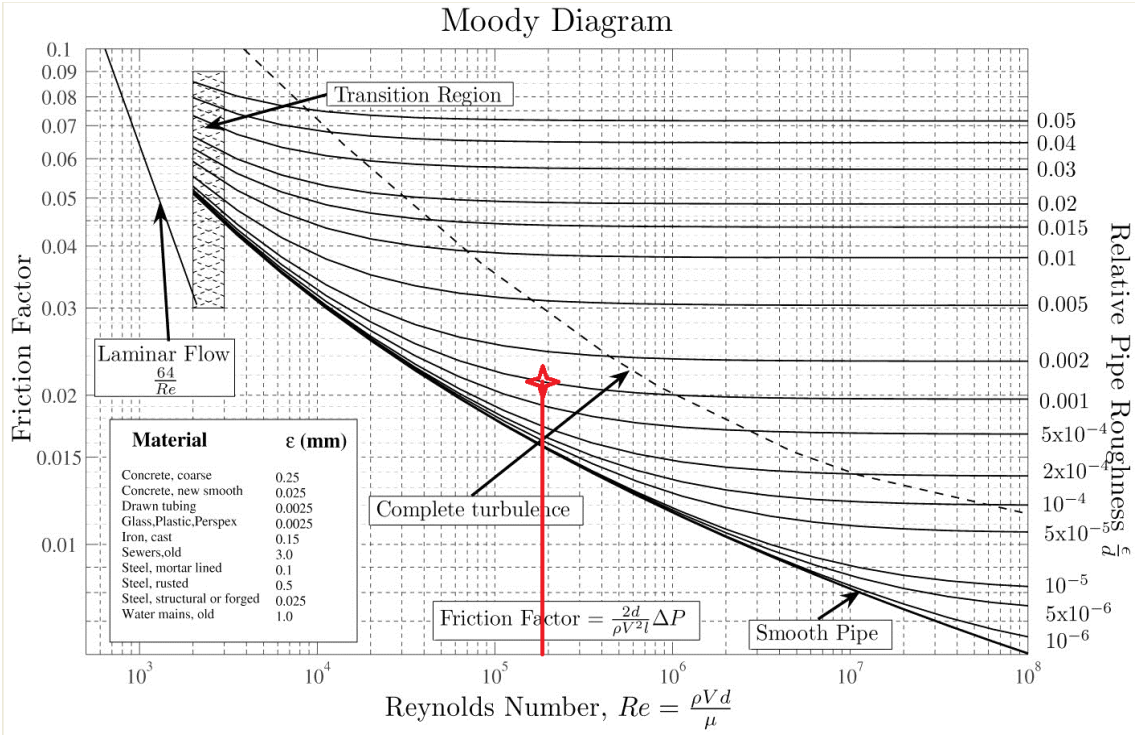

Figure 58: Moody diagram

Then, using the Moody diagram, given in Figure 58, the friction factor f is found, Re and relative pipe roughness 0.001 were taken into account. Friction factor f=0.0215, so, Darcy friction factor f_d=4·0.0215=0.086.

Also, as density had to be calculated, pressure and temperature are extracted from result file the program.

$$\rho = \frac{p}{RT}$$

$$\rho = \frac{5.03\ 10^5}{287\ 320} = 5.476\ kg/m^3$$

Using the Darcy-Weisbach equation, the length of the pipe is found by use of given pressure difference, pipe diameter etc.

$$\Delta p = \frac{8 f_d L Q^2}{\pi^2 \rho d^5}$$

Finally, for the diameter 25mm, length of the pipe is found as 15 m.

If the same procedure is repeated for 50mm pipe, length of the pipe is equal to 420m.

Similar calculations and simulations can be done for the system with unlimited quantity of tanks similar to combination presented on Figure 59.

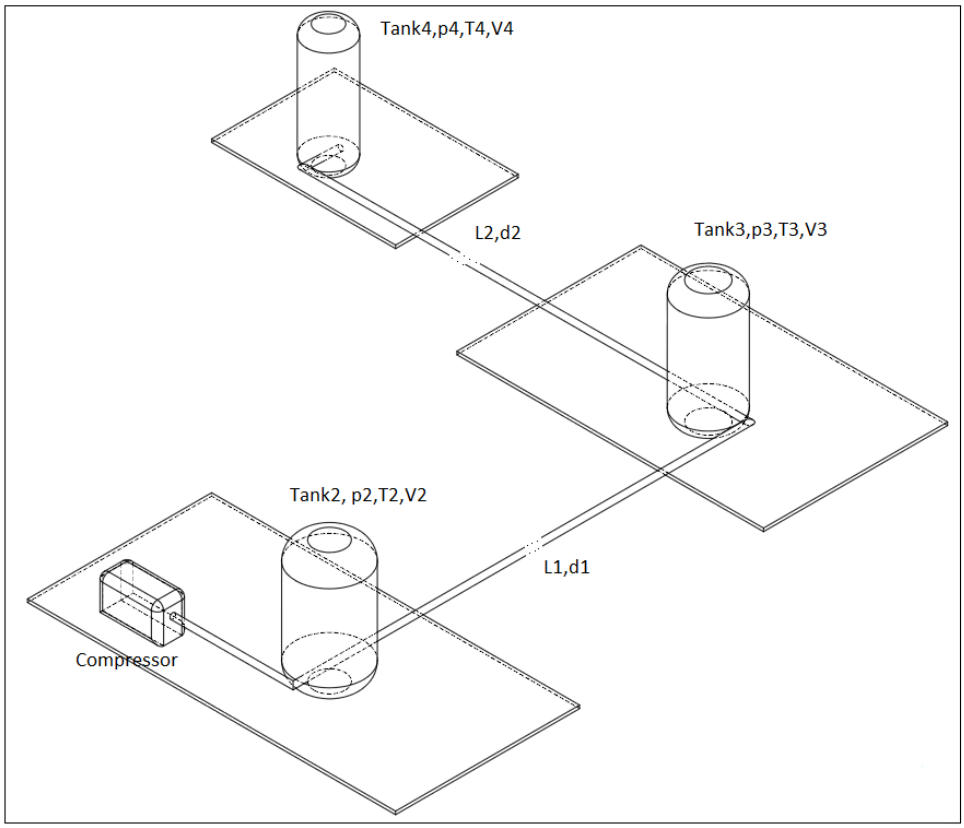

Figure 59: Alternative screw compressor plant scheme

8.4. Simulation of Steady and Intermittent Modes in order to Estimate Plant Performance

A preliminary investigation was also carried out to determine how power consumption differs between steady and intermittent operation as a result of varying the valve area.

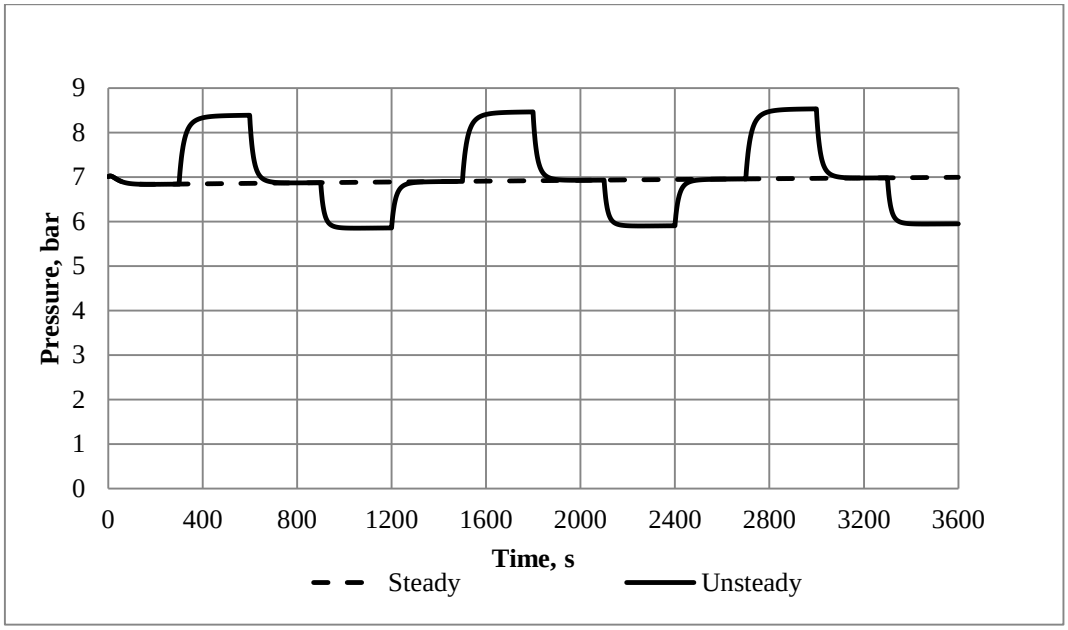

Figure 60: Pressure variation in the tank resulting from sudden valve area changes

The results of the analysis of a case where the steady state discharge pressure is 7 bar and the valve area is 50mm^2 are shown in Figure 60 when the valve area varies between 40 mm^2 and 60 mm^2. The power consumption for both cases was calculated and the difference was found to be about 1%.

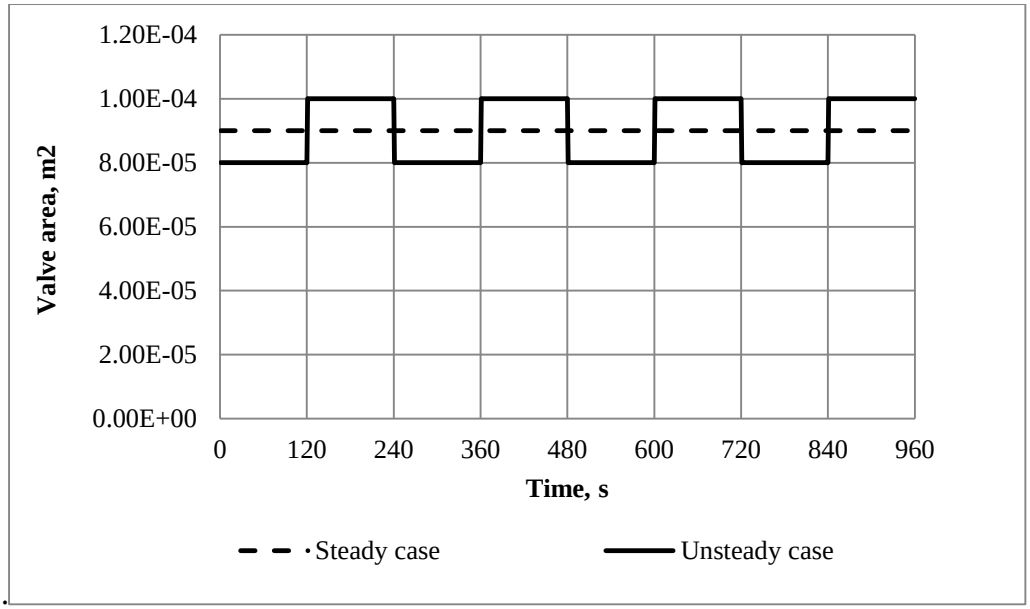

Figure 61: Valve area variation for steady and unsteady modes

The valve area changes required to effect the pressure changes are shown in Figure 61.

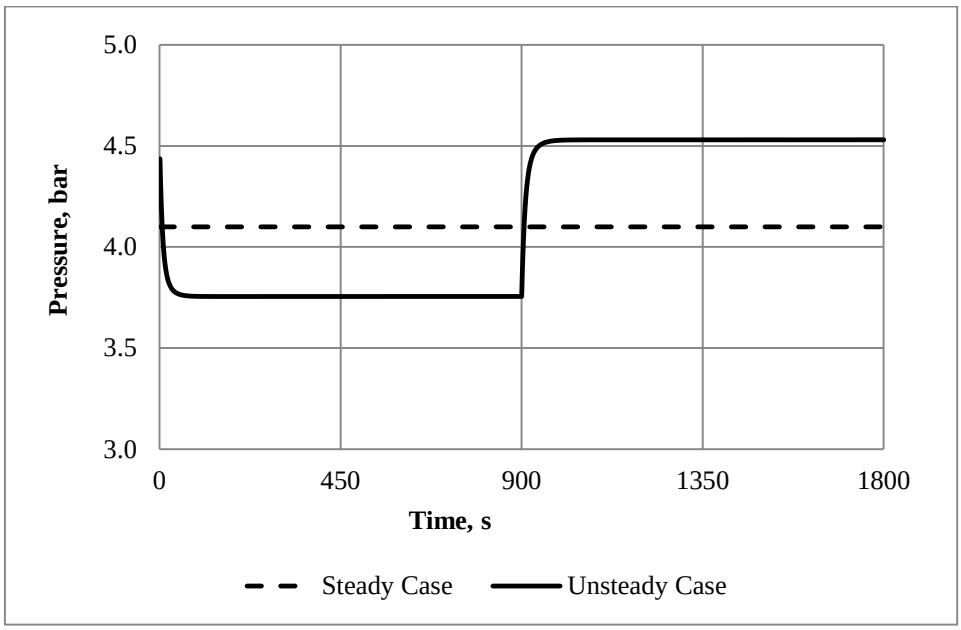

Figure 62: Pressure in the system for steady and unsteady cases, example 1

The pressure does not always rise linearly with the valve area, as shown in Figure 62 which shows the pressure in the system for steady and intermittent modes when the valve area at steady conditions is 90mm^2, and is varied between 80mm^2 and 100mm^2.

Table 7: System parameter comparison, example 1

		Steady	Intermittent	delta, %
Power	kW	15.949	16.065	0.72
Sp. Power,	kW/m3/min	4.081	4.112	0.76

As can be seen from Figure 62 and Table 7 the average power and specific power for the steady and intermittent cases differ by approximately 1%. But if larger area changes are made as shown in Figure 63 and Table 8, the pressure changes are of the order of 12%, and power and specific power consumption change by 8-9%. And as can be seen again, the pressure change with area is not linear.

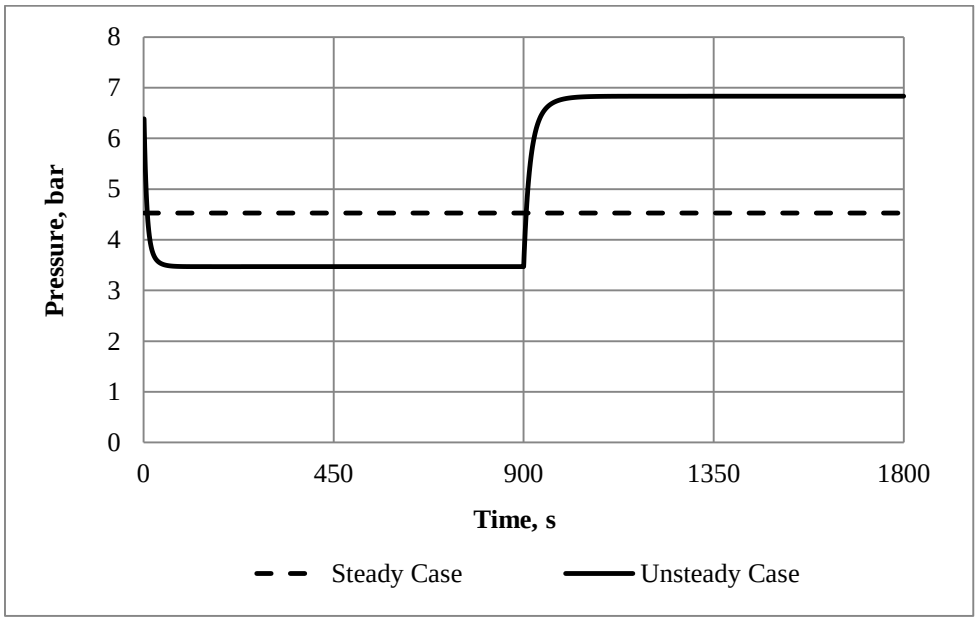

Figure 63: Pressure variation in the system for steady and unsteady cases, example 2

Table 8: System parameters comparison, example 2

		Steady	Intermittent	delta, %
Power	kW	17.044	18.540	8.06
Sp. Power,	kW/m3/min	4.378	4.791	8.62

8.5. Pressure Range Limit Simulation

Another scenario considered was how the pressure varies during intermittent shutdown. The plant model was modified to include maximum and minimum speeds as well as maximum and minimum pressures as input limiting conditions. The program then simulated the process of the pressure rising at maximum speed until it achieved its maximum value. The shaft speed then became equal to its minimum speed, which was zero in our case since this corresponds to shut off. The pressure then decreased until it attained its minimum value. The shaft speed then increased to its maximum value and the entire process was repeated. The results of this study are shown in Figure 63 and Table 9.

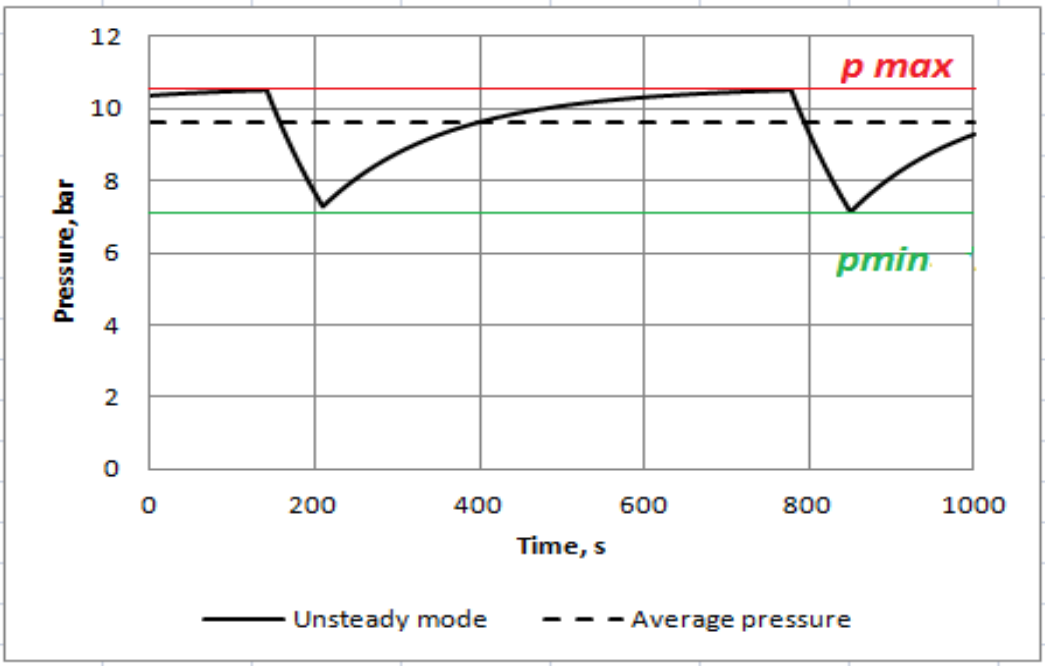

Figure 64: Pressure for simulated switch off and switch on

Table 9: Initial parameters of the system

V [m^3]	Speed max [rpm]	Speed min [rpm]	P max [bar]	P min [bar]	A_v [mm^2]	Cycle length, [s]	Figure
0.325	6000	0	10.5	7.5	48.5	650	65
0.325	6000	0	8	6	58.5	25	66

Thus, the model enables all kind of scenarios for system shut down to be analysed and enables the time it takes for the pressure to drop to p_{min} and then back to p_{max} and the results are shown in Figure 65. This will vary depending on the tank volume or the valve area for different initial values of s_{max}/s_{min} and $p_{max}/p_{min.}$ and would be of value for control engineers.

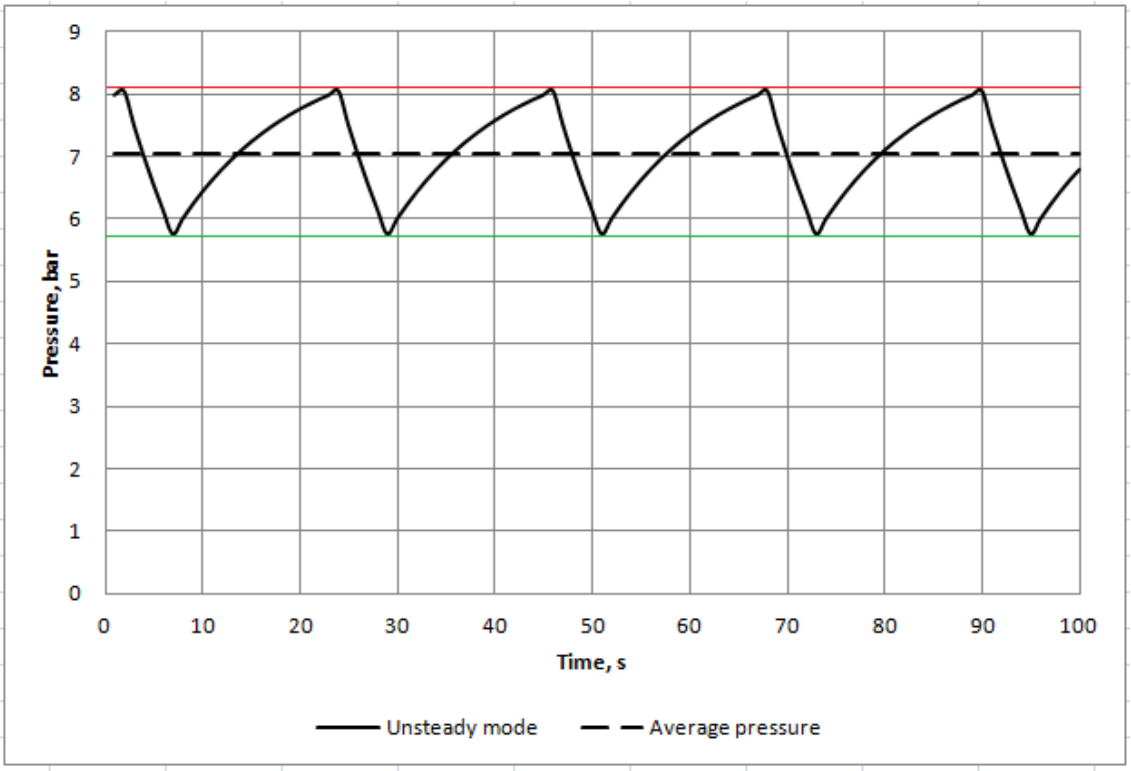

Figure 65: Pressure curve for simulated switch repetitive on/off operation

9. Conclusions

The intermittent character of everyday operation of industrial plant, using compressors, requires special attention to be paid to ensure their reliable and efficient operation. Systems operating with reciprocating and centrifugal machines have previously been investigated and computer programs that simulate their operation under these conditions already exist. But, due to the complex geometry of screw compressors, no such programs were found to be available, in the public domain, to analyse the performance of systems operating with these machines.

Accordingly, the aim of this research was to develop and verify a mathematical model to analyse screw compressor driven plant during both continuous and intermittent operation. This has been achieved by:

- Development of a model, based on the differential equations of conservation of mass and energy, which is suitable for air, process gas and refrigeration plant by the inclusion of equations for the prediction of real gas properties;
- The testing of this model by comparison of predicted performance with test data. The difference between them is within 5% for all analysed parameters and less than 2% for the majority of the cases considered;
- The use of this model to predict a variety of operating scenarios. These include any number of gas storage tanks of various sizes, located at different positions, pressure reduction valves and condensers and evaporators;
- The model can predict compressor plant performance such as power, specific power and efficiency during intermittent operation. This enables the plant performance to be estimated at any instant;
- Startup and shutdown simulation can be performed within defined pressure and speed intervals. This may be useful for control engineers.

10. Recommendations for Future Work

The model can be extended to expand possible options for modelling of screw compressor plant operating under intermittent conditions. This includes, refrigeration applications, which have been only mentioned in Chapter 8, and multiple tanks in parallel, as shown in Figure 66. Also, experimental work can be further extended to verify refrigeration plant predictions.

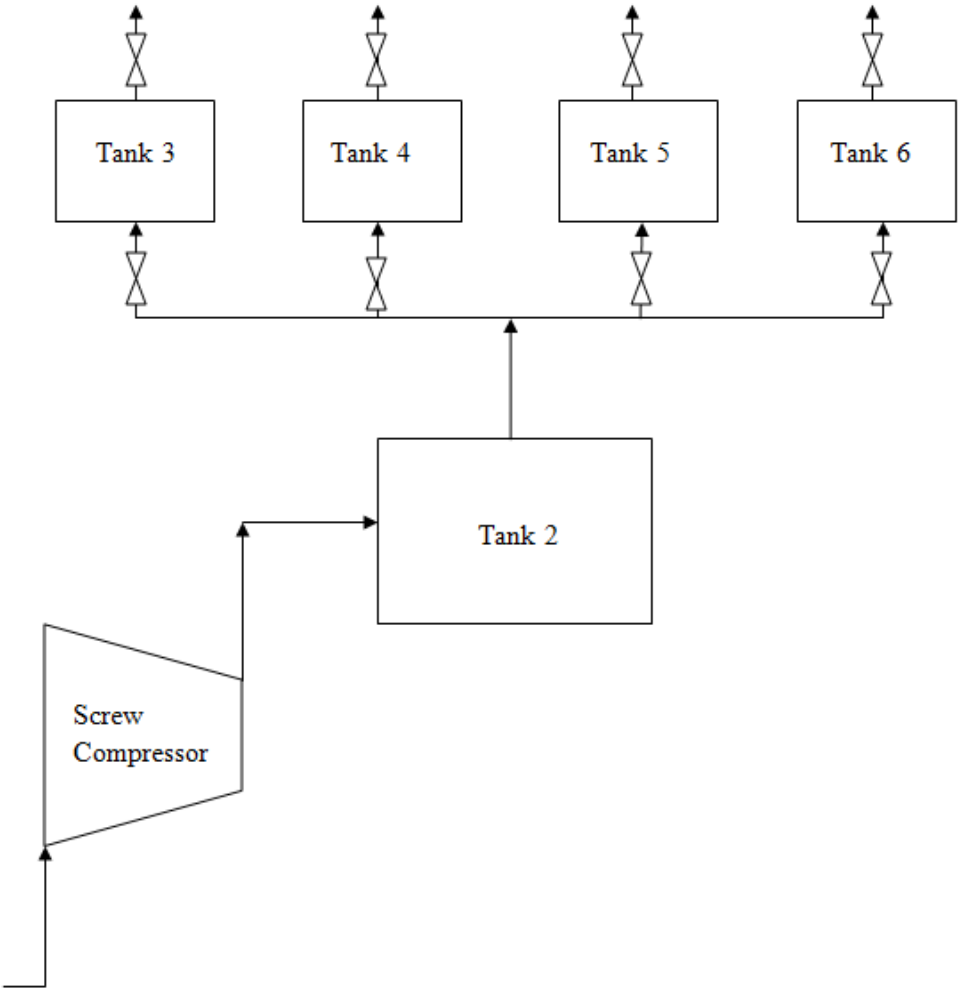

Figure 66: Multiple tank configuration for further modelling

.

Bibliography

Amosov, P. E., 1977. *Vintovie kompressornye mashiny (Screw Compressors Machines).* Leningrad: Mashinostroenie.

Andreev, P. A., 1961. *Vintovye kompressornye mashiny (Screw Compressor Machines).* Leningrad: SUDROM.

Anon., 2012. *Honywell Process Solutions.* [Online]
Available at: https://www.honeywellprocess.com/library/marketing/notes/service-note-on-dynamic-engineering-studies.pdf
[Accessed March 2014].

Bendapudi, S. & Braun, J. E., 2002. *A review of literature on dynamic models of vapour compression equipment,* s.l.: ASHRAE.

Bezzo, F. et al., 2004. *Using Process Simulators for Steady-state and Dynamic Plant Analysis.* Chemical Engineering Research and Design, 82(A4), pp. 499-512.

Bloch, H. P., 2006. *Compressors and modern process applications.* Hoboken, New Jersey: John Wiley&Sons.

Brownrigg, N., 2014. *Protecting compressors with dynamic simulation,* s.l.: AspenTech.

Brown, R. N., 1997. *Compressors: selection and sizing.* Houston: Butterworth-Teinemann.

Cetin Kocak, M., 1980. *Dynamic Simulation of Chemical Plant.* Birmingham: University of Aston, Thesis.

Chukanova, E., Stosic, N. & Kovacevic, A., 2013. *Experimental Investigation and Numerical Modelling of Dynamic Behaviour of Screw Compressor Plant.* Universal Journal of Engineering Science, Volume 1, pp. 68-79.

Chukanova, E., Stosic, N. & Kovacevic, A., 2013. *Numerical Analysis of Unsteady Behaviour of a Screw Compressor System.* London, s.n.

Chukanova, E., Stosic, N. & Kovacevic, A., 2014. *Modelling and Experimental Investigation of Unsteady Behaviour of a Screw Compressor Plant.* London, International Refrigeration and Air Conditioning Conference at Purdue.

Chukanova, E., Stosic, N., Kovacevic, A. & Dhunput, A., 2012. *Investigation of Start Up Process in Oil Flooded Twin Screw Compressors.* Purdue, USA, s.n.

Chukanova, E., Stosic, N., Kovacevic, A. & Rane, S., 2012. *Identification and Quantification of Start Up Process in Oil Flooded Screw Compressors.* s.l., s.n.

Ding, G., 2007. Recent developments in simulation techniques for vapour-compression refrigeration systems. *International Journal of Refrigeration,* Volume 30, pp. 1119-1133.

Fleming, J. S., Tang, Y. & You, C. X., 1996 19(6). *Shutdown process simulation of a refrigeration plant having a twin screw compressor.* International Journal of Refrigeration, pp. 422-428.

Golovintsov, A. G., 1964. *Rotatsionnye kompressory (Rotary Compressors).* Moscow: Mashinostroenie.

Hisameev, I. G. & Maksimov, V. A., 2000. *Dvuhrotornye vintovye i pryamozubye kompressory: teoriya, raschet i proektirovanie.* Kazan: FEN.

Honeywell, n.d. *Dynamic Simulation services for process design, control and troubleshooting.* [Online]
Available at: https://www.honeywellprocess.com/library/marketing/notes/service-note-on-dynamic-engineering-studies.pdf
[Accessed 12 November 2013].

Jun, W. & Yezheng, W., 1988. *On the On-Off Operation in a Reciprocating Compressor Refrigeration System with Capillary.* Purdue, s.n.

Jun, W. & Yezheng, W., 1990 13 (3). Start-up and shut-down operation in a reciprocating compressor refrigeration system with capillary tubes. *International Journal of Refrigeration,* pp. 187-190.

Koshkin, N. N., Sakun, I. A. & Bambushek, E. M., 1985. *Holodilnye mashiny (Refrigeration machines).* Leningrad: Mashinostroenie.

Koury, R., Machado, L. & Ismail, K., 2001. Numerical simulation of a variable speed refrigeration system. *International Journal of Refrigeration,* Volume 24, pp. 192-200.

Kovacevic, A., Mujic, E., Stosic, N. & Smith, I. K., 2007. *An Integrated Model for the Performance Calculation of Screw Machines.* s.l., s.n.

Kovacevic, A., Stosic, N. & Smith, I. K., 2007. *Screw Compressors: Three Dimensional Computational Fluid Dynamics and Solid Fluid Interaction.* s.l.:Springer-Verlag Berlin Heidelberg.

Krichel, Susanne, V. & Sawodny, O., 2011 21. Dynamic Modeling of Compressors Illustrated by an Oil-flooded Twin Helical Screw Compressor. *Mechatronics,* pp. 77-84.

Liang, N., Shao, S., Tian, C. & Yan, Y., 2010. Dynamic simulation of variable capacity refrigeration systems under abnormal conditions. *Applied Thermal Engineering,* Volume 30, pp. 1205-1214.

Liang, N., Shao, S., Xu, H. & Tian, C., 2010. Instability of refrigeration system - A review. *Energy Conversion and Management,* Volume 51, pp. 2169-2178.

Li, B. & Allyene, A. G., 2010 33(3). A dynamic model of a vapor compression cycle with shut-down and start-up operations. *International Journal of Refrigeration,* pp. 538-552.

Link, R. & Deschamps, C. J., 2011 34(6). Numerical modeling of start up and shut down transients in reciprocating compressors. *International Journal of Refrigeration,* pp. 1398-1414.

Llopis, R., Cabello, R. & Torrella, E., 2007. A dynamic model of shell-and-tube condenser operating in a vapour compression refrigeration plant. *International journal of Thermal Sciences,* Volume 47, pp. 926-934.

Mokhatab, S. & Towler, B., 2007. Dynamic Simulation of Offshore Production Plants. *Petroleum Science and Technology,* 25(6), pp. 741-757.

Mujic, E., 2009. *A Numerical and Experimental Investigation of Pulsation Induced Noise in Screw Compressors,* PhD Thesis, City University London: s.n.

Ndiaye, D. & Bernier, M., 2010 30(8-9). Dynamic model of a hermetic reciprocating compressor in on–off cycling operation. *Applied Thermal Engineering*, pp. 792-799.

Ogbonda, J. E., 1987. *Dynamic Simulation of Chemical Plant.* Birmingham: University of Aston, Thesis.

Okasinski, M. & Liu, Y., n.d. *Dynamic Simulation of C3-MR LNG Plants with Parallel Compression Strings.* [Online]
Available at: http://www.airproducts.com/~/media/downloads/white-papers/D/en-dynamic-simulation-of-c3-mr-lng-plants-with-parallel-compression-strings-whitepaper.pdf?industryItem=industries&subIndustryItem=Energy&segment=LNG&applicationChildItem=lng-applications&Product
[Accessed 12 November 2013].

Okasinski, M. & Schenk, M., 2007. *Dynamic of Baseload Liquefied Natural Gas Plants - Advanced Modellling and Control Strategies.* [Online]
Available at: http://www.ivt.ntnu.no/ept/fag/tep4215/innhold/LNG%20Conferences/2007/fscommand/PO_31_Okasinski_s.pdf
[Accessed 12 November 2013].

O'Neill, P. A., 1993. *Industrial compressors: theory and practice.* Oxford: Butterworth-Heinemann Ltd.

Powell, G., Weathers, B. & Sauls, J., 2006. *Transient Thermal Analysis of Screw Compressors, Part I: Use of Thermodynamic Simulation to Determine Boundary Conditions for Finite Element Analyses.* Purdue, s.n.

Rinder, L., 1979. *Schraubenverdichter (Screw Compressors).* New York: Springer Verlag.

Sakun, I. A., 1960. *Vintovye kompressory (Screw compressors).* Leningrad: Mashinostroenie.

Sauls, J., Powel, G. & Weathers, B., 2007. *Thermal Deformation Effects on Screw Compressor Rotor Design*. American Standard.

Sauls, J., Weathers, B. & Powell, G., 2006. *Transient Thermal Analysis of Screw Compressors, Part III: Transient Thermal Analysis of a Screw Compressor to Determine Rotor-to- Rotor Clearances.* Purdue, s.n.

Stosic, N., Smith, I. K. & Kovacevic, A., 2003; 217; 3. Opportunities for innovation with screw compressors. *Process Mechanical Engineering,* p. 157.

Stosic, N., Smith, I. K. & Kovacevic, A., 2005. *Screw Compressors: Mathematical Modelling and Performance Calculation.* s.l.:Springer-Verlag Berlin Heidelberg.

Stosic, N., Smith, I. K., Kovacevic, A. & Mujic, E., 2010. *Three Decades of Modern Practice in Screw Compressors.* Purdue, s.n.

Stosic, N., Smith, I. K., Kovacevic, A. & Mujic, E., 2011 12(4). Geometry of screw compressor Rotors and their tools. *Journal of Zhejiang University-SCIENCE A (Applied Physics & Engineering),* pp. 310-326.

Weathers, B., Sauls, J. & Powell, G., 2006. *Transient Thermal Analysis of Screw Compressors, Part II: Transient Thermal Analysis of a Screw Compressor to Determine Rotor-to-Housing Clearances.* Purdue, s.n.

Wu, J., Feng, J., Dasgupta, S. & Keith, I., 2007. *A Realistic Dynamic Modelling Approach to Support LNG Plant Compressor Operations.* LNG Journal.

Appendix 1. Screw Compressor Working Principle

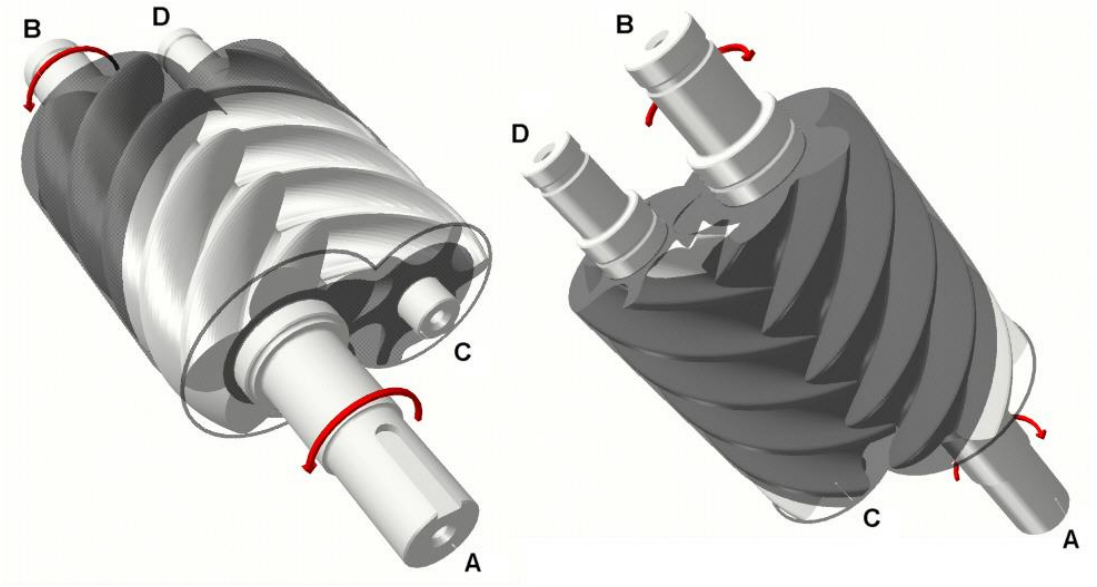

View from Front and Top View from Bottom and Rear

Figure 67: Compression process inside of screw compressor

Screw Compressor working principle description including Figure 67 are taken from Stosic et al, 2005.

Its principle of operation is based on volumetric changes in three dimensions rather than two. As shown, it consists, essentially, of a pair of meshing helical lobed rotors, contained in a casing. The flutes formed between the lobes on each rotor form a series of working chambers in which gas or vapour is contained. Beginning at the top and in front of the rotors, shown on the left, there is a starting point for each chamber where the trapped volume is initially zero. As rotation proceeds in the direction of the arrows, the volume of that chamber then increases as the line of contact between the rotor with convex lobes, known as the male rotor, and the adjacent lobe of the female rotor advances along the axis of the rotors towards the rear. On completion of one revolution i.e. 360^{o} by the male rotor, the volume of the chamber is then a maximum and extends in helical form along virtually the entire length of the rotor. Further rotation then leads to reengagement of the male lobe with the succeeding female lobe by a line of contact starting at the bottom and front of the rotors and advancing to the rear, as shown on the right. Thus, the trapped volume starts to decrease. On completion of a further 360^{o} of rotation by the male rotor, the trapped volume returns to zero.

The dark shaded portions show the enclosed region where the rotors are surrounded by the casing, which fits closely round them, while the light shaded areas show the regions of the rotors, which are exposed to external pressure. Thus the large light shaded area on the left corresponds to the low pressure port while the small light shaded region between shaft between ends B and D on the right corresponds to the high pressure port.

Exposure of the space between the rotor lobes to the suction port, as their front ends pass across it, allows the gas to fill the passages formed between them and the casing until the trapped volume is a maximum. Further rotation then leads to cut off of the chamber from the port and progressive reduction in the trapped volume. This continues until the rear ends of the passages between the rotors are exposed to the high pressure discharge port. The gas is then expelled through this at approximately constant pressure as the trapped volume returns to zero.

An important feature of such machines is that if the direction of rotation of the rotors is reversed, then gas will flow into the machine through the high pressure port and out through the low pressure port and it will act as an expander. The machine will also work as an expander when rotating in the same direction as a compressor provided that the suction and discharge ports are positioned on the opposite sides of the casing to those shown since this is effectively the same as reversing the direction of rotation relative to the ports. When operating as a compressor, mechanical power must be supplied to shaft A to rotate the machine. When acting as an expander, it will rotate automatically and power generated within it will be supplied externally through shaft A.

Appendix 2. Instrumentation and Instruments Calibration

All measuring transducers have been calibrated for the compressor test and their characteristics were implemented into the data acquisition software input. The torque meter was calibrated using an arm of known length and applied load as shown in Figure 68. The torque meter readings were found to be in good agreement with the applied torque and the results can be seen in Figure 69.

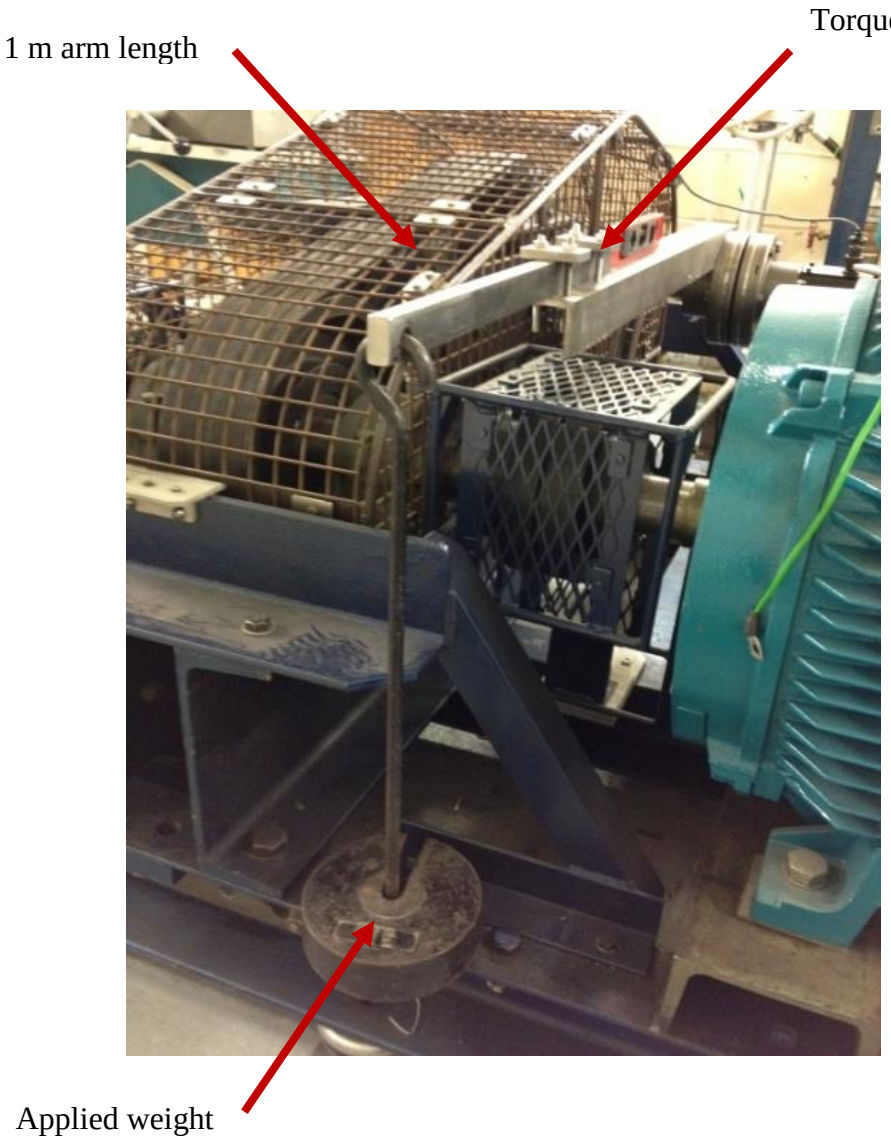

Figure 68: Torque meter calibration

The calibration of the pressure transducer was done by Budenberg hydraulic dead weight tester, Figure 70. Several sets of measurements of known pressures were made and the corresponding output of the transducers, in millivolts, was recorded. Then a calibration coefficient of each pressure transducer was obtained.

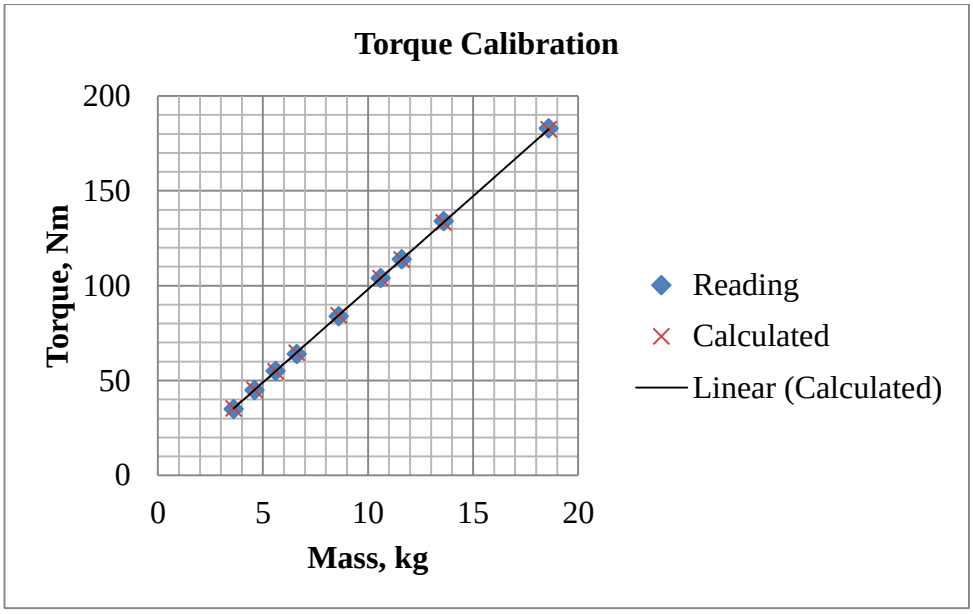

Figure 69: Torque meter calibration results

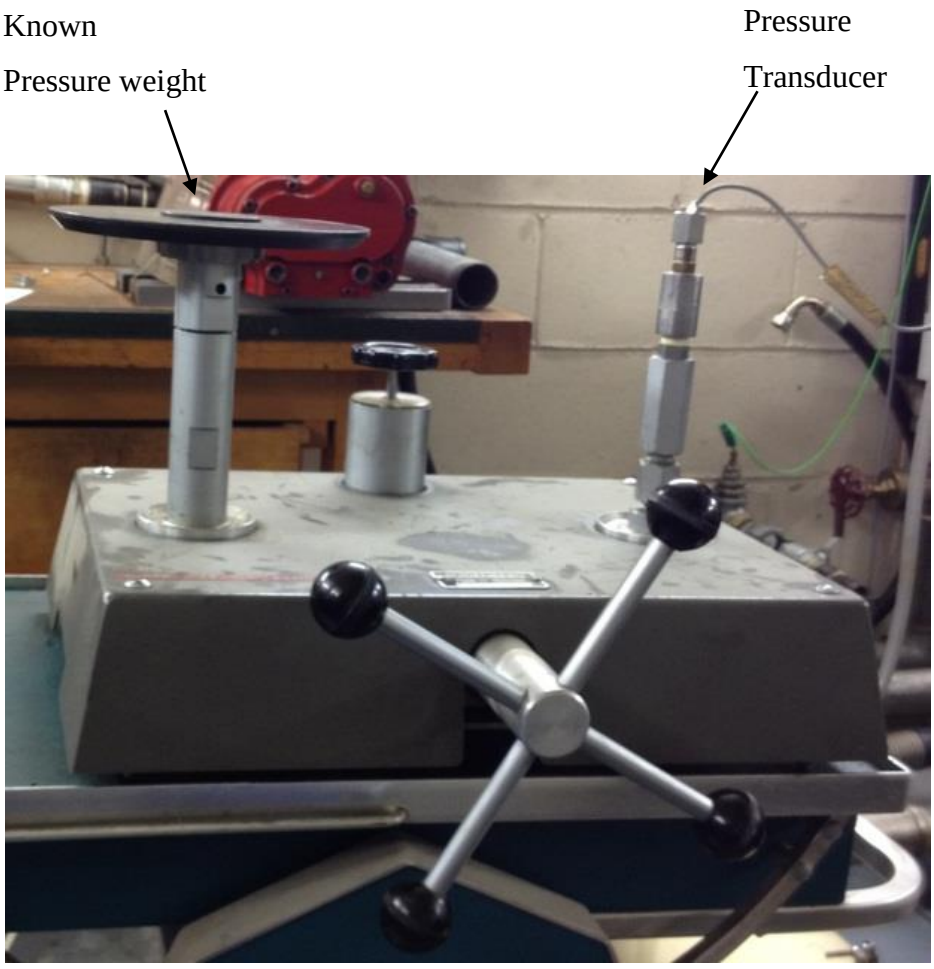

Figure 70: Hydraulic dead weight tester

The digital tachometer on the shaft of the compressor was verified with an optical tachometer and both readings were found to be in good agreement with each other. Where appropriate the K-type thermocouples were verified with either a mercury or infrared thermometer.

Table 10 below gives the list of installed instruments used for measurement the operating parameters of a compressor.

Table 10: Description of the test rig instruments

Measured Parameter	**Instrument**	**Specifications**
Compressor Speed, n	Tachometer (RPM transducer)	0 TTL pulses per revolution, Accuracy= 0.1%
Compressor Torque, M	TRP-500 torque meter (strain gauge transducer)	max torque: 500Nm, Calibration level: 335Nm Range = 0 - 6000 rpm, Supply volt=10v dc, Accuracy= 0.25 % of max torque
inlet pressure, p	PDCR 110/w -pressure transducer (piezoresistive type)	Operating range = 3.5bar(abs) Excite voltage=10V dc, Accuracy =0.6%,
inlet temperature , T_1	K- type thermocouple (based on Ni/Cr-Ni/Al alloy)	Range= -200^{0}C to 1300^{0}C, Accuracy= ±2.2^{0}C sensitivity = 41 µV/°C
outlet pressure, p	PDCR 922-pressure transducer (piezoresistive type)	Operating range =15 bar (abs) Excite voltage=10V dc, Output voltage= 100 mV Accuracy =0.6%
outlet temperature, T_2	K- type thermocouple (based on Ni/Cr-Ni/Al)	Range= -200^{0}C to 1300^{0}C, Accuracy=± 2.2^{0}C sensitivity = 41 µV/°C

Appendix 3. Data Acquisition and processing

All the data from the transducers were collected by a data acquisition system. It consists of a National Instrument Compact-RIO, CRIO-9022 Real-Time with an 8 slots chassis CRIO-9114. It has an industrial 533 MHz real-time processor for reliable real-time applications. Compact _RIO has 256 MB of DDR2 RAM and 2 GB of non-volatile storage for holding programs and logging data. The unit also permits the acquisition of signals from the measurement transducers simultaneously during the experiment that are inputs to the unit itself and connected to a computer via an Ethernet cable. The programming was done using LabVIEW Field Programmable Gate Array which is suitable for high frequency data acquisition. The measurements obtained from the transducers are acquired on the CRIO and send to the PC which is programmed to instantaneously calculate values of the compressor power consumption, air flow rate, specific quantities and efficiency. All required information is displayed on a computer monitor in real time as presented in Figure 4 and Figure 6.

Measurement records were collected twice a second and saved in a separate file which was used for further analysis. Before the measurements, the compressor and its plant were run for 30 minutes to obtain steady temperature in the compressor casing and to bring the oil temperature to its working level.

Appendix 4. Reynolds Transport Theorem

Reynolds Transport Theorem defines a change of variable ϕ in a control volume V limited by area **A** which vector of local normal is d**A** and which travels at local speed **v.** This control volume may, but not necessarily coincides with the engineering or physical material system. The rate of change of variable ϕ in time within the volume is:

$$\left(\frac{\partial \phi}{\partial t}\right)_V = \frac{\partial}{\partial t}\int_V \rho\phi dV \tag{1}$$

Therefore, it may be concluded that the change of variable ϕ in the volume V is caused by:

- change of the specific variable $\varphi=\Phi/m$ in time within the volume because of sources (and sinks) in the volume, $\left(\frac{\partial \varphi}{\partial t}\right)dV$ which is called a local change and
- the movement of the control volume which takes new space with variable φ in it and leaves old space, causing a change in time of φ for $\rho\varphi\mathbf{v}.d\mathbf{A}$ and which is called convective change.

The first contribution may be represented by a volume integral:

$$\int_V \frac{\partial(\rho\varphi)}{\partial t} dV \tag{2}$$

while the second contribution may be represented by a surface integral:

$$\int_A \rho\varphi\, \mathbf{v}\cdot d\mathbf{A} \tag{3}$$

Therefore:

$$\left(\frac{\partial \phi}{\partial t}\right)_V = \frac{d}{dt}\int_V \rho\varphi dV = \int_V \frac{\partial(\rho\varphi)}{\partial t} dV + \int_A \rho\varphi\, \mathbf{v}\cdot d\mathbf{A} \tag{4}$$

which is a mathematical representation of Reynolds Transport Theorem.

Applied to a material system contained within the control volume V_m which has surface A_m and velocity **v** which is identical to the fluid velocity **w,** Reynolds Transport Theorem reads:

$$\left(\frac{\partial \phi}{\partial t}\right)_{Vm} = \frac{d}{dt}\int_{Vm} \rho\varphi dV = \int_{Vm} \frac{\partial(\rho\varphi)}{\partial t} dV + \int_{Am} \rho\varphi \mathbf{w}\cdot d\mathbf{A} \tag{5}$$

If that control volume is chosen in one moment to coincide with the control volume V, the volume integrals are identical for V and V_m and the surface integrals are identical for A and A_m, however, the time derivatives of these integrals are different, because the control volumes will not coincide in the next time interval. However, there is a term which is identical for the both times intervals:

$$\int_{V} \frac{\partial(\rho\varphi)}{\partial t} dV = \int_{Vm} \frac{\partial(\rho\varphi)}{\partial t} dV \tag{6}$$

therefore,

$$\left(\frac{\partial \phi}{\partial t}\right)_{Vm} - \int_{Am} \rho\varphi \mathbf{w}\cdot d\mathbf{A} = \left(\frac{\partial \phi}{\partial t}\right)_{V} - \int_{A} \rho\varphi \mathbf{v}\cdot d\mathbf{A} \tag{7}$$

or:

$$\left(\frac{\partial \phi}{\partial t}\right)_{Vm} = \left(\frac{\partial \phi}{\partial t}\right)_{V} + \int_{A} \rho\varphi(\mathbf{w}-\mathbf{v})\cdot d\mathbf{A} \tag{8}$$

If the control volume is fixed in the coordinate system, i.e. if it does not move, **v**=0 and consequently:

$$\left(\frac{\partial \phi}{\partial t}\right)_{V} = \int_{V} \frac{\partial(\rho\varphi)}{\partial t} dV \tag{9}$$

therefore:

$$\left(\frac{\partial \phi}{\partial t}\right)_{Vm} = \int_{V} \frac{\partial(\rho\varphi)}{\partial t} dV + \int_{A} \rho\varphi \mathbf{w}\cdot d\mathbf{A} \tag{10}$$

Finally application of Gauss theorem leads to the common form:

$$\left(\frac{\partial \phi}{\partial t}\right)_{Vm} = \int_{V} \frac{\partial(\rho\varphi)}{\partial t} dV + \int_{V} \nabla\cdot(\rho\varphi \mathbf{w}) dV \tag{11}$$

As stated before, a change of variable ϕ is caused by the sources q within the volume V and influences outside the volume. These effects may be proportional to the system mass or volume or they may act at the system surface. The first effect is given by a volume integral and the second effect is given by a surface integral.

$$\left(\frac{\partial \phi}{\partial t}\right)_{Vm} = \int_{Vm} q_V dV + \int_{Am} q_A \cdot d\mathbf{A} = \int_V \left(q_V + \nabla \cdot q_A\right) dV = \int_V q dV \tag{12}$$

q can be scalar, vector or tensor.

A combination of the two last equations gives:

$$\begin{aligned} &\int_V \frac{\partial(\rho\varphi)}{\partial t} dV + \int_A \rho\varphi \mathbf{w} \cdot d\mathbf{A} = \int_V q dV \quad \text{or} \\ &\int_V \left[\frac{\partial(\rho\varphi)}{\partial t} + \nabla \cdot (\rho\varphi \mathbf{w}) - q\right] dV = 0 \end{aligned} \tag{13}$$

Omitting integral signs gives:

$$\frac{\partial(\rho\varphi)}{\partial t} + \nabla \cdot (\rho\varphi \mathbf{w}) - q = 0 \tag{14}$$

This is well known conservation law form of variable $\phi=\rho\varphi$. Since for $\varphi=1$, this becomes continuity equation: $\frac{\partial \rho}{\partial t} + (\nabla \cdot \rho \mathbf{w}) = 0$ finally it is:

$$\begin{aligned} &\varphi\left[\frac{\partial \rho}{\partial t} + (\nabla \cdot \rho \mathbf{w})\right] + \rho \frac{\partial \varphi}{\partial t} + \rho(\mathbf{w} \cdot \nabla \varphi) - q = 0 \quad \text{or} \\ &\frac{D\varphi}{dt} = \rho \frac{\partial \varphi}{\partial t} + \rho(\mathbf{w} \cdot \nabla \varphi) = q \end{aligned} \tag{15}$$

$D\varphi/dt$ is the material or substantial derivative of variable φ. This equation is very convenient for derivation of particular conservation laws. As previously mentioned $\varphi=1$ leads to continuity equation, $\varphi=\mathbf{u}$ to momentum equation, $\varphi=e$, where e is specific internal energy, leads to energy equation, $\varphi=s$, to entropy equation and so on.

If the surfaces where fluid carrying variable Φ goes into or exits from the control volume can be identified, a convective change may conveniently be written:

$$\int_A \varphi \rho \mathbf{w} \cdot d\mathbf{A} = \int \varphi \, d\dot{m} = \left(\bar{\varphi}\dot{m}\right)_{in} - \left(\bar{\varphi}\dot{m}\right)_{out} = \dot{\Phi}_{in} - \dot{\Phi}_{out} \qquad (16)$$

where bar denotes the variable average at entrance/exit surface sections. This leads to macroscopic form of the conservation law:

$$\left(\frac{d\Phi}{dt}\right)_V = \left[\frac{d\left(\rho\varphi\right)}{dt}\right]_V = \dot{\Phi}_{in} - \dot{\Phi}_{out} + Q = \left(\bar{\varphi}\dot{m}\right)_{in} - \left(\bar{\varphi}\dot{m}\right)_{out} + Q \qquad (17)$$

which states in words: (rate of change of Φ)=(inflow Φ)-(outflow Φ)+(source of Φ)

Appendix 5. Publications

Attended Conferences and published papers are presented in Table 11 below.

Table 11: Attended conferences

Conference/Journal	Date	Paper
City University Student Research Simposium 2012, CUL, London	June 2012	Investigation of Start Up Process in Oil Flooded Twin Screw Compressors
21st International Compressor Conference at Purdue University, USA	July 2012	Investigation of Start Up Process in Oil Flooded Twin Screw Compressors
ASME Congress 2012, Texas, USA	November 2012	Identification and Quantification of Start Up Process in Oil Flooded Screw Compressors
International Conference on Compressors and their Systems, City University London	September 2013	Numerical Analysis of Unsteady Behaviour of a Screw Compressor System
Compressor Engineering Refrigeration and Air Conditioning Conference at Purdue	July 2014	Modelling and Experimental Investigation of Unsteady Behaviour of a Screw Compressor Plant

Published papers:

E. Chukanova, N. Stosic, A. Kovacevic and A. Dhunput, "Investigation of Start Up Process in Oil Flooded Twin Screw Compressors," in *International Compressor Engineering Conference at Purdue*, Purdue, USA, 2012.

E. Chukanova, N. Stosic, A. Kovacevic and S. Rane, "Identification and Quantification of Start Up Process in Oil Flooded Screw Compressors," in *ASME Congress*, 2012.

E. Chukanova, N. Stosic, A. Kovacevic, “Numerical Analysis of Unsteady Behaviour of a Screw Compressor System,” in *International Conference on Compressors and their Systems*, City University London, 2013.

E. Chukanova, N. Stosic , A. Kovacevic (2013). Experimental Investigation and Numerical Modelling of Dynamic Behaviour of Screw Compressor Plant. *Universal Journal of Engineering Science, 1 ,* 68 - 79.

E. Chukanova, N. Stosic, A. Kovacevic, “Modelling and Experimental Investigation of Unsteady Behaviour of a Screw Compressor Plant” in *International Compressor Engineering Conference at Purdue*, Purdue, USA, 2014.

E. Chukanova, N. Stosic, A. Kovacevic, “Verification and Calibration of Dynamic Model of Screw Compressor Plant” in *ASME Congress*, 2015.